Identification of novel Parkinson's Disease genes involved in Parkin mediated mitophagy

Valerie Lefebvre

This thesis is submitted in partial fulfillment of the M.Sc. program in Cellular and Molecular Medicine

November 21, 2013

Department of Cellular and Molecular Medicine

Faculty of Medicine

University of Ottawa

Abstract

Mitochondrial dysfunction has been implicated as one of the primary causes of Parkinson's disease (PD). The proteins PINK1, a serine-threonine kinase, and Parkin, an E3 ubiquitin ligase, are mutated in many genetic cases of PD. In healthy individuals, Parkin is recruited to damaged mitochondria and leads to autophagic degradation of mitochondria in a process termed mitophagy. Following depolarization of the mitochondrial membrane, PINK1 is stabilized on the outer mitochondrial membrane, and triggers Parkin translocation from the cytosol to mitochondria. Precisely how this phenomenon is regulated is still unclear. We employed RNA interference (RNAi) technology in a 384-well format to identify novel genes that are required for Parkin recruitment to mitochondria. We identified ATPase inhibitory factor 1 (IF1) as the strongest hit required for Parkin recruitment following treatment with the protonophore CCCP. We show that IF1 is upstream of PINK1 and Parkin, and required to sense mitochondrial damage by allowing the loss of membrane potential. In cells treated with CCCP, the absence of IF1 permits the ATP synthase to run freely in reverse, consuming ATP to maintain potential across the inner mitochondrial membrane, thus blocking PINK1 and Parkin activation. Interestingly, Rho0 cells, that lack mitochondrial DNA, have downregulated endogenous expression of IF1 in order to maintain mitochondrial function. Overexpression of IF1 in Rho0 cells results in the depletion of mitochondrial membrane potential and the initiation of mitophagy. These data demonstrate a unique role for IF1 in the regulation of mitochondrial quality control that has not been explored in the etiology of PD.

Table of Contents

List of Figures

List of abbreviations

$\Delta\Psi_m$	change in potential across the mitochondrial inner membrane
$\Delta\Psi_P$	change in potential across the plasma membrane
AAA	ATPases Associated with diverse cellular Activities
ATG5	Autophagy related gene 5
ATG8/LC3	Autophagy related gene 8
ATG12	Autophagy related gene 12
ATG14L	Autophagy related gene 14-like (Barkor)
ATG16L	Autophagy related gene 16-like
ATP	adenosine triphosphate
ATP13A2	ATPase 13A2
BAX	BCL-2 associated X protein
BCL-2	B-cell lymphoma 2
CCCP	Carbonyl cyanide m-chlorophenyl hydrazine
cDNA	coding DNA
DA	dopamine
DHE	dihydroethidium
DJ-1	Parkinson protein 7
DNA	deoxyribonucleic acid
DRP1	dynamin-related protein 1
ETC	electron transport chain
FIS1	mitochondrial fission 1

GCL	glutamate-cysteine ligase
GTP	guanosine triphosphate
GWAS	genome-wide association study
H2O2	hydrogen peroxide
HRP	horseradish peroxidase
HK1	hexokinase 1
HK2	hexokinase 2
iAAA	intermembrane AAA protease
IF1	ATPase Inhibitory Factor 1 (ATPIF1)
IKK	IkappaB kinase
IMM	inner mitochondrial membrane
IPS	induced-pluripotent stem cells
LC3	microtubule-associated protein 1 light chain 3 alpha (MAP1LC3A)
LRRK2	Leucine Repeat Rich Kinase
mAAA	matrix AAA protease
MCL1	myeloid cell leukemia 1
MEF	mouse embryonic fibroblast
MFF	mitochondrial fission factor
MFN1	Mitofusin 1
MFN2	Mitofusin 2
MIRO	mitochondrial Rho GTPase
MnSOD	manganese superoxide dismutase
MPTP	mitochondrial permeability transition pore

MPTP	1-methyl-4-phenyl-1,2,3,4-tetrahydropyridine
mATG13	mammalian autophagy-related gene 13
mtDNA	mitochondrial DNA
mTORC1	mammalian transducer of rapamycin 1
NEMO	NF-kappaB essential modifier
NF-κB	nuclear factor-kappaB
Nrf2	nuclear factor erythroid-2
OMA1	zinc metallopeptidase
OMM	outer mitochondrial membrane
OPA1	optic atrophy protein 1
PARL	Presenilins-associated rhomboid-like protein
PD	Parkinson's disease
PGC-1α	peroxisome proliferator-activated receptor-γ co-activator 1α
PINK1	PTEN Inducible Kinase 1
PtdIns3K	phosphatidylinositol 3-kinase
PVDF	polyvinylidene difluoride
RNA	ribonucleic acid
ROS	reactive oxygen species
SNCA	α-synuclein
STS	staurosporine
TBS	TRIS bufferes saline
TOMM20	translocase of outer mitochondrial membrane 20
TOMM70	translocase of outer mitochondrial membrane 70

TRIS	tris(hydroxymethyl)aminomethane
TRX1	Thioredoxin 1
Ub	Ubiquitin
UBL	Ubiquitin-like
ULK1	unc-51-like kinase 1
ULK2	unc-51-like kinase 2
UVRAG	ultraviolet irradiation resistance-associated gene
VDAC1	voltage-dependent anion channel 1
VDAC2	voltage-dependent anion channel 2
VDAC3	voltage-dependent anion channel 3
WT	wild type

Acknowledgments

I would like to extend my gratitude to my supervisor Rob Screaton for his support and guidance during this project. In addition I would like to thank all my fellow lab mates, past and present, for their advice and help they provided. A special mention goes towards Stephen Baird who was always available for help in the HTS facility as well as his tremendous help running the genome screen and designing the computer algorithms required for data analysis during and after the screen. Andy Ng was great help in the design and troubleshooting of the genome screen. Qiujiang Du for his help during the screen as well as all the work he did during the validation steps, and virus design and production. Mirna Nascimento and Qiujuang Du for their assistance in the analysis of the mtDNA mutant cell lines. Other members who provided help, advice, and company in the lab including Chantal Depatie, Calie Fu, Darcey Miller, Chandra Eberhard, Jen Crichton, Courtney Reeks, Jun-Ichi Sakamaki, Matt Norton, Matt Gaetz, Emily Xu, Karine Robitaille, Joanne McBane, Yasir Mohamud, Edgardo Montez, Jim Yang, Myddryn Ellis, and Eliane Barras. Thank you to Lynn Kelly and Kathleen Frost for managing and the research institute and keeping it running.

I would additionally like to thank my thesis advisory committee members David Park, Michael Schlossmacher, and Steffany Bennett who provided so much support and guidance. Thank you to my thesis examiners Bob Korneluk and Michael Schlossmacher who have taken the time out of their busy schedules to read this thesis. Thank you as well to our collaborators who provided both advice and reagents Heidi McBride, Edward Fon, Michelangelo Campanella, Eric Shoubridge, and David Park.

I would also like to acknowledge the Michael J Fox Foundation, which has provided funding for this project. Thank you as well for scholarships provided by the Parkinson Society of Canada and the Queen Elizabeth II Graduate Scholarship in Science and Technology. Finally, thank you to the CHEO Research Institute and the Department of Cellular and Molecular Medicine at the University of Ottawa including Sylvie Deblois and Blanche Dinelle.

Chapter 1. Introduction

1.1 Parkinson's Disease

Parkinson's Disease (PD) is the second most common neurodegenerative disease. It is caused by the death of dopaminergic neurons in the substantia nigra pars compacta [1]. Loss of dopamine (DA) producing neurons results in many debilitating mental and motor symptoms. PD is clinically diagnosed during early stages of the disease based on the following motor symptoms: resting tremor, bradykinesia, postural instability, and rigidity [2]. Later stages of PD can manifest psychological issues such as depression, sleep disturbances, and dementia [3]. Pathologically, PD can be identified by the formation of inclusions called Lewy bodies composed primarily of α-synuclein and ubiquitin, although they are not present in all cases of parkinsonism [4].

The only existing therapies for PD, such as dopamine supplementation or deep brain stimulation, merely treat the symptoms. Although these treatments alleviate the day-to-day stress of living with the motor symptoms of PD, patients still suffer from the psychological stresses, as these therapies are no true cure nor do they prevent the progression of the disease. A major obstacle in finding a cure for PD has been our incomplete understanding of the mechanisms by which the pathology occurs.

1.2 Cause of PD

Nearly 200 years have passed since the original publication of James Parkinson's *An Essay on the Shaking* Palsy (1817), and yet how dopaminergic death occurs and its

cause is still poorly understood. Three major risk factors contribute to the probability of developing PD: age, genetics, and environment.

1.2.1 Age as a risk factor for PD

As with most neurodegenerative diseases, age is highly correlated with incidence of PD. Even in cases where a patient has a genetic predisposition for PD, age is still a major determining factor for whether the patient will have the disease. Indeed, at the age of 60 years old, 0.5-1% of the population will develop PD, and the prevalence increases to 3% of the population at 80 years of age [5]. Despite the increasing evidence for genetic factors that may predispose an individual to PD, age remains to be the greatest risk factor [6]. Importantly, a rise in the average life expectancy has increased the size of this high-risk age group and the number of individuals afflicted with PD accordingly.

1.2.2 Environmental risk factors for PD

Many recent reports have linked exposure to environmental toxins with PD. The most well known case occurred in response to a side product produced during the production of meperidine called 1-methyl-4-phenyl-1,2,3,6-tetrahydropyridine (MPTP) [7, 8]. Similar cases have been observed in cases of repeated exposure to certain insecticides such as paraquat, maneb, and rotenone [9]. As such, a strong correlation has been identified between PD and gardening, farming, occupational agriculture, and rural living [10]. Exposure to the solvents trichloroethylene and perchlorothylene has also resulted in the development of all features of PD [11]. Interestingly, all of these

toxins share the common property that they are all inhibitors of complex I of the electron transport chain (ETC) and lead to mitochondrial dysfunction.

1.2.3 Genetic risk factors for PD

Although genetic causes have only been identified in 5-10% of PD cases, studying these patients can help identify factors that are instrumental to the progression of the disease [12]. It was not until the 1990s that the first signs of a genetic contribution were identified in autosomal dominant or recessive cases of PD. Since this time up to 28 chromosomal regions have been identified that confer risk for developing PD [13]. This number is likely to increase with time given the advent of deep-sequencing technologies, and genome-wide association studies (GWAS). Of these chromosomal locations, 6 have been validated as the cause of a monogenic form of PD. Mutations in two genes, SNCA (α-synuclein, PARK1) [14], and LRRK2 (leucine-rich repeat 2, PARK8) [15] have been implicated in autosomal dominant cases of PD. Mutations in PINK1 (PTEN induced putative kinase 1, PARK6) [16], Parkin (PARK2) [17], DJ-1 (PARK7) [18], and ATP13A2 (ATPase type 13A2, PARK9) [19] are associated with autosomal recessive cases of PD. Interestingly, many of these genes are involved in a common pathway of mitochondrial control, further highlighting the importance of mitochondrial health in PD pathology.

1.3 Mitochondrial Quality Control

Mitochondria are double membrane bound organelles found within the cell tasked with coordinating a medley of cellular functions. They are unique in that although the majority of mitochondrial proteins are encoded by nuclear DNA, a small

subset of the genes that make up the complexes of the ETC are encoded by the mitochondria's own DNA (mtDNA). Not only are mitochondria responsible for a large portion of the energy production for most cells through the ETC, they also participate in iron synthesis, Ca^{2+} buffering, β-oxidation, metabolite biosynthesis, and apoptosis. These processes result in the production of the majority of ROS found within a cell, which can contribute to damage and ageing if improperly regulated [20]. Accumulation of ROS leads to damage of mtDNA, lipids, and proteins causing impaired bioenergetics due to mitochondrial dysfunction and finally death [21]. Consequently, mitochondrial function is crucial for the survival of the cell, resulting in the evolution of multiple quality control mechanisms to ensure their health.

1.3.1 Mitochondrial fission and fusion

Despite what is typically conceived about mitochondria in textbooks, mitochondria are extremely dynamic organelles. Mitochondria within a cell are now recognized as a dynamic network where they are constantly undergoing processes termed mitochondrial fission and fusion, where a mitochondrion can be joined with another mitochondrion, or split to produce two mitochondria (reviewed in [22]). These fission and fusion events allow for rapid repair of damaged mitochondria through the sharing and redistribution of key metabolites and proteins.

The state of the mitochondrial network has been shown to be important for many biological events. Mitochondrial fission is required for cell division or cell death (reviewed in [23]). Additionally, mitochondrial fusion is implicated in cases were increased Ca^{2+} buffering or ATP stores are required. As such, significant research has been aimed at understanding how the balance between fusion and fission states is

controlled within cells, and has revealed the involvement of many proteins and molecular events. Due to the structure of mitochondria, consisting of both inner and outer mitochondrial membranes, the regulation of mitochondrial fission and fusion is especially complicated.

Mitochondrial fission of the outer mitochondrial membrane (OMM) is largely regulated by the cytosolic dynamin GTPase DRP1 [24, 25]. Loss of DRP1 results in a highly connected mitochondrial network due to ongoing fusion events in the absence of fission [24]. DRP1 recruitment to the surface of mitochondria is thought to be mediated by interaction with the mitochondrially anchored proteins FIS1 (mitochondrial fission 1) [26, 27] and MFF (mitochondrial fission factor) [28]. This process has not been clearly elucidated in mammalian cells but they appear to recruit DRP1 through independent pathways. The recruitment of DRP1 to the mitochondrial membrane results in the oligomerization of a ring of DRP1 around a mitochondrion where it exerts a GTP-dependent constriction of the membrane [29, 30].

Mitochondrial fusion of the OMM is mediated by the paralogous large GTPases mitofusin 1 and 2 (MFN1 and MFN2) that are situated at the outer mitochondrial membrane [31]. These proteins are believed to act as docking sites for adjacent mitochondria where MFN1 and 2 can join via an antiparallel coiled-coil motif to then use their GTPase activity to drive membrane fusion [32].

The dynamin related large GTPase optic atrophy protein 1 (OPA1) mediates fusion of the inner mitochondrial membrane (IMM) [33]. Upon import into mitochondria, OPA1 can be alternatively processed by the proteases PARL (presenilins-

associated rhomboid-like) [34, 35], as well as the AAA proteases (ATPases Associated with diverse cellular Activities) mAAA (matrix AAA protease) and iAAA (intermembrane AAA protease) [36-38], and OMA1 (zinc metallopeptidase) [39]. This results in the formation of eight different isoforms that can alternatively regulate IMM fusion and cristae formation. The regulation of cristae by OPA1 is important in the control of apoptosis; regulated opening of cristae causes release of cytochrome c, an early event in the apoptosis pathway [40]. The long non-soluble isoforms of OPA1 are responsible for membrane docking whereas the short isoforms exert the GTPase functions required for membrane mixing [41, 42].

Notably, the mitofusins and OPA1 are required for mixing of matrix contents [43, 44]. Sharing of mitochondrial components is important for the biogenesis of new organelles where fusion allows for mixing of mitochondrial components and fission results in the production of two new morphologically distinct mitochondria (reviewed in [45]). Mixing of mitochondrial components via fusion can rescue damaged mitochondria by replacing its non-functional components. Since mitochondria each possess their own mtDNA, mitochondrial defects caused by damaged mtDNA can be repaired by complementation through fusion with a mitochondrion that has non-mutant mtDNA to restore impaired respiratory activity [46, 47]. Additionally, fission serves as a quality control mechanism by severing the damaged portion of a mitochondrion for recycling by autophagy [48].

Mitochondrial dynamics play a particularly important role for the maintenance of neuronal function, as the unique energy requirements of dendritic spines and

synapses depends on highly functional mitochondria [49]. Dopamine metabolism and elevated iron levels contribute to high levels of ROS and put these mitochondria at greater risk of damage [50]. mtDNA is subject to damage by ROS due to proximity to the ETC [51]. As such, mitochondrial quality control pathways in neurons are crucial due to the elevation in damage that they experience.

Impaired mitochondrial morphology has been observed to play an important role in the etiology of PD. Cybrid cell lines generated using mitochondria derived from the platelet cells of PD patients had swollen mitochondria with damaged cristae [52]. Following the observation that complex I inhibitors cause PD, it was found that they also induce mitochondrial fragmentation in a DRP1-dependent manner [53, 54]. Concurrent with these findings, the PD genes DJ-1, LRRK2, PINK1, and Parkin all increase mitochondrial fragmentation when knocked down or inactivated [55-58]. Overall, impaired mitochondrial fission and fusion appear to contribute to the mitochondrial dysfunction observed in PD.

1.3.2 ER-mitochondria contacts

Increasing evidence suggests that the interaction between the endoplasmic reticulum (ER) and mitochondria is important for the maintenance of cell homeostasis. ER-localized MFN2 is involved in the tethering of ER to mitochondria through complexes with MFN1 or MFN2 on the OMM [59]. Sites of ER contact on mitochondria appear to mark sites for mitochondrial fission as they are often colocalized with the fission factors DRP1 and MFF [60]. It has been suggested that the ER participates in the initial constriction of mitochondria prior to DRP1 mediated fission. This is supported by

the fact that DRP1 oligomers do not exceed 100nm in diameter, a value much smaller than the diameter of an unconstructed mitochondria [29]. Although loss of MFN2 reduces the number of ER-mitochondria contact sites within the cell, it is likely not the only factor involved in the interaction between ER and mitochondria as mitochondrial constriction by ER can still occur in the absence of MFN2 [59, 60].

Interaction between ER and mitochondria is additionally beneficial for increased Ca^{2+} buffering from the ER to mitochondria [61]. Ca^{2+} buffering is facilitated from the inositol 1,4,5-triphsophate receptor ($Ins(1,4,5)P_3R$) channel on the ER to the voltage-dependent anion channel 1 (VDAC1) on the OMM of mitochondria [62, 63]. Transfer of Ca^{2+} across the IMM is further facilitated by the mitochondrial calcium uniporter (MCU) [64].

Ca^{2+} signaling into the mitochondria is beneficial for several reasons. MIRO (mitochondrial Rho GTPase) is responsible for tethering of mitochondria to the cytoskeleton, and subsequent mitochondrial translocation and morphology. Ca^{2+} has been shown to bind the EF hands of MIRO and thereby block mitochondrial motility [65]. Interestingly MIRO is situated in punctae where ER-mitochondria contacts occur [66]. High concentrations of Ca^{2+} also activate the fission protein DRP1 in a MIRO-dependent fashion [67] and are required for the activation of other mitochondrial proteins in the TCA (tricarboxylic acid) cycle to enhance ATP production [68]. The concentrations required for activation of these proteins are greater than Ca^{2+} levels found within the cytoplasm of the cell suggesting that these ER-mitochondria contacts are necessary for their activation. The absence of proper calcium buffering between ER

and mitochondria triggers apoptosis through the opening of the mitochondrial permeability transition pore (MPTP) and subsequent release of cytochochrome c [69].

Finally, the connection between ER and mitochondria are especially important in the formation of autophagosomes. There is now evidence that autophagosome formation occurs at ER-mitochondria contact sites [70]. Indeed, loss of MFN2 results in impaired starvation-induced mitophagy [71]. This connection permits the regeneration of mitochondrial membranes during the formation of autophagosomes [71].

Impaired or unregulated ER-mitochondria contacts have been implicated in the progression of neurodegenerative diseases. Their impairment is thought to contribute to the progression of Alzheimer's disease, which is associated with mitochondrial dysfunction similar to PD [72]. Given that ER-mitochondria contacts can improve mitochondrial function, it has been hypothesized that they can also play a role in the pathogenesis of PD. Overexpression of several PD genes, notably DJ-1, PINK1, and Parkin, have been associated with an increase in ER-mitochondrial contacts, leading to better mitochondrial calcium buffering and protect against ER-stress [73-75].

1.3.3 Mitophagy

Mitophagy is the selective autophagy of mitochondria that occurs during several physiological processes. The first is during the selective removal of paternal mitochondria and mtDNA from the fertilized oocyte [76, 77]. Mitophagy also occurs during the formation of red blood cells (reticulocytes) to prevent them from consuming the O_2 that they are transporting [78]. Finally, mitophagy acts as a last line of defense in mitochondrial quality control [79]. This quality control pathway is regulated by PINK1 and Parkin, which identify and target damaged mitochondria for destruction [80].

1.3.3.1 Autophagy

Autophagy is a process of "self-eating" by which components of a cell are degraded and recycled. Mitophagy is considered to be a type of macroautophagy whereby the cellular contents to be degraded are delivered to the lysosome via a double membrane bound vesicle [81]. Macroautophagy (Figure I) is generally considered to be a cytoprotective mechanism as it occurs under normal conditions to degrade damaged or unnecessary organelles, or it is activated in cases of nutrient stress in order to provide the necessary metabolites required for survival [82]. Dysfunctional autophagy can result in many different pathologies including: diabetes, cancer, ageing, and neurodegeneration (reviewed in [83]).

Macroautophagy is initiated at ER-mitochondria contact sites to form what is termed a phagophore [70, 71]. The phagophore grows until it envelops the desired cargo ranging in size from 0.5 to 1.5 μm [84]. Phagophore formation is initiated by the ULK complex downstream of the mammalian target of rapamycin complex 1 (mTORC1). This complex consists of the unc-51-like kinases 1 and 2 (ULK1 and ULK2), ATG13, and FIP200 [85-87]. ATG13 forms a complex with ULK1 and 2 following mTORC1-dependent phosphorylation. Further growth and elongation of the phagophore is dependent on the ubiquitin-like proteins ATG12 and ATG8/LC3 [82]. ATG12 is conjugated to ATG5, which then interacts with ATG16L to oligomerize into the ATG16L complex. This complex dictates sites of LC3 cleavage [88]. The lipidated form of cleaved LC3 termed LC3-II decorates both the inner and outer membrane of the growing autophagosome [89].

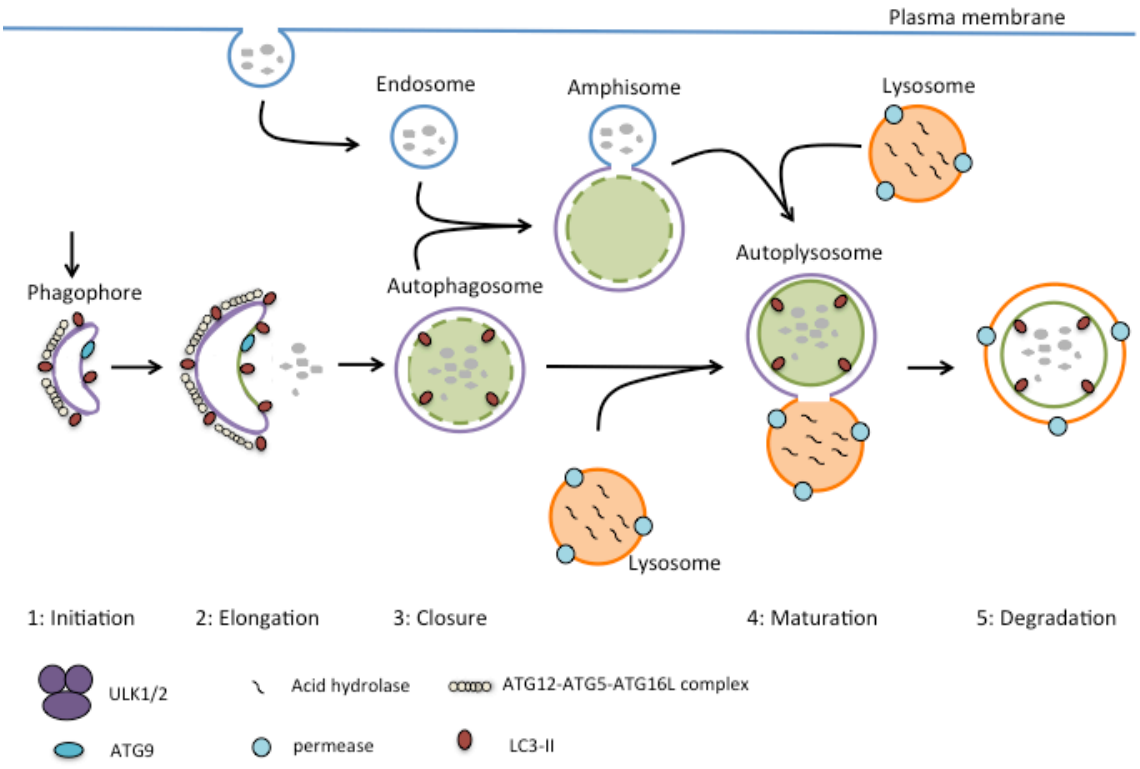

Figure I- Process and core machinery of mammalian macroautophagy. Phagophore formation is initiated by the ULK1/2 complex. The phagophore contains LC3-II, the ATG12-ATG5-ATG16L complex, and Atg9 which are required for the formation of the double-membrane bound autophagosome containing the cellular constituents to be degraded. The mature autophagosome then fuses directly with the lysosome or first with an endosome to form what it called an autolysome. The lysosome contains acid hydrolases that breaks down cargo, which are then released through permeases. Modified from Figure 1 in Yang, Z, Klionsky DJ. Eaten alive: a history of macroautophagy. Nat Cell Biol 12(9): 814-22, 2010. [90]

The class III phosphatidylinositol 3-kinase (PtdIns3K) complex is responsible for linking the newly formed phagophore to the autophagosome machinery. It consists of ATG14L (Barkor), ultraviolet irradiation resistance-associated gene (UVRAG), Beclin1, and p150 [91-93]. ATG14L interaction with ATG16L and LC3 positive structures and is necessary for the recruitment of class III PtdIns3K complexes [94]. UVRAG then promotes fusion of mature autophagosomes with a lysosome [95].

Once the autophagosome has fully formed, enveloping the cargo destined for destruction, it fuses with a lysosome to form what is termed an autolysosome. The autolysosome degrades cargo using acid hydrolases. The newly reformed metabolites are then released back into the cytosol via permeases where they can be re-used [90].

1.3.3.2 PINK1-Parkin mediated mitophagy

Mitophagy is seen as the last line of defense in mitochondrial quality control (Figure II). This was initially observed by Lemasters *et al.,* who saw that loss of membrane potential in mitochondria resulted in their selective removal by autophagosomes [96]. This is a process that is mediated through the PD associated genes PINK1, a serine-threonine kinase, and Parkin an E3-ubiquitin ligase. It was observed that GFP-tagged Parkin relocalizes from the cytoplasm to mitochondria following depolarization with the protonophore CCCP [97]. Prolonged treatment with CCCP resulted in selective loss of the mitochondrial network in cells overexpressing Parkin via autophagy [97]. Importantly, Parkin recruitment was only observed following complete loss of potential across the IMM ($\Delta\Psi_m$). Pathological Parkin mutants were incapable of either relocalizing to mitochondria, or clearing the mitochondrial network [98, 99].

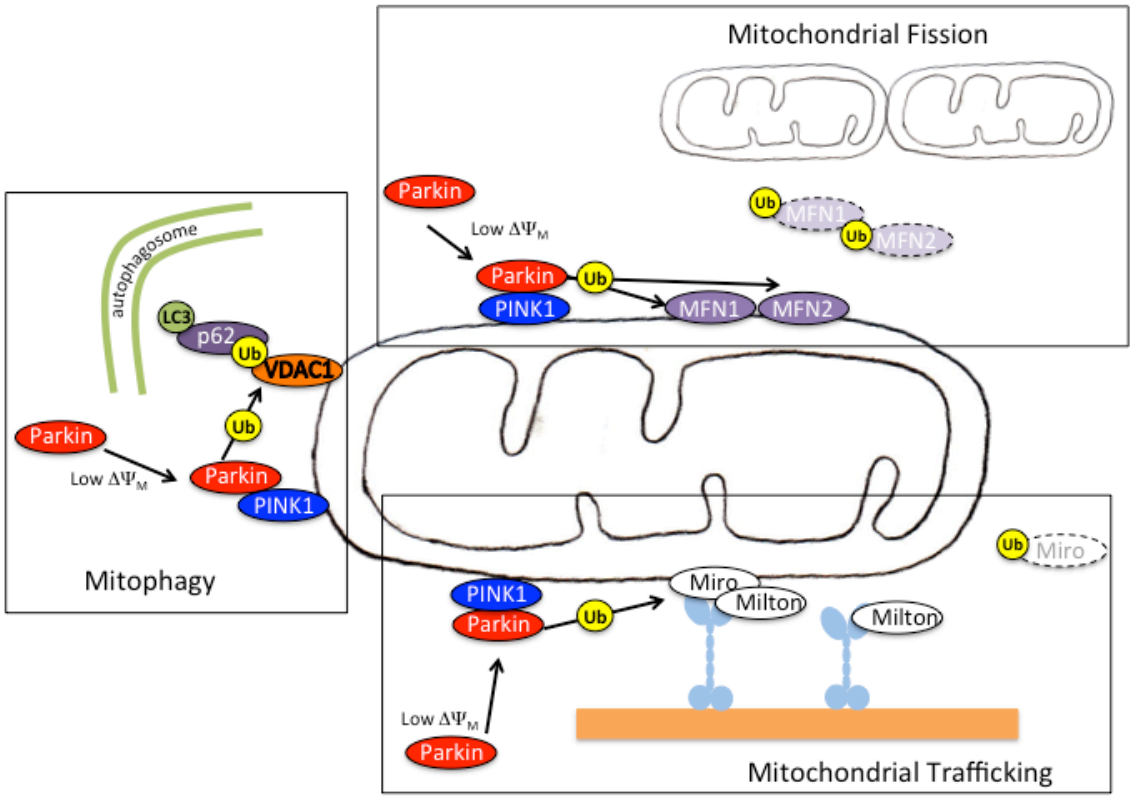

Figure II- Roles of PINK1/Parkin during mitophagy. PINK1/Parkin are responsible of for multiple steps during mitophagy. Ubiquitination and degradation of Miro halts trafficking of damaged mitochondria along microtubules. Ubiquitination and degradation of MFN1/2 results in the fission of damaged mitochondria from the mitochondrial network. Additional ubiquitination of other OMM proteins including VDAC1 signals the recruitment of the p62 adaptor protein and autophagosome formation around the damaged mitochondria. Modified from Figure 2 in Rosa L.A. de Vries, Serge Przedborski. Mitophagy and Parkinson's disease: Be eaten to stay healthy. Mol Cell Neurosci. 55: 37–43, 2013.

PINK1 and Parkin have long been considered to interact in a common pathway for mitochondrial maintenance [100-102]. Interestingly, Parkin recruitment is dependent on PINK1 [99, 103, 104]. Under normal conditions PINK1 is imported into mitochondria where it is cleaved by the mitochondrial proteases MPP and PARL resulting in a 52 kDa form which is further degraded by the proteasome [105-107]. Depolarization of mitochondria halts import of PINK1 such that the full-length 64 kDa

version is localized on the OMM, with the kinase domain facing the cytosol, leading to Parkin recruitment [103]. Furthermore, the recruitment of Parkin to mitochondria is dependent on the kinase activity of PINK1, such that pathological PINK1 mutants fail to recruit Parkin [108]. The downstream substrates of PINK1 following mitochondrial depolarization have been difficult to identify. There is some evidence that PINK1 phosphorylates Parkin, however the evidence is weak and has only been shown in *in vitro* assays [109]. Recent evidence suggests that PINK1 phosphorylates MFN2 following depolarization and that this phosphorylation is a necessary step in the progression of mitophagy [110].

Once targeted to mitochondria, Parkin ubiquitinates a host of OMM proteins. Ubiquitination and proteasomal degradation of proteins on the OMM is required for the recruitment of autophagy machinery to damaged and depolarized mitochondria [111]. TOMM70, VDAC1-3, MFN1/2, HK1/2, FIS1, BAX, and MCL1 are a few of the OMM proteins that are thought to be ubiquitinated by Parkin during mitophagy [112-114]. VDAC ubiquitination has been shown to recruit p62 and the autophagy machinery, although it does not appear to be essential for the process [112, 115]. Among these proteins, MFN1/2 are the only proteins shown to be ubiquitinated by endogenous Parkin [116-120]. This degradation may reflect a need for fission of mitochondria prior to their autophagic elimination [48]. Fission can segregate the healthy and damaged components of mitochondria as well as reduce the size of a mitochondrion permitting its encapsulation by autophagosomes.

Another target for PINK1/Parkin that has been recently identified is MIRO. MIRO and Milton work in conjunction to anchor mitochondria to kinesins and dyneins,

allowing their transport along microtubules in the cell. This transport is particularly important in neurons where mitochondria need to be transported to axons to provide energy for synaptic activity [121, 122]. PINK1 was found to form a complex with MIRO and Milton, with MIRO was found to be downstream of the fragmentation effect of PINK1 silencing on mitochondria [123]. Additional evidence demonstrated that PINK1 and Parkin target MIRO for degradation, resulting in arrested mitochondrial trafficking following loss of $\Delta\Psi_m$ [124]. CCCP treatment in mouse cortical neurons also appears to result in decreased anterograde movement of mitochondria [125]. These data suggest that freezing of mitochondrial movement may be an important step in preparing mitochondria for degradation.

1.3.3.3 Mitophagy in PD

The majority of research addressing the role of PINK1 and Parkin in mitophagy has been performed in immortalized cell lines using overexpressed Parkin and has not been confirmed in a physiological setting. This has made it difficult to draw strong conclusions on the role of mitophagy in PD. It has long been understood that mitochondrial dysfunction contributes to the progression of PD and thus it is logical that PINK1/Parkin mediated-mitophagy would provide a link between mitochondrial quality control and PD. The lack of convincing physiological data is in part due to the fact that the pharmacologic tools that are used to observe mitophagy are difficult to use with neurons [126]. Neurons are reliant on their mitochondria for all energy production and as such are incapable of switching to a glycolytic metabolism in cases of mitochondrial stress [127].

Despite the shortcomings of studying mitophagy in neurons, there has been some success in this field. Parkin recruitment has been observed in neurons derived from induced-pluripotent stem cells (IPS) following treatment with valinomycin. This recruitment was dependent on functional PINK1 as neurons derived from patients with mutant PINK1 were unable to recruit Parkin [128]. Additional evidence has been found in cortical neurons cultured from mouse embryos. In these studies, adjustments were made to the media in order to achieve Parkin recruitment. Cai *et al* found that culturing neurons with the apoptotic inhibitor Z-VAD over the course of a 24h CCCP treatment allowed them to observe recruitment of Parkin [125]. Additionally, Joselin *et al* discovered that the antioxidant properties in B27 neuronal supplement prevents the response of Parkin recruitment and thus observed that neurons cultured in the absence of B27 displayed robust Parkin recruitment to mitochondria following a 4h CCCP treatment [129]. In all cases, the current evidence for Parkin recruitment and mitophagy in neurons has been dependent on overexpressed Parkin. Research done by Rakovic *et al* in IPS-derived neurons suggests that endogenous levels of PINK1 and Parkin are capable of Parkin recruitment but not mitophagy [130].

Importantly, mitophagy has also been observed under physiological conditions suggesting it can occur during steady-state conditions in the absence of pharmacological inhibitors. Parkin recruitment has been observed in cells harboring mtDNA mutations. This recruitment was selective to mutant mitochondria in heteroplasmic cell lines indicating its use in providing mitochondrial quality control to cells [131]. Parkin recruitment has also been observed in fusion-incompetent cell lines in the absence of any other pharmacological stimulus [97]. This recruitment was likely a

reflection of an inability to repair mitochondrial damage through fusion and sharing of proteins and metabolites. These data suggest that Parkin recruitment and mitophagy of damaged mitochondria play an important physiological role in cells however further research on this pathway in PD is required.

Mitophagy has been observed *in vivo* in drosophila where it has been demonstrated that PINK1 or Parkin mutation leads to a decreased mitochondrial protein turnover [132]. Additional inhibition of mitophagy through binding of p53 to Parkin in mice leads to cardiac dysfunction indication that mitochondrial quality control plays an important role in maintaining functional cardiomyocytes [133]. Evidence of active mitophagy in a neuronal context has however remained elusive. Investigation of Parkin activity in the MitoPark mouse model, which develops PD-like symptoms as a result of respiratory chain deficiency in DA neurons [134], found that Parkin was not recruited to impaired mitochondria in vivo nor did its absence affect clearance of damaged mitochondria [135]. Given that ablation of any genes related to PD in murine models does not manifest symptoms of PD, another system for studying the molecular physiology of the disease should be investigated. Investigation of PINK1 and Parkin in the dopaminergic neurons of medaka fish has provided evidence for their protective capabilities in an alternative vertebrate model [136].

1.4 Mitochondrial Dysfunction and PD

Recent hypotheses suggest that mitochondrial dysfunction is the underlying cause of PD and that all other defects contribute to loss of mitochondrial integrity [137]. Mitochondrial dysfunction can arise from defects in mtDNA, nuclear encoded

mitochondrial proteins, or impaired metabolism. Mitochondria are subject to constant stress from active metabolites and reactive oxygen species (ROS), thus an inability to maintain healthy mitochondria can lead to a build-up of damage. Damaged or dysfunctional mitochondria, leads to loss of $\Delta\Psi_m$, which could in turn activate apoptotic-signaling pathways [138]. The discovery of the genetic factors that influence PD have given insight into sporadic cases as well highlighting an overwhelming contribution of mitochondrial dysfunction in what has been termed the mitochondrial cascade hypothesis by Cardoso [139].

1.4.1 SNCA and mitochondrial dysfunction

SNCA encodes a soluble protein found primarily in neural tissue. Point mutations in SNCA result in early-onset autosomal dominant cases of PD, whereas duplications or triplications of SNCA are associated with late-onset sporadic cases of the disease [4]. Importantly SNCA represents the majority of protein found in Lewy bodies, the pathological hallmark of the disease. Whether these SNCA aggregates are the cause of PD progression or if they are the consequence of a protective mechanism is not well understood. Complex I inhibitors have been found to interact with SNCA and suggest a potentially protective role during oxidative stress [140]. Mutant SNCA results in increased rotenone induced cell toxicity due to oxidative stress [141].

Although the precise function of SNCA in the cell is unclear, it has been found to be associated with mitochondrial membranes [142, 143]. Import of SNCA into mitochondria promotes mitochondrial fragmentation [144]. Additionally, expression of pathological A53T SNCA or overexpression of WT SNCA results in a fragmented mitochondrial network, whereas siRNA knockdown of SNCA results in an elongated

mitochondrial network [144, 145]. Expression of A53T SNCA results in inhibition of complex I in neurons and subsequent mitophagy leading to neuronal death [146, 147]. The inhibition of complex I by SNCA has also been observed in the brains of PD patients [148]. Overall, current evidence suggests that SNCA mutation or overexpression contributes to PD pathology by contributing to mitochondrial damage and interference of mitochondrial fusion.

1.4.2 DJ-1 and mitochondrial dysfunction

DJ-1 mutation is associated with an autosomal recessive form of PD [18]. Although its function is not fully understood, it is widely associated with oxidative stress. A cysteine residue (C106 in humans), which is conserved all the way down to yeast, is oxidized to sulfinic acid in response to oxidative stress [149, 150]. The oxidation of DJ-1 results in its accumulation at mitochondria [151]. This accumulation appears to play a protective role. Mutagenesis of C106 to alanine prevents the accumulation of DJ-1 to the mitochondria following oxidative damage. Additionally, overexpression of WT but not C106A DJ-1 can protect cells from rotenone induced cell death. These data suggest that the formation of sulfinic acid at C106 is intrinsic to the protective capabilities of DJ-1 [152].

Although the protective mechanism of DJ-1 is not properly understood, it is thought to modulate the cell's response to oxidative stress through transcriptional regulation. DJ-1 has been shown to upregulate the expression of the antioxidants manganese superoxide dismutase (MnSOD) and glutamate-cysteine ligase (GCL) via interaction with peroxisome proliferator-activated receptor-γ co-activator 1α (PGC-1α) ultimately leading to a decrease in ROS [153, 154]. DJ-1 is also capable of stabilizing

nuclear factor erythroid-2 (Nrf2), the master regulator of detoxifying enzymes and antioxidant proteins [155]. It has been shown that DJ-1 exerts at least a portion of its protective capacity by inducing the expression of Thioredoxin 1 (Trx1) through the Nrf2 pathway [156]. Transgenic mice expressing Trx1 have been shown to resist loss of DA neurons following treatment with MPTP [157].

Studies using DJ-1 knockout in mice have demonstrated that loss of DJ-1 results in a sensitization to oxidative stress by MPTP [158]. Additionally, DJ-1 is responsible for the attenuation of oxidative stress in DA neurons during their regular pacemaking functions, whereas loss of DJ-1 results in an accumulation of mitochondrial oxidative damage [159]. DJ-1 knockout in mouse embryonic fibroblasts (MEFs), and neuroblastoma cell lines, results in fragmented mitochondria, and impaired oxygen consumption and mitophagy [160, 161]. The interaction of DJ-1 with the mitophagy pathway remains controversial as loss of DJ-1 in DA neurons has also been shown to increase Parkin recruitment to mitochondria, and mitophagy, by increasing the amount of ROS production [129]. It is generally agreed however that the oxidative protection abilities of DJ-1 are important for maintaining a healthy mitochondrial population.

1.4.3 LRRK2 and mitochondrial dysfunction

LRRK2 is a multi-domain protein kinase whose mutation results in autosomal-dominant cases of parkinsonism [15]. Although its function is not well known, mutations in LRRK2 are responsible for the largest portion of heritable cases of PD [162]. LRRK2 is found in the cytoplasm as well as localized to various organelles including ER and mitochondria [163]. Interaction between LRRK2 and organelles appears to affect organelle function including mitochondrial homeostasis. Mutant

LRRK2 fibroblasts derived from PD patients display mitochondrial impairments including a disrupted network, lowered ATP levels, and decreased $\Delta\Psi_m$ [164]. Overexpression of mutant LRRK2 resulted in a similar phenotype in SH5Y cells and rat cortical neurons. The effect on the mitochondrial network can be rescued by WT-MFN1 or a dominant-negative form of DRP1, indicating that DRP1 and MFN1/2 are involved in its regulation [58]. How LRRK2 affects mitochondrial fission and fusion as well as other aspects of mitochondrial function remains to be understood.

1.4.4 Parkin and mitochondrial dysfunction

Parkin is a RING type E3-ubiquitin ligase whose mutation is associated with autosomal recessive juvenile parkinsonism [17]. It is capable of catalyzing multiple types of ubiquitinatation such as monoubiquitination, and both Lysine-48 and Lysine-63 polyubiquitin chains. To date, over 100 pathogenic mutations have been identified, resulting in impaired Parkin function due to either misfolding, loss of E3 activity, or mutations in its ubiquitin-like (UBL) domain [165]. Research into Parkin's role in neurons has revealed that it is in large part neuroprotective. Notably, overexpression of Parkin has been found to protect neurons from death following many damaging stimuli including ER-stress, excitotoxins, and mitochondrial toxins [166-170].

Mutant Parkin models in drosophila revealed that loss of function resulted in mitochondrial dysfunction [56]. Interestingly, Drosophila expressing mutant PINK1 displayed similar defects in mitochondrial dysfunction, a phenotype that was rescued by Parkin, placing these two genes in a common pathway governing mitochondrial quality control [101, 102]. Parkin is also able to rescue the effects on mitochondrial

pathology in human cell lines following PINK1 knockdown [55]. Additionally, silencing of Parkin in human cells lines results in mitochondrial fragmentation in a DRP1 dependent manner [171]. It is now well accepted that PINK1 and Parkin work in concert during mitophagy (reviewed above) although it is not known whether PINK1 is involved in Parkin's other protective mechanisms.

The recently identified Parkin substrate PARIS (Parkin-interacting substrate) has suggested a role for Parkin in promoting mitochondrial biogenesis. PARIS represses expression of the transcriptional co-activator PGC1α, which plays an important role in the promotion of mitochondrial biogenesis [172]. Degradation of PARIS through the ubiquitin-proteasome system is mediated through ubiquitination by Parkin, thus promoting mitochondrial biogenesis [173].

The neuroprotective properties of Parkin have also been linked to the NF-κB pathway. It has previously been observed that Parkin mediated its neuroprotective abilities through the activation of the IKK/NF-κB (IkappaB kinase/nuclear factor-kappaB) pathway by ubiquitination of NEMO (NF-kappaB essential modifier) [174]. The linear ubiquitination of NEMO has been reported to protect against TNFα (Tumour necrosis factor α) induced apoptosis through activation of NF-κB [175]. Incidentally, Parkin has been found to mediate linear-ubiquitination of NEMO to upregulate NF-κB resulting in downstream upregulation of OPA1 [176]. OPA1 promotes increased mitochondrial integrity and provides protection against cell-death through maintenance of cristae junctions and IMM fusion [40, 165]. This pathway was found to occur independent of PINK1 and mitophagy.

1.4.5 PINK1 and mitochondrial dysfunction

PINK1 is a serine-threonine kinase targeted to mitochondria whose loss of function results in autosomal recessive PD [16]. Over 50 mutations in the kinase and regulatory domains of PINK1 have been identified in PD patients and result in impaired function [165]. Silencing of PINK1 in human cells lines results in mitochondrial fragmentation, decreased ATP production, and decreased $\Delta\Psi_m$ [55, 171, 177, 178]. Additionally, PINK1 knockout mice display impaired mitochondrial respiration and increased sensitivity to oxidative stress [179]. Loss of PINK1 results in an imbalance in calcium homeostasis [180], suggesting impaired ER-mitochondria contacts contribute to the cause of neuronal death in PINK1-associated cases of PD [181]. PINK1, along with Parkin, are understood to reduce mitochondrial dysfunction via activation of mitophagy in mitochondria lacking $\Delta\Psi_m$ as described earlier [182]. Whether PINK1 has functions outside of the mitophagy pathway is not well understood.

Among possible substrates for PINK1 is the mitochondrial chaperone TRAP1 (TNF-receptor associated protein 1) [183]. PINK1 has been shown to phosphorylate TRAP1 in response to oxidative stress resulting in impaired cytochrome c release [183]. Loss of TRAP1 in drosophila results in mitochondrial dysfunction, whereas its upregulation was able to rescue the PINK1 mutant phenotype [184]. PINK1 has also been found to interact with the mitochondrial protease HtrA2/OMI (high-temperature requirement factor A2)[185]. HtrA2 is proposed to work in a common pathway with PINK1 based on evidence from drosophila models [186].

1.5 Screening for novel regulators of PINK1/Parkin mediated mitophagy

With the recent discovery of PINK1 and Parkin as a quality control checkpoint for mitochondrial health, precisely how Parkin is recruited and retained on mitochondria is of intense interest. Further research on the upstream events of this pathway is required to provide a better understanding of how mitophagy is linked to the etiology of PD [187].

Functional genomic screening provides an unbiased high-throughput approach that can be used to delineate cell-signaling pathways. By implementing the use of RNA interference (RNAi) libraries, one can pinpoint the role of a gene in a specific context by measuring a change in phenotype. In a pilot kinome screen, systematic siRNA knockdown of all kinases identified PINK1 as the only kinase required for Parkin recruitment to mitochondria, thus validating our screening approach. These results have been confirmed by several publications [103, 104, 120] showing that PINK1 is stabilized on the mitochondrial outer membrane following loss of mitochondrial membrane polarization ($\Delta\Psi_m$) prior to Parkin translocation.

Hypothesis: Functional genomic screening can be used to identify novel genes that function upstream of Parkin relocalization to mitochondria in response to oxidative damage.

While PINK1 is required for Parkin recruitment to mitochondria, it is not clear whether it binds to or phosphorylates Parkin directly. Thus, several other critical proteins are likely to be involved in the PINK1-Parkin pathway. **Our ultimate goal is to**

identify genes that regulate the events upstream of Parkin relocalization to mitochondria in response to oxidative damage. We predict that the results from functional genomic screening will help to fully elucidate the components involved in mitochondrial quality control of diseased neurons and will bring us closer to novel therapeutics for the treatment of PD. Using this approach we have identified that ATPase inhibitory factor 1 (IF1) plays an essential role in the identification of mitochondria designated for recycling via mitophagy.

Chapter 2. Methods

2.1 Reagents

Carbonyl cyanide m-chlorophenyl hydrazone (CCCP), dihydroethidium (DHE), oligomycin, N-acetyl cysteine (NAC,), and staurosporine were obtained from Sigma. MitoTracker Red CM-H_2XRos, MitoTracker Green FM, TMRE, and Hoechst 33342 were obtained from Invitrogen/Molecular Probes.

Antibodies were from the following sources: TOMM20 (Santa Cruz, sc11415), ATPIF1 (Sigma, SAB2100188), beta actin (Sigma, A5441), PINK1 (Novus, BC100-494), LRRK2 (MJFF2, Epitomics, 3514-1), ATP5B (3D5) (Abcam, ab14730).

2.2 Cell culture

HeLa cells (from Dr. Heidi McBride) and 143B cells (Dr. Eric Shoubridge) were cultured in DMEM with 25 mM glucose at 37°C in a humidified incubator with 5% CO_2. Rho0 cell (Dr. Eric Shoubridge) (derived from 143B) medium was supplemented with 1 mM

pyruvate and 50 µg/ml uridine. U2OS cells were cultured in McCoy's 5a medium (Gibco, 16600-082). All media contained 10% FBS and streptomycin/penicillin.

2.3 Imaging screen

Pools of four siRNA SMARTpool duplexes targeting 692 genes (Qiagen) or 18,255 human genes (Dharmacon siGenome) were spotted into 384-well plates using a Janus automated workstation. 10 nM of siRNA was reverse transfected into 450 HeLa cells using 0.025 µl of Lipofectamine RNAiMAX (Invitrogen). Coincident with transfection, cells were infected with an adeno-associated virus (AAV) expressing N-terminally tagged GFP-Parkin. 72 h later, 5 µM CCCP or vehicle (DMSO) was added to the cells for 1 h prior to fixation. Cells were washed with PBS, permeabilized with 0.1% Triton X-100 for 15 min, and subsequently stained with rabbit anti-TOMM20 primary antibody and AlexaFluor goat anti-rabbit secondary antibody (Sigma-Aldrich; A11012). Images of 10 fields per well were collected using a Cellomics Arrayscan Vti with a 40x objective and an XF53 filter set. Nuclei were counterstained with 1 µg/mL Hoechst 33342 and cell boundaries were approximated using a 40-pixel radius from the edge of the nucleus or the midpoint between two neighboring nuclei. Cells expressing GFP-Parkin were analyzed using Thermo Scientific's Cellomics vHCS:Scan software to differentiate cytoplasmic and mitochondrial GFP-Parkin signal. Each well was then scored based on the percentage of cells containing cytoplasmic GFP-Parkin. The level of GFP-Parkin associated with the mitochondria, as designated by TOMM20 fluorescence, was measured using the Matthews correlation coefficient of the two signals. A cutoff value for the correlation coefficient was set where greater than 85% of DMSO-treated cells were considered as having only cytoplasmic GFP-Parkin. Following algorithm analysis,

images from hit wells were manually inspected to verify failure of PARK2 mitochondrial recruitment.

2.4 Plasmids and vectors used

AAV packaging (given by Dr. David Park): pAAV-GFP-Parkin, pHelper, pNL-rep/cap

Lentiviral packaging (obtained from Addgene): PCMV 8.74, PMD2.G, pLenti6/v5, pLKO.1-non-targetting

Lentiviral constructs: pLenti6-IF1siRES-v5, pLenti6-IF1_E55A_Y58A-v5, pLenti6-mPINK1-V5, pLenti6-MTCH2-V5 (Darcey Miller), pLKO.1-shIF1(Qiujiang Du)

2.5 Western blotting

Proteins were harvested in 1X SDS sample buffer. Samples were run on 8% (for PINK1) or 12% (for IF1) polyacrylamide gels with a 4% upper stacking gel in Tris-Glycine running buffer. Proteins were transferred to a 0.45 μm polyvinylidene difluoride (PVDF) (for PINK1) or 0.20 μm PVDF membrane using a Tris/glycine/methanol transfer buffer for 80 min at 100 V. Membranes were blocked with 5% skim milk in Tris buffered saline containing 0.1% Tween-20 (TBS-T). Membranes were incubated for 1 hr at room temperature or overnight at 4 ^{o}C with the primary antibody in 5% milk in TBS-T + 0.05% sodium azide. Membranes were washed 3-5 times with 1X TBS-T and incubated with horseradish peroxidase (HRP)-conjugated secondary antibodies (Sigma) at 1:5000 for 1 hr at room temperature. Antibodies were used at the following concentrations: TOMM20 (1:2000), IF1 (1:1000), beta actin (1:20000), PINK1 (1:200), LRRK2 (1:500), ATP5B (β subunit, 1:2000)

2.6 ΔΨ measurements

MitoTracker Red staining was achieved by incubating cells with 300 nM of dye for 30 min following treatment with DMSO or CCCP. Cells were then fixed and stained for imaging as in the imaging screen. TMRE measurements were performed by live imaging on the Perkin Elmer Opera automated confocal microscope acclimatized to 37°C and 5% CO_2 and using a 20X water objective. Cells were incubated with 40 nM TMRE and 1 µg/ml Hoechst for 30 min prior to imaging and treatment. TMRE intensity per cell was evaluated with Columbus software (Perkin-Elmer) using an algorithm to look at the signal intensity of TMRE within a 30-pixel radius from the nucleus.

2.7 ATP assay.

siRNA knockdown was conducted in a white opaque 384-well plate as detailed above for the imaging screen. 72 h later, wells were treated for 1 h with 5 µM CCCP or DMSO. Staurosporine treatment (1 µM for 3 h) was included as a positive control for ATP depletion. The plate was equilibrated at room temperature for 30 min prior to the addition of an equal volume of Cell-Titre Glo (Promega, G7570). Contents were mixed for 2 min at 600 rpm on a microplate shaker and equilibrated for 10 min. Luminescence values were determined using a Synergy2 plate reader (BioTek) and normalized based on cell number using Hoechst nuclear stain.

2.8 Mitochondrial stress test

10 nM of siRNA was reverse transfected into HeLa cells using 0.5 µl of Lipofectamine RNAimax into a Seahorse XF24 cell culture plate. Cells were seeded at 5,000 cells per

well in 100 µl. After 4 h 400 µl of media was added per well. After 72 h cells were washed 3x with 500 µl of Seahorse XF assay medium. The mitochondrial stress test was performed using 2.5 µM of Oligomycin, FCCP, and Antimycin A. Oxygen consumption and glycolysis were measured using a Seahorse bioscience plate reader equilibrated to 37°C. Protein lysates were collected afterwards and measured by BCA assay for normalization.

2.9 ROS measurements

ROS was measured using the fluorescent dye Dihydroethidium at 20 µM. Cells. DHE was added to cells for 1 h with DMSO, Antimycin A, or CCCP and ROS was measured based on fluorescence intensity using a Synergy plate reader. Values were normalized to cell number using Hoechst nuclear stain.

2.10 RT-qPCR

RNA was harvested from a confluent 48-well dish using a QIAGEN RNeasy kit. Subsequently, cDNA was prepared from 750 ng of RNA in a reaction containing 1 mM dNTP, 50 µg/mL oligo dT, 10 mM DTT, 1X First strand buffer and SuperScript^{TM} II Reverse Transcriptase (Invitrogen). qPCR was performed using QuantiTech SYBR Green PCR kits (QIAGEN) with a minimum of 37.5 ng of cDNA and 10 µM of primers in an Eppendorf Mastercycler epigradient S thermocycler. Transcriptional changes in gene expression were normalized to 36B4 by the ΔCT method.

Chapter 3. Results

3.1 Development of a screen to identify genes involved in Parkin recruitment

To test for genes required for Parkin recruitment to mitochondria, we applied arrayed siRNAs libraries to an assay we developed to monitor Parkin localization following mitochondrial depolarization by the protonophore CCCP, or the complex III inhibitor Antimycin A (Figure 1a). HeLa cells were infected with an adeno-associated virus (AAV) expressing N-terminally tagged GFP-Parkin. This allowed us to visually monitor cellular localization of Parkin and to observe robust Parkin translocation from the cytoplasm to mitochondria following mitochondrial depolarization in control cells. A computer algorithm was generated to detect the percentage of cytoplasmic GFP-Parkin relative to the area of the cell comprised of TOMM20 stained mitochondria (Figure 1b-c, Stephen Baird). Following 72 h of gene knockdown, cells were stimulated with CCCP for 1 h prior to imaging. Genes were considered as hits required for mitochondrial Parkin recruitment if close to 100% of cells maintain cytoplasmic localization. PINK1 siRNA was used as a positive control. Genes that were not required for Parkin recruitment had scores closer to the scrambled non-targeting control siRNA where less than 60% of cells had cytoplasmic Parkin.

3.2 PINK1 is a suitable positive control for a genome-wide siRNA screen

A pilot screen was performed implementing a library of over 600 siRNA pools targeting all of the protein kinases found in the human genome. From this pilot screen PINK1 was the only protein kinase found to be required for Parkin recruitment (Appendix I). Three out of four siRNAs targeting PINK1 but not siRNAs against the PD

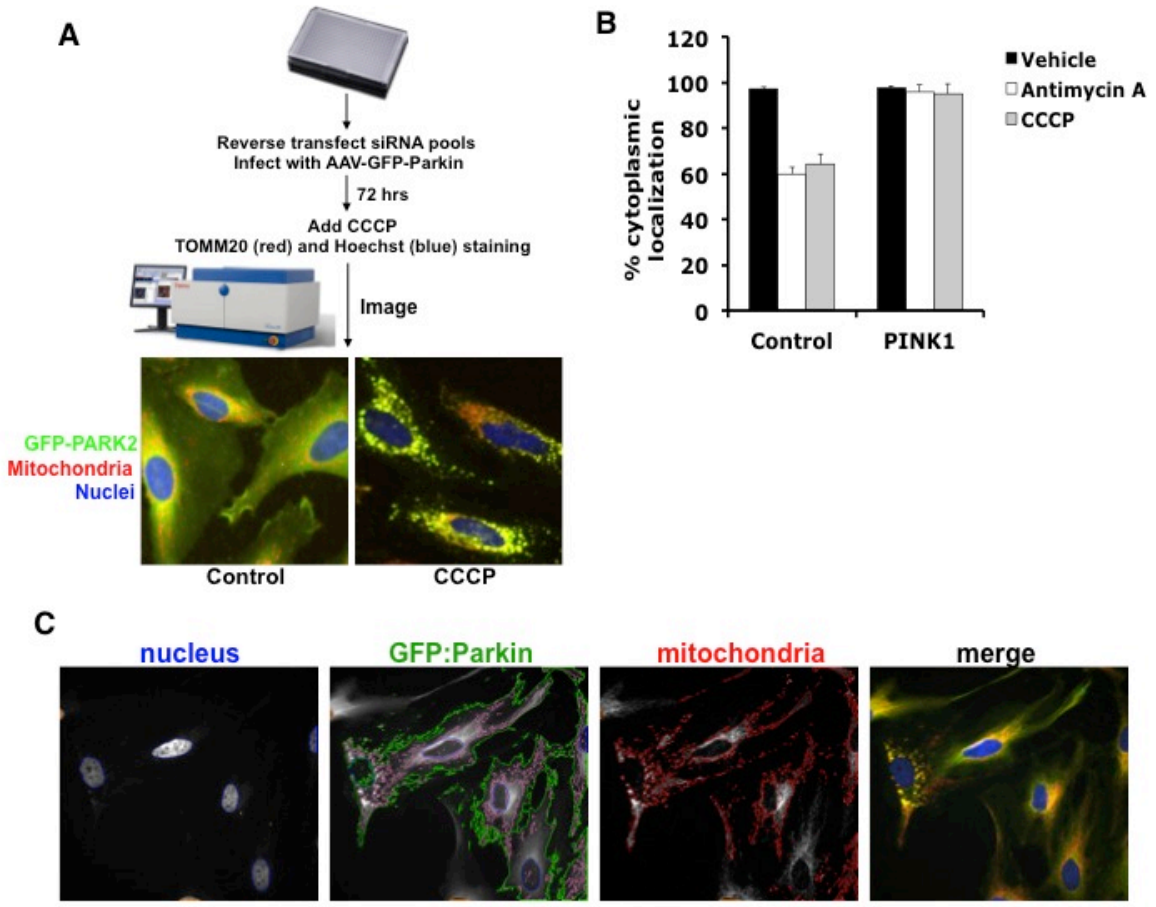

Figure 1-Development of an assay to identify genes required for Parkin recruitment. (A) Schematic of the screening layout. Pools of siRNAs are daughtered into 384 well imaging plates and are reverse transfected into HeLa cells. Cells are simultaneously infected with AAV-GFP-Parkin. Following 72 hrs of gene knockdown cells are treated with 5 μM CCCP for 1 hour prior to formaldehyde fixation. Hoechst dye is applied to reveal the nuclei, and an immunofluorescent antibody directed against TOMM20 to reveal mitochondria. Plates are subsequently imaged at 40x using a Cellomics HTI automated microscope. (B) Bar plot demonstrating the ability of an algorithm to detect between control (negative control) and PINK1 (positive control) siRNA following an hour of treatment with 5 μM CCCP or 40 μM Antimycin A. (C) Images demonstrating the detection of the nucleus (blue), GFP-Parkin (green), and the mitochondria (red) by the Cellomics software.

gene LRRK2 prevented CCCP induced Parkin recruitment (Figure 2) [188]. Additionally, reintroduction of a V5-tagged mouse PINK1 cDNA using a lentivirus was able to rescue the effect of PINK1 knockdown and restore Parkin recruitment (Figure 3). Introduction of another mitochondrially targeted protein MTCH2 had no effect. Genetic rescue is the only way to truly demonstrate that the effects observed by an siRNA are a product of loss of gene expression and not off-target.

3.3 IF1 is required for Parkin recruitment

We performed a genome-wide siRNA screen targeting over 18,000 genes in the human genome. Values from this screen were normalized and ranked based on variation from the mean to generate a Q-Q plot (Figure 4a, with Qiujiang Du) [188]. Genes whose scores fell within that of the positive control (PINK1), and passed manual inspection, were kept under consideration as hits. Deconvoluted siRNAs were ordered for these potential hits and the 4 individual siRNAs from the original pool were tested to determine the number of siRNAs that recapitulated the inhibition of Parkin translocation observed in the screen (Appendix II, with Qiujiang Du).

ATPase Inhibitory Factor 1 (ATPIF1 or hereinafter referred to as IF1) was selected as a top hit in the genome screen as three out of four siRNAs effectively blocked Parkin translocation (Figure 4b,c) [188] and knocked down IF1 protein levels (Figure 4d) [188]. Using lentivirus to deliver an shRNA against IF1 also blocked Parkin recruitment (Figure 4e, Qiujiang Du) [188]. To ensure that the effect of IF1 siRNA was not off-target, we generated an siRNA resistant cDNA against IF1 by mutating the IF1 coding sequence in the siRNA seed region such that the amino acid sequence was conserved but the siRNA targeting IF1 was no longer complimentary. The effect of IF1

knockdown on Parkin recruitment was rescued following introduction of this siRNA resistant IF1 (Figure 5) [188].

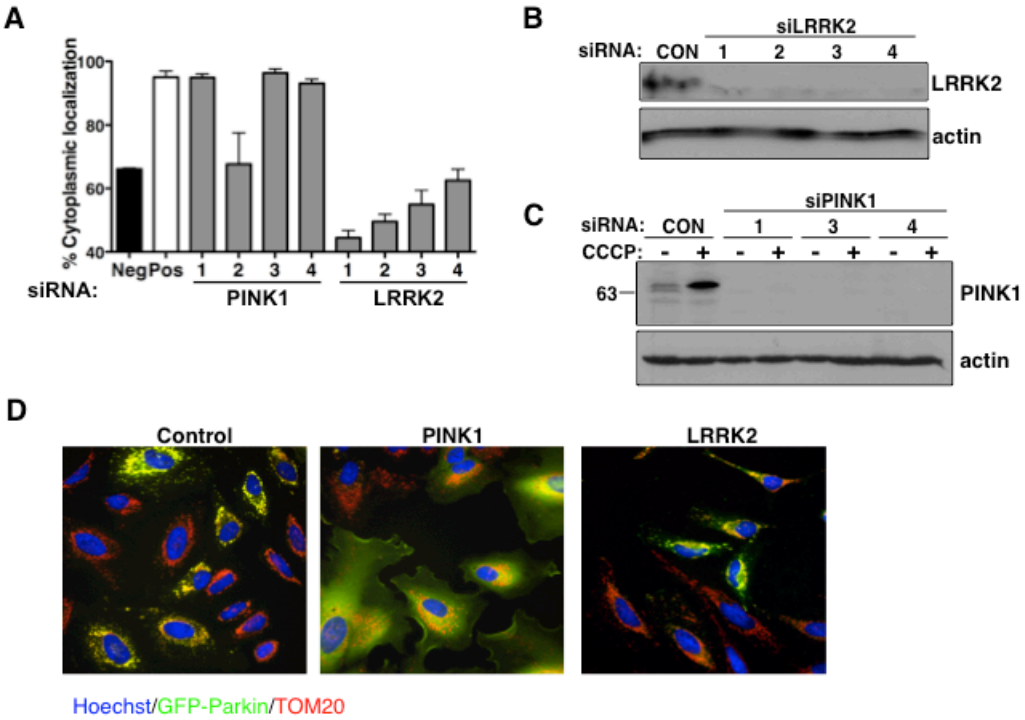

Figure 2- Kinome screen reveals PINK1 as the only protein kinase required for Parkin recruitment. (A) Quantitation of cytoplasmic localization in HeLa cells following 1 h of 5 μM CCCP treatment. Cells were simultaneously transfected with siRNAs and infected with AAV-GFP-Parkin 72 h before treatment and staining. Neg corresponds to the scrambled negative control siRNA, and Pos corresponds to the pooled positive PINK1 siRNA. (B) Western blot showing effective protein knockdown of LRRK2 following 72 h siRNA transfection in HeLa cells. Actin is shown as a loading control. (C) Western blot showing effective protein knockdown of PINK1 in HeLa cells following 72 h siRNA transfection. Cells were treated for 1 hour with either DMSO or 5 μM CCCP prior to harvesting protein. Actin is shown as a loading control. (C) Fluorescent micrographs showing localization of GFP-Parkin in HeLa cells following a 1 hr treatment with 5 μM CCCP in control, PINK1, and LRRK2 siRNA knockdown conditions. Hoechst stained nuclei are shown in blue, GFP-Parkin in green, and TOMM20 stained mitochondria in red.

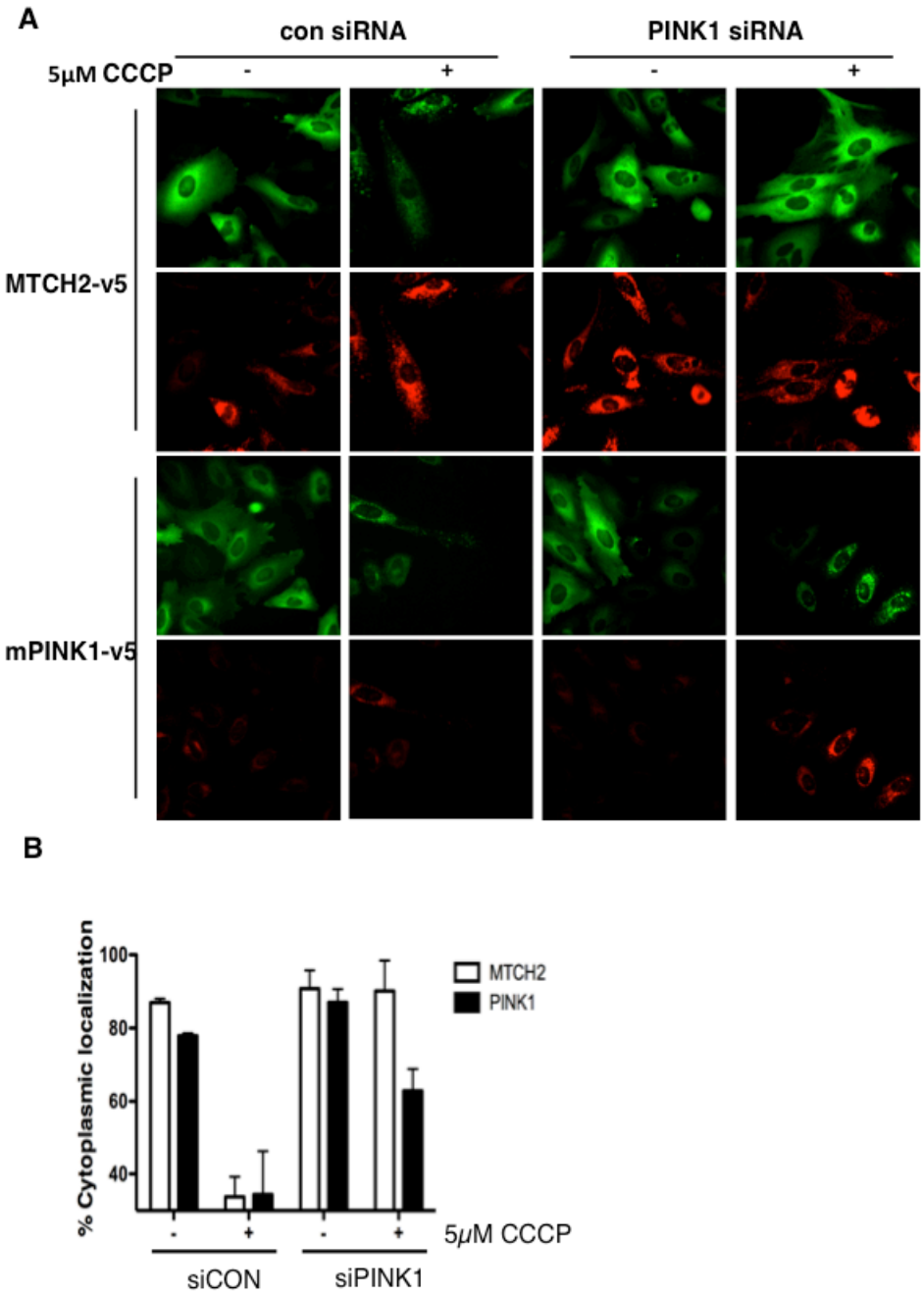

Figure 3- PINK1 knockdown phenotype is rescued using a lentivirus encoding mouse PINK1 (mPINK1). (A) Immunofluorescence showing restoration of GFP-PARKIN localization to mitochondria in CCCP treated cells following overexpression of mPINK1 but not MTCH2 in HeLa cells. Cells were simultaneously transfected with control or PINK1 siRNA and lentivirus expressing V5-tagged mPINK1 or MTCH2. Following 72 h of gene knockdown, cells were treated for 1 h with either DMSO (-) or 5 μM CCCP (+) prior to fixation and staining. GFP:PARKIN is shown in green and V5 staining is shown in red. (B) Quantification of cytoplasmic localization is shown.

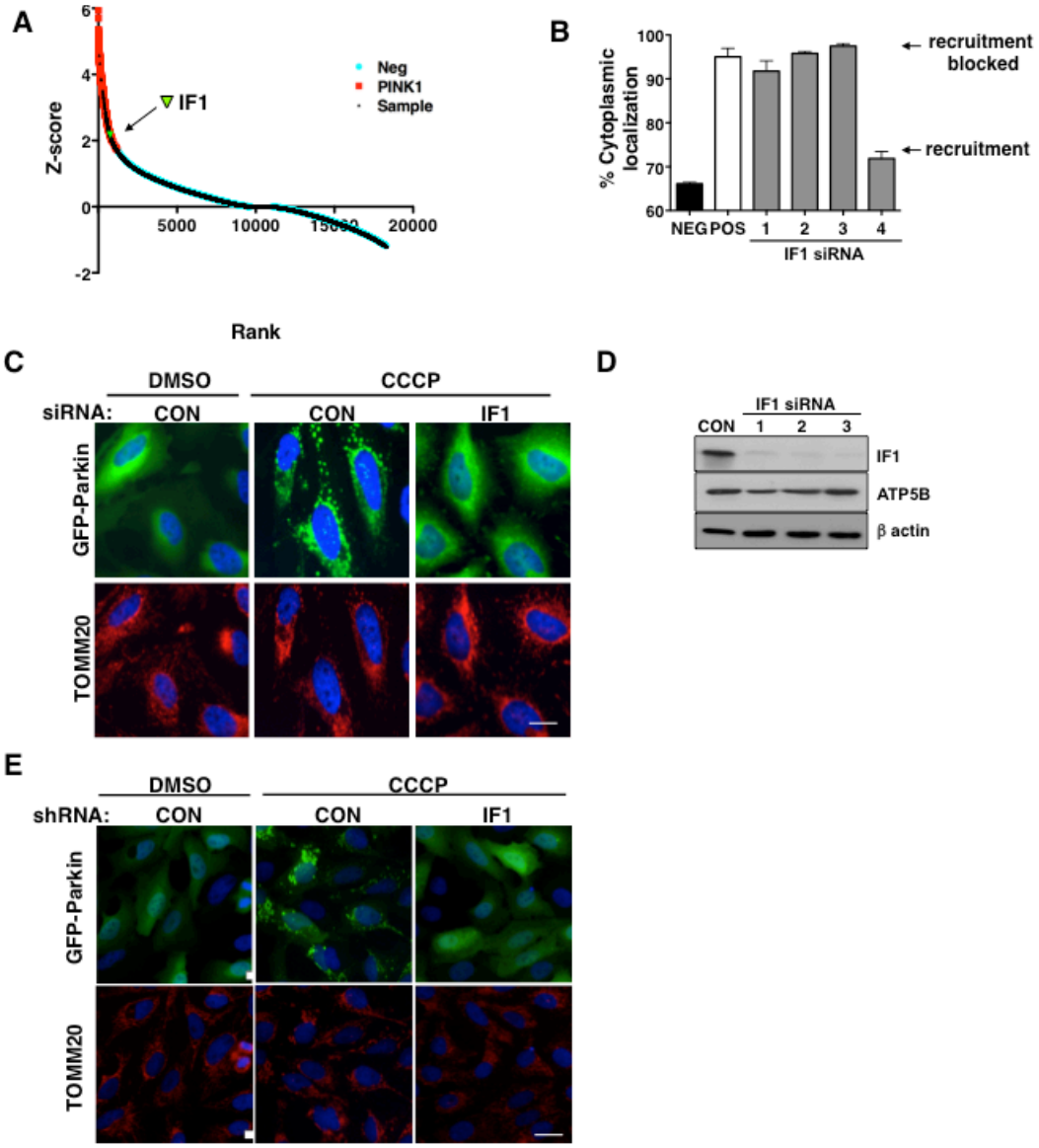

Figure 4- Genome-wide siRNA screen identifies IF1 as a strong candidate for Parkin recruitment. (A) Q-Q plot showing the Z-score ranking of genes from the genome screen (black circles) among the positive PINK1 siRNA controls (red squares) and negative scrambled siRNA (turquoise squares). The ranking of IF1 is demonstrated by a green triangle. (B-C) HeLa cells were simultaneously infected with AAV-GFP-Parkin and siRNA. Following 72 h cells were treated with 5 μM CCCP for 1 h prior to fixation and staining. (B) Bar plot showing the effect of the deconvoluted IF1 siRNAs on Parkin recruitment. (C) Representative image of GFP-Parkin distribution with control or IF1 siRNA. Scale bar = 25 μm. (D) Western blot showing effective knockdown of IF1 protein levels. Protein lysates were collected from HeLa cells following 72 h siRNA transfection. The ATPase ATP5B subunit, and actin are shown as loading controls. (E) An shRNA targeting IF1 prevents Parkin recruitment in U2OS cells. U2OS cells were simultaneously infected with lentivirus expressing GFP-Parkin and shRNA targeting IF1, then treated with 5 μM CCCP, fixed, and stained 72 h later.

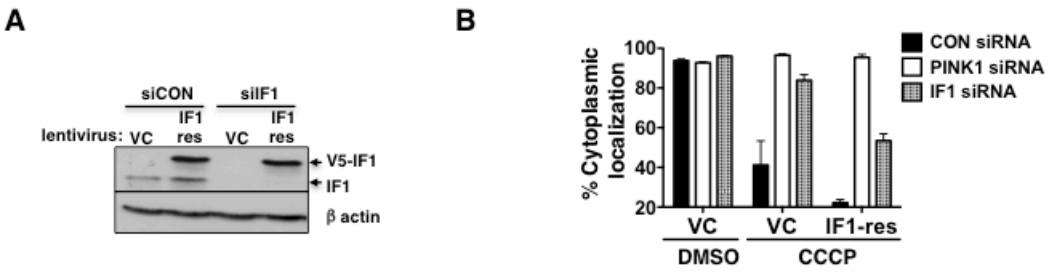

Figure 5- Introduction of an siRNA resistant IF1 cDNA rescues Parkin recruitment. (A) Western blot demonstrating efficient restoration of IF1 protein levels following IF1 knockdown. HeLa cells were transfected with either control (siCON) or IF1 (siIF1) siRNA and infected with lentivirus expressing a vector control (VC) or siRNA resistant IF1 cDNA (IF1 res). Protein was collected 72 h later and ran on an SDS-PAGE gel. Membrane was probed for IF1 protein with actin as a loading control. (B) Quantitation of Parkin recruitment following restoration of the siRNA resistant cDNA.

IF1 is a mitochondrial matrix protein that inhibits the F_1F_o-ATP synthase from running in reverse as an ATPase [189, 190]. This process occurs when the electron transport chain becomes impaired such as in cases of oxygen deprivation, making it favourable to consume ATP to restore $\Delta\Psi_m$ [191]. When a drug such as CCCP is used to disrupt $\Delta\Psi_m$, IF1 blocks the ATPase, preventing the cell from using up ATP and allowing depolarization of mitochondria [192]. To test whether the role of IF1 in Parkin recruitment was dependent on its interaction with the F_1F_o- ATPase we mutated amino acids E55 and Y58 to alanine. These residues have been shown to be required for binding of bovine IF1 to the ATPase in vitro [193]. Introduction of an siRNA resistant E55A-Y58A mutant IF1 cDNA to HeLa cells failed to restore Parkin recruitment in the context of IF1 knockdown (Figure 6) [188].

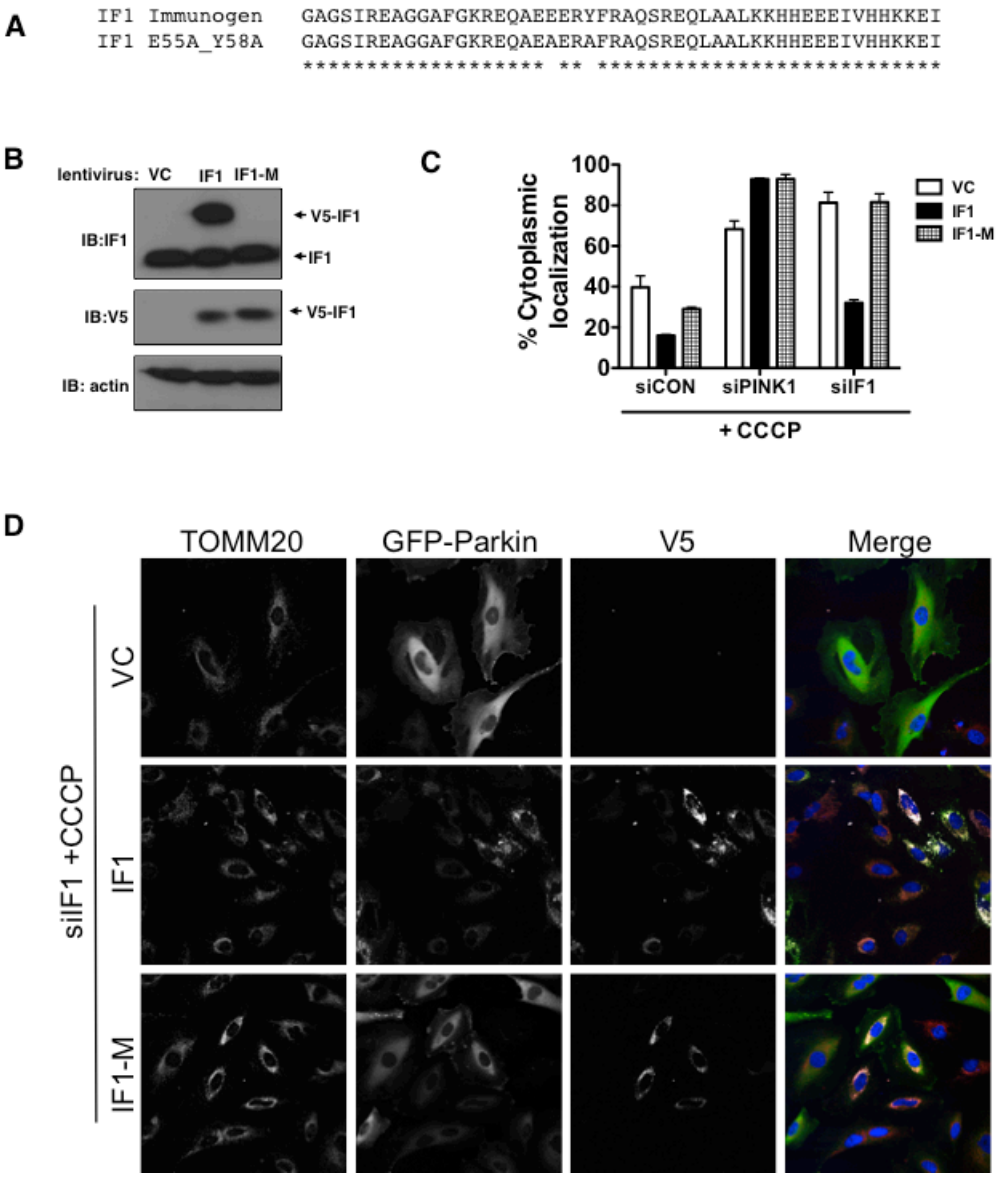

Figure 6- An E55A-Y58A mutant of IF1 is unable to rescue Parkin recruitment. (A) Alignment of the commercial IF1 antigen with the mutant cDNA sequence. (B) Western blot demonstrating equivalent expression of both WT siRNA resistant and mutant (IF1-M) siRNA resistant V5-tagged IF1 protein following 72 h expression by lentiviral infection in HeLa cells. A lentivirus expressing the empty vector was used as a control (VC). Membrane was probed with both IF1 antibody to show endogenous protein levels, and a V5 antibody to show mutant protein levels. Actin is shown as a loading control. (C-D) Expression of mutant IF1 is unable to rescue Parkin recruitment. HeLa cells were infected with AAV-GFP-Parkin and lentivirus expressing the empty vector (VC), WT IF1 (IF1), or mutant IF1 (IF1-M) following siRNA transfection. After 72h cells were treated with 5 μM CCCP for 1 h then fixed and stained. (C) Quantitation of % cytoplasmic Parkin. (D) Representative fluorescent images with GFP-Parkin in green, Hoechst in blue, TOMM20 in red, and V5 in white.

3.4 IF1 inhibits the F_1F_O-ATP synthase to allow loss of $\Delta\Psi_m$

Given that the interaction of IF1 with the F_1-ATPase is required for Parkin recruitment, we tested if the use of Oligomycin would also be able to rescue Parkin recruitment. Oligomycin inhibits both the forward and reverse reaction of the F_1F_O-ATP synthase mimicking the action of IF1 [194]. Indeed, we observed that in the presence of 2.5 μM Oligomycin, IF1 knockdown no longer prevented Parkin recruitment following mitochondrial depolarization by either CCCP or Antimycin A (Figure 7) [188]. These data provide further indication that the inhibition of the F_1F_O-ATP synthase by IF1 is required for Parkin recruitment.

Provided that IF1 inhibits the F_1F_O-ATP synthase from running in reverse to maintain a proton gradient across the inner mitochondrial membrane, we hypothesized that knockdown of IF1 prevented depolarization of mitochondria following CCCP treatment. This was confirmed using mitotracker red staining to identify mitochondria that maintained $\Delta\Psi_m$ (Figure 8a) [188]. In addition we were able to measure the dynamic loss of $\Delta\Psi_m$ with the potentiometric dye TMRE to show that IF1 can maintain higher levels of $\Delta\Psi_m$ relative to control following a 1 h treatment with either CCCP or Antimycin A (Figure 8b-c) [188]. Additionally, the maintenance of $\Delta\Psi_m$ was collapsed in the presence of Oligomycin (Figure 8 b-c). An issue associated with using these cationic dyes is that their loading can be sensitive to changes in potential across the plasma membrane ($\Delta\Psi_P$). Elevated $\Delta\Psi_P$ results in increased loading of dye into the cell, which in turn leads to an increase in signal [195]. To test whether IF1 KD was affecting dye loading, changes in $\Delta\Psi_P$ were measured using the anionic dye $DiBAC_4(3)$ [196]. A decrease in the intensity of $DiBAC_4(3)$ indicates an increase in $\Delta\Psi_P$ and vice versa.

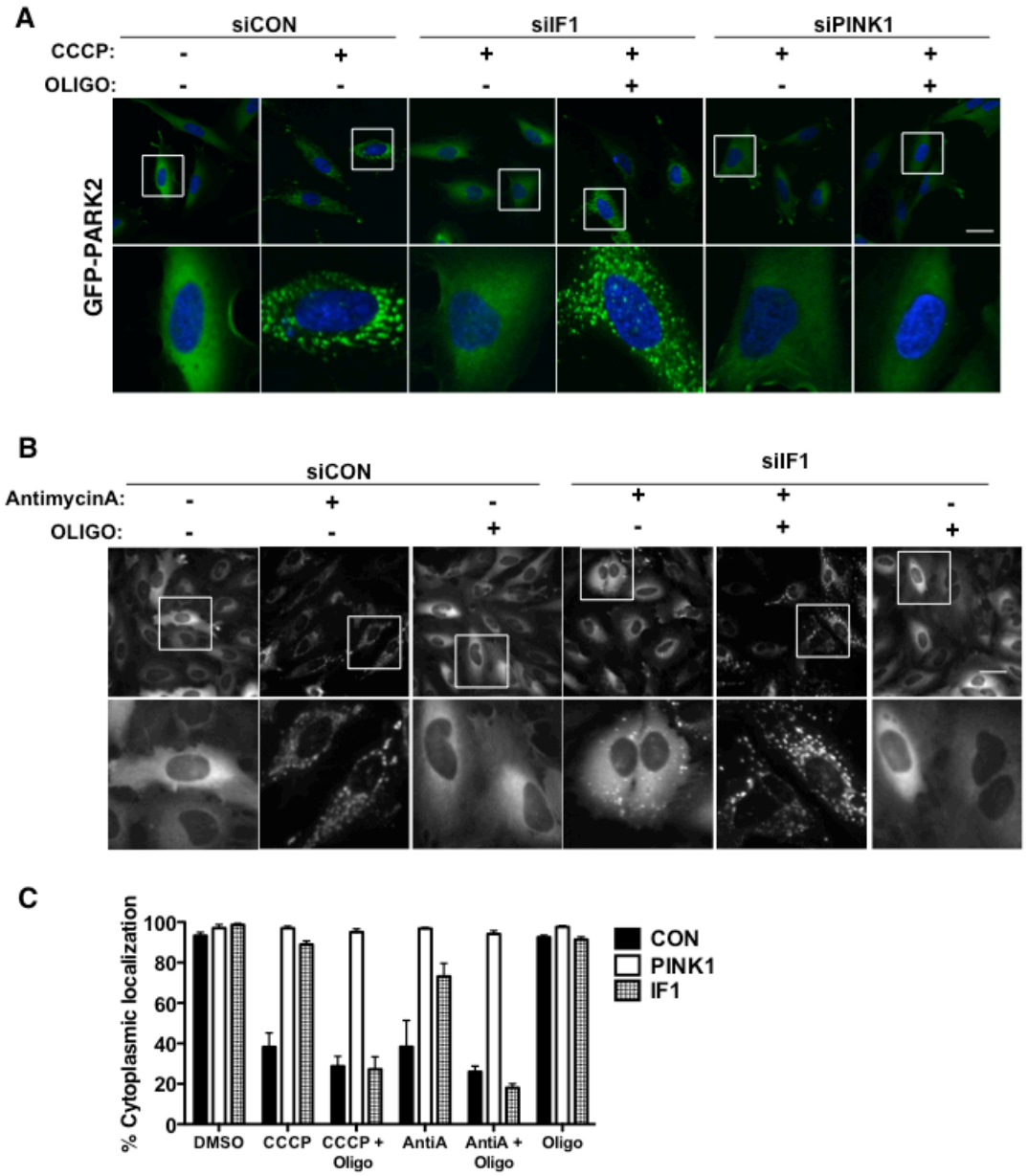

Figure 7- Oligomycin rescues Parkin recruitment in the context of IF1 knockdown. HeLa cells were transfected with siRNA and infected with AAV-GFP-Parkin 72 hrs prior to treatment, fixation, and staining with Hoechst and TOMM20. (A) Representative images of HeLa cells following treatment with either DMSO (-), 5μM CCCP, or CCCP and 2.5 μM Oligomycin for 1 h. Hoechst staining is shown in blue and GFP-Parkin in green. Scale bar = 50 μm. (B) Representative images of GFP-Parkin distribution in HeLa cells following treatment with either DMSO (-), 40 μM Antimycin A, or Antimycin A and 2.5 μM Oligomycin for 1 hr. Scale bar = 50 μm. (C) Quantitation of % Cytoplasmic GFP-Parkin localization.

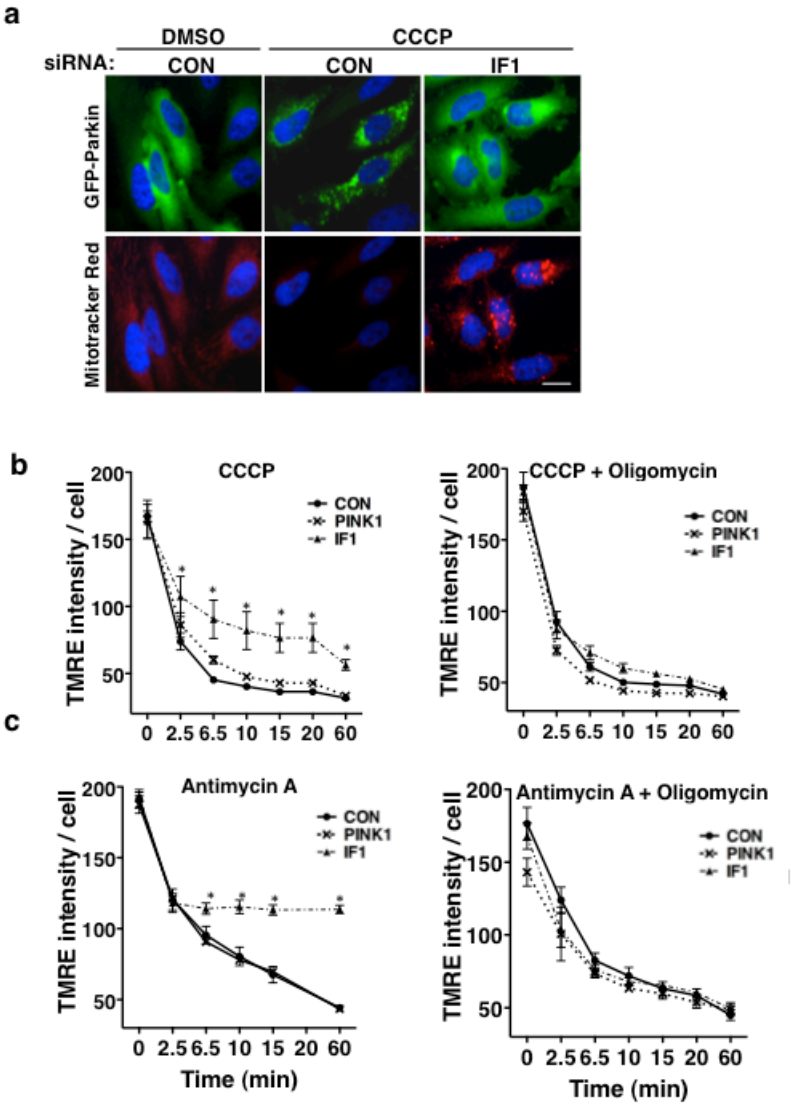

Figure 8- IF1 knockdown prevents loss of $\Delta\Psi_m$. (A) Fluorescent micrographs of Mitotracker Red staining and GFP-Parkin localization in HeLa cells following treatment with either DMSO or 5 µM CCCP. HeLa cells were transfected with either control or IF1 siRNA and infected with AAV-GFP-Parkin 72 h prior to CCCP treatment. Following a 1 h of treatment with either DMSO or CCCP, cells were loaded with 300 nM of Mitotracker red then fixed and imaged. Localization of GFP-Parkin is shown in green, Hoechst staining of nuclei in blue, and Mitotracker Red in red. Scale bar = 50 µm. (B-C) Graphical representation of the average amount of TMRE fluorescence measured per cell over time. Cells were transfected with siRNAs 72 h prior to loading with 40 nM TMRE and Hoechst. Images were taken at time 0 and then at corresponding time-points following addition of 5 µM CCCP, 40 µM Antimycin A, or co-treatment with 2.5 µM Oligomycin.

We observed no significant difference between cells with control siRNA or IF1 siRNA following treatment with DMSO or 5 μM CCCP however, treatment with 100 mM KCl resulted in an increase in $DiBAC_4(3)$ signal (Figure 9). This indicates that in the conditions where $\Delta\Psi_m$ were measured by TMRE or Mitotracker Red, changes in $\Delta\Psi_P$ were not a confounding factor in the results observed.

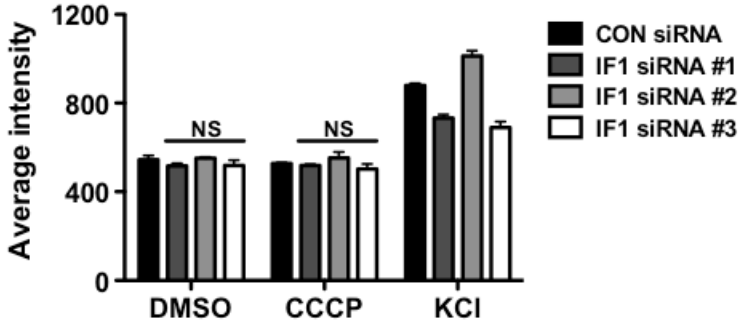

Figure 9- Knockdown of IF1 has no effect on potential across the plasma membrane. HeLa cells were subjected to 72 h siRNA knockdown prior to loading with 1 μM $DiBAC_4(3)$ and Hoechst. Intensity of $DiBAC_4(3)$ was measured following a 1 h treatment with DMSO or 5 μM CCCP as well as 30 min depolarization by 100 mM KCl.

Since $\Delta\Psi_m$ is maintained in cells lacking IF1, we hypothesized that IF1 functions upstream of PINK1. In the absence of IF1, $\Delta\Psi_m$ is no longer collapsed which we expect would allow PINK1 transport into mitochondria to continue unhindered where it can be cleaved by mitochondrial proteases and targeted for degradation [103]. This was confirmed by western blot analysis by demonstrating that in the absence of IF1, full length (63kD) PINK1 is no longer stabilized on the outer mitochondrial membrane following CCCP treatment. Addition of Oligomycin restored PINK1 stabilization in IF1 KD cells (Figure 10) [188].

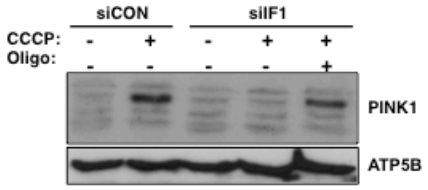

Figure 10- IF1 knockdown prevents the accumulation of full-length PINK1 protein. HeLa cells were subjected to a 1 hr treatment with DMSO (−), 5 μM CCCP (+), or 2.5 μM Oligomycin (+) following 72 h of siRNA knockdown with a control siRNA (siCON) or and IF1 siRNA (siIF1). Protein lysates were run on an SDS-PAGE gel then probed for PINK1 and ATP5B as a loading control.

3.5 IF1 prevents ATP consumption by the F_1-ATPase

To support the hypothesis that the ATP synthase is running freely in reverse in the absence of IF1, we looked at ATP levels in cells treated with CCCP and observed that ATP levels were significantly decreased in IF1 knockdown cells (Figure 11a). This bolstered the idea that ATP is being consumed by the ATP synthase to restore mitochondrial potential. In addition basal levels of ATP were marginally lower in both IF1 and PINK1 knockdown cells which was coupled to a decrease in O2 consumption (Figure 11). It has been previously observed that loss of PINK1 reduces O2 consumption due to a decrease in Ca^{2+} buffering [180, 181].

3.6 IF1 does not block ROS induced Parkin recruitment

Stimuli that contribute to Parkin recruitment result in the production of ROS. As such, we decided to look at how ROS production affected IF1 dependent Parkin recruitment. Treatment with CCCP and Antimycin A resulted in the production of superoxide as measured by an increase in DHE intensity(Figure 12a). Additionally this ROS could be quenched by pre-treatment with the antioxidant N-acetyl cysteine (NAC) (Figure 12b). Knockdown of IF1 had no significant of effect on ROS production

indicating that its effect was exerted solely on F_1F_o-ATPase, independent of ROS production.

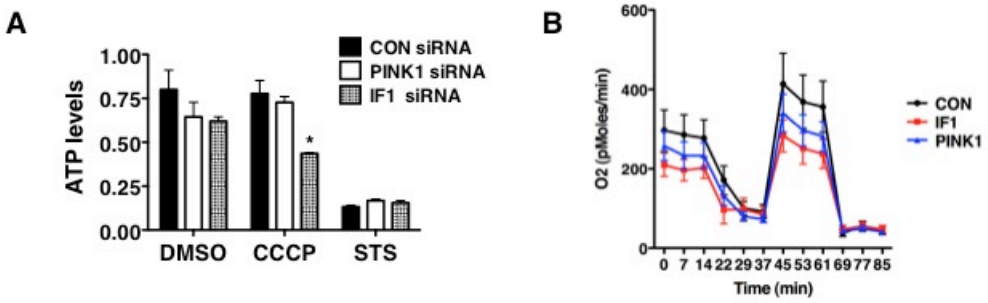

Figure 11- IF1 knockdown results in lower ATP levels and a decrease in oxygen consumption. (A) Measurement of ATP levels following treatment with DMSO or CCCP, STS treatment was used as a control. HeLa cells were subjected to 72 h of siRNA knockdown prior to treatment with DMSO, 5 µM CCCP, or 1 µM STS. (B) Measurement of O_2 consumption during a mitochondrial stress test. O_2 consumption from HeLa cells was measured basally (1-14 min), and following treatment with 2.5 µM Oligomycin (22-37 min), 2.5 µM FCCP (25-61 min), and 2.5 µM Antimycin A (69-85 min).

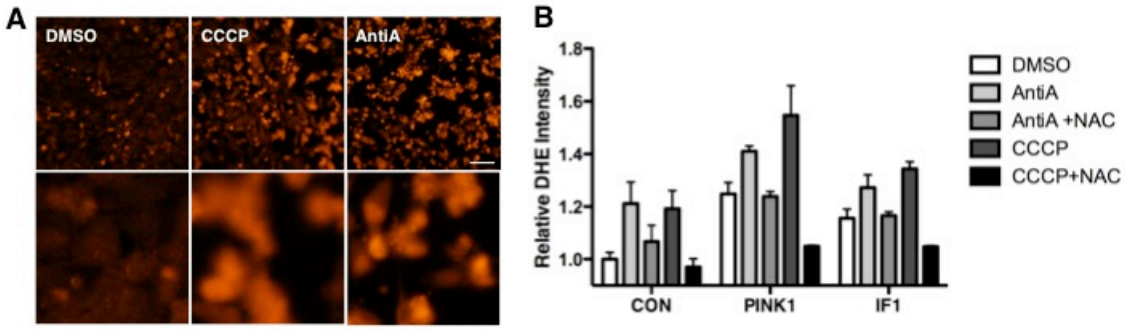

Figure 12- Treatment of cells with CCCP or Antimycin A generates ROS. HeLa cells were loaded with 20 µM DHE to detect superoxide production following treatment with DMSO, 5 µM CCCP, or 40 µM Antimycin A (AntiA). (A) Fluorescent micrographs showing DHE fluorescence following treatment. Lower panels are a 5X zoom of upper panels. (B) Quantitation of mean fluorescence intensity per cell. DHE intensity was measured in HeLa cells following 72 h of siRNA knockdown. 10 mM NAC was preloaded into cells for 1 h prior to treatment with CCCP or Antimycin A.

Pre-treatment with NAC not only reduced the accumulation of ROS, but it also prevented CCCP induced Parkin recruitment (Figure 13 a, b). Interestingly, this dose of NAC did not prevent Antimycin A induced Parkin recruitment. This suggests that loss of $\Delta\Psi_m$ by the protonophore CCCP on Parkin recruitment is propagated by ROS generation whereas loss of $\Delta\Psi_m$ by Antimycin A is exerted through deficiency of the ETC to transport protons across the IMM. Measurement of $\Delta\Psi_m$ by TMRE fluorescence revealed that NAC pre-treatment did indeed block loss of $\Delta\Psi_m$ following CCCP treatment to similar levels as those seen by IF1 KD (Figure 13c). This result was not affected by treatment with Oligomycin supporting the idea that IF1 does not prevent Parkin recruitment by modulating ROS.

ROS production following CCCP or Antimycin A treatment occurs as a byproduct of their effect on the ETC. The direct addition of ROS with treatment of H_2O_2 or Menadione was also sufficient to stimulate Parkin recruitment. This recruitment is blocked by PINK1 knockdown but not by IF1 knockdown (Figure 14). This likely reflects the fact that some forms of mitochondrial damage cannot be restored by the reversal of the ATP synthase. It is possible that in these circumstances damage to the ETC and the mitochondrial membrane is so severe that even provided an endless supply of ATP to pump ions back across the IMM, $\Delta\Psi_m$ still can not be restored. Indeed, treatment of HeLa cells with increasing doses of CCCP can also overwhelm the ability of IF1 to prevent Parkin recruitment (Figure 15).

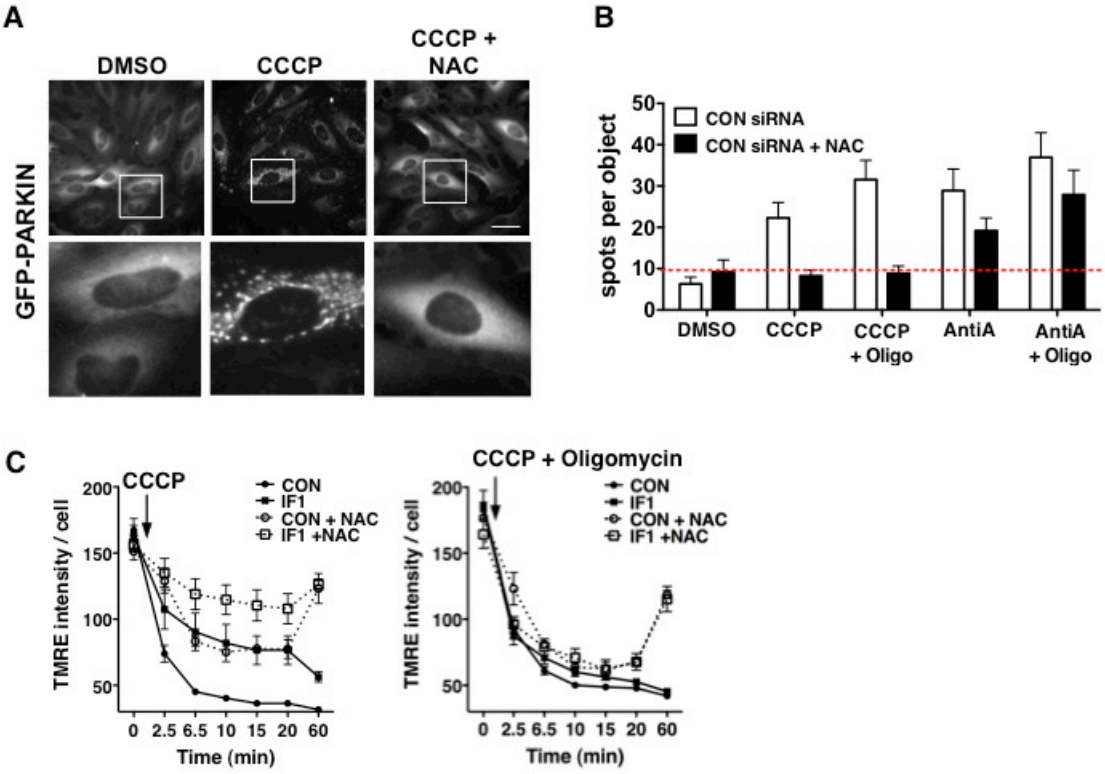

Figure 13- NAC but not loss of IF1 can modulate the response of Parkin to ROS. HeLa cells were pre-treated with 10 mM NAC for 1 h prior to treatment with DMSO, 5μM CCCP, or 40 μM Antimycin A (AntiA) (A) Fluorescent micrographs showing the distribution of GFP-Parkin in HeLa cells following treatment. Lower images are blown up insets from the white boxes above. (B) Quantification of the number of GFP-Parkin foci (spots per object) following treatment. (C) Measurement of TMRE intensity per cell in HeLa cells following 72 h of siRNA knockdown. TMRE intensity is shown following treatment with with CCCP alone (left) and CCCP with Oligomycin (right).

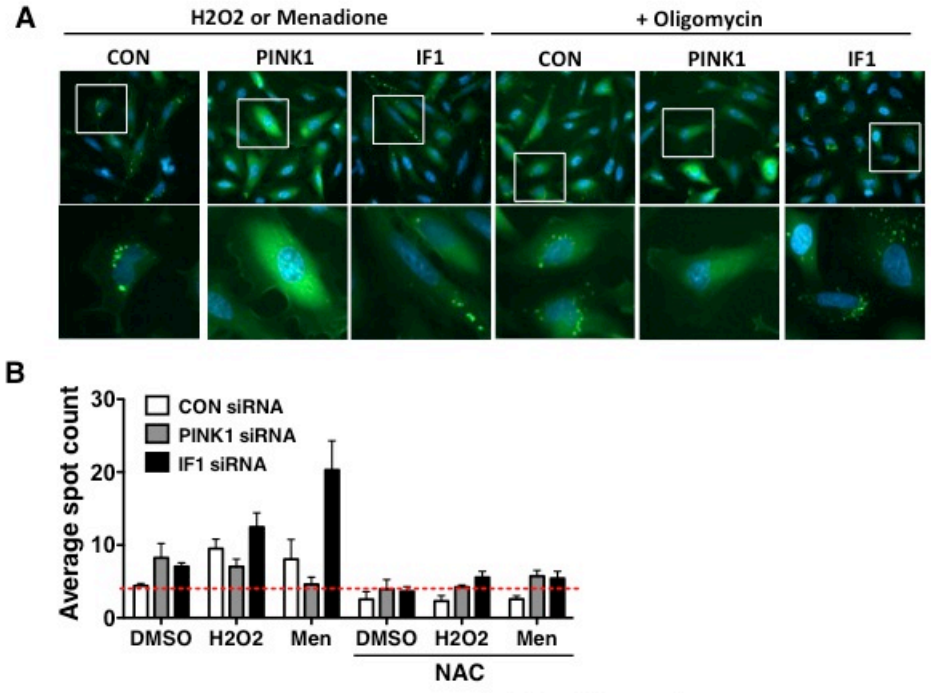

Figure 14- IF1 does not prevent Parkin recruitment in response to direct ROS. HeLa cells were treated for 3 h with either 50 μM H_2O_2 or 30 μM menadione following 72 h of siRNA knockdown. (A) Fluorescent micrographs of GFP-Parkin distribution following 3 h of treatment with H_2O_2 or Menadione +/- 2.5 μM Oligomycin. GFP-Parkin is shown in green and Hoechst staining of the nuclei in blue. (B) Quantitation of GFP-Parkin foci (Average spot count) following treatment with H_2O_2 or Menadione +/- and a 1 h pretreatment with 10 mM NAC.

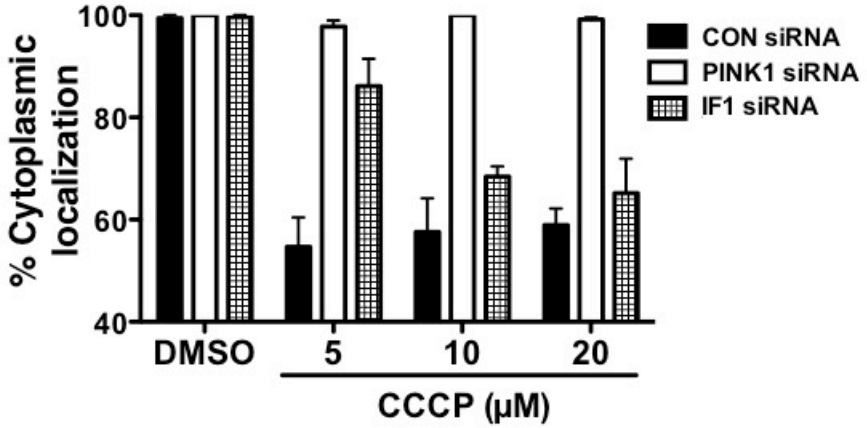

Figure 15- IF1 knockdown does not inhibit Parkin recruitment following treatment with higher doses of CCCP. HeLa cells were treated with 5, 10, or 20 μM CCCP for 1 h following 72 h of siRNA knockdown. Treatment with DMSO is shown as a vehicle control.

3.7 IF1 is downregulated to preserve damaged mitochondria

To test whether IF1 was differentially regulated in PD cell-types we examined the expression of IF1 in a variety of tissue types from mice. It has been shown that IF1 expression levels are higher in oxidative cells than glycolytic cells [197] so we were not surprised to see elevated levels of IF1 in murine brain tissue and neurons relative to levels of the β-subunit of the ATP synthase (Figure 16).

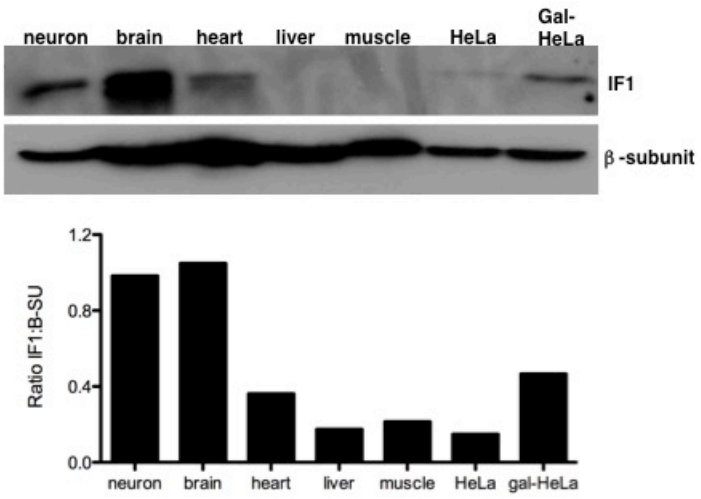

Figure 16- Expression levels of IF1 differ between oxidative and glycolytic cell types. Western blot of a variety of mouse tissue types as well as HeLa cells cultured in both regular medium and in galactose medium (Gal-HeLa). 40 μg of protein was loaded per lane as normalized by BCA assay. Membrane was probed for IF1 and for the β-subunit of that ATP synthase as a control. Quantitation of IF1 protein levels relative to the β-subunit by densitometry is shown below.

Parkin has been demonstrated to protect mtDNA integrity through mitophagy [131]. It is possible that cells with extremely impaired mitochondria will lower IF1 protein levels to help preserve their mitochondria for use in processes other than energy production. Thus, whether IF1 plays a role in the selection of healthy versus diseased mtDNA was of interest. To examine whether IF1 expression is regulated in response to mitochondrial dysfunction we examined IF1 protein and message levels in

a panel of different mitochondrial dysfunction patient cell lines. IF1 levels were variable, however there was no consistent correlation with disease state (Appendix III, with Qiujiang Du and Mirna Nascimento). Interestingly, the protein levels of IF1 in Rho0 cells (Figure 17a,b) [188] were markedly decreased, relative to the parental 143B cell line.

Rho0 cells are devoid of any mtDNA, and thus are incapable of maintaining $\Delta\Psi_m$ through classical pumping of protons (H^+) by the electron transport chain. In order to maintain mitochondrial function (protein import, Ca^{2+} buffering, iron metabolism, etc.), Rho0 cells maintain potential via the reverse reaction of the ATP synthase [198-200]. It is logical that these cells have repressed IF1 expression to allow the ATPase to run freely in reverse to maintain $\Delta\Psi_m$. Indeed, overexpression of a V5-tagged IF1 in Rho0 cells resulted in a dramatic reduction in $\Delta\Psi_m$ (Figure 17c) [188], as well as recruitment of GFP:Parkin to mitochondria under basal conditions (Figure 17d, e) [188]. Importantly, the effect measured on $\Delta\Psi_m$ was independent of mitochondrial mass (Figure 18). Western blot analysis confirmed an increase in full-length (activated) PINK1 in Rho0 cells overexpressing IF1 (Figure 17f) [188], confirming that the decrease in $\Delta\Psi_m$ was sufficient to induce Parkin recruitment and mitophagy. Additionally, overexpression of mutant IF1 in Rho0 cells failed to decrease $\Delta\Psi_m$ or induce Parkin recruitment to mitochondria (Figure 17a, e).

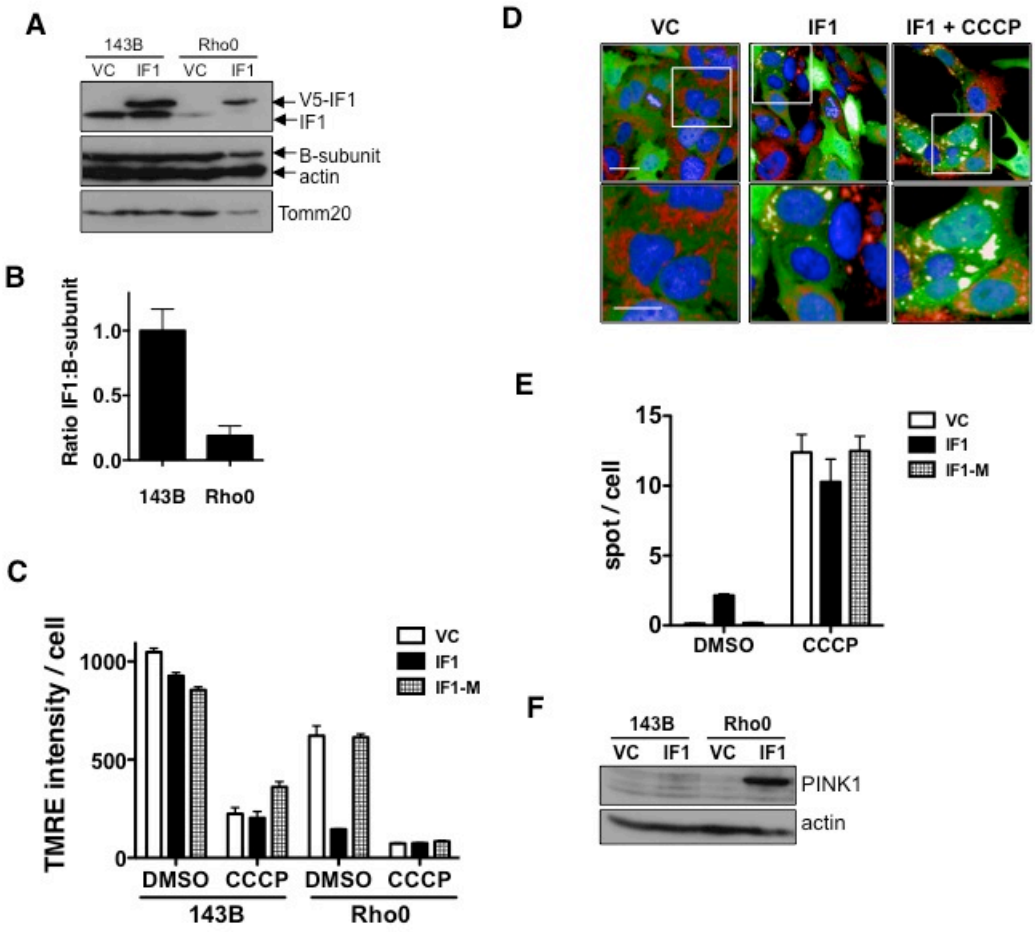

Figure 17- IF1 overexpression in Rho0 cells induces Parkin recruitment. (A) Western blot showing endogenous (VC) and overexpressed (IF1) levels of IF1 protein in 143B control and Rho0 cells following overexpression of V5-tagged IF1 by lentiviral infection. Protein lysates were collected following 72 h of infection. The β-subunit of the ATP synthase, actin, and TOMM20 are shown as loading controls. (B) Histogram showing the ratio of IF1 protein relative to the F_1F_o-ATP synthase β1 subunit measured by densitometry. Data are mean ± SD of 4 individual samples. (C) TMRE staining intensity in 143B control and Rho0 cells infected with control (VC), V5-IF1 (IF1), or mutant IF1 (IF1-M) lentivirus. Effect of treatment with DMSO vehicle control and 10 μM CCCP is shown. Data are mean ±SD of 3 independent experiments. (D) Fluorescence micrographs of GFP-Parkin in Rho0 cells infected with control (VC) or V5-IF1 (IF1) lentivirus, treated with DMSO or 5 μM CCCP. Scale bar = 50 μm (top) and 125 μm (bottom). (E) Histogram showing GFP-Parkin spots on mitochondria in 143B and Rho0 cells infected with control (VC), V5-IF1 (IF1), or mutant V5-IF1 (IF1-M) lentivirus as determined by imaging analysis using Columbus software. Data are mean ± SD of 3 independent experiments. (F) Western blot showing level of PINK1 in control (VC) or V5-IF1 infected 143B and Rho0 cells. Actin is shown as a loading control.

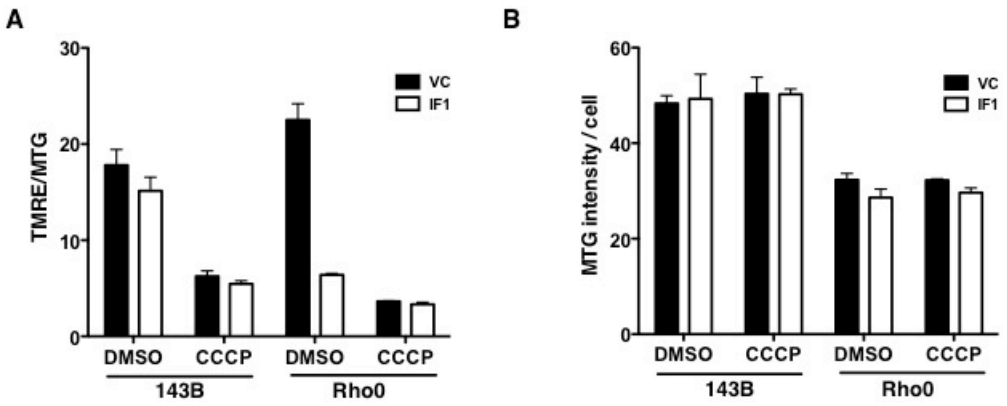

Figure 18- Mitochondrial potential in Rho0 cells with restored IF1 expression is unaffected by mitochondrial mass. 143B and 143B Rho0 cells were infected with control (VC) or IF1-V5 (IF1) lentivirus 72 h prior to preloading with TMRE, Mitotracker green (MTG), and Hoechst followed by a 1 hour treatment with 5 μM CCCP. (a) TMRE intensity is plotted relative to MTG (b) Histogram showing MTG intensity/cell.

We were interested by the observation that the decrease in IF1 protein levels in Rho0 cells was not accompanied by a decrease in IF1 mRNA levels (Figure 19a). We treated cells with the proteasomal inhibitor MG132 to see if IF1 was being turned over by proteasomal degradation. A 6 h treatment with 10 μM MG132 did not have any effect of the accumulation of endogenous (Figure 18b) or overexpressed (Figure 18c) IF1. This suggested that IF1 levels were not regulated through the ubiquitin machinery. Whether IF1 expression is regulated via a mitochondrial protease, or at the translational level has not been tested.

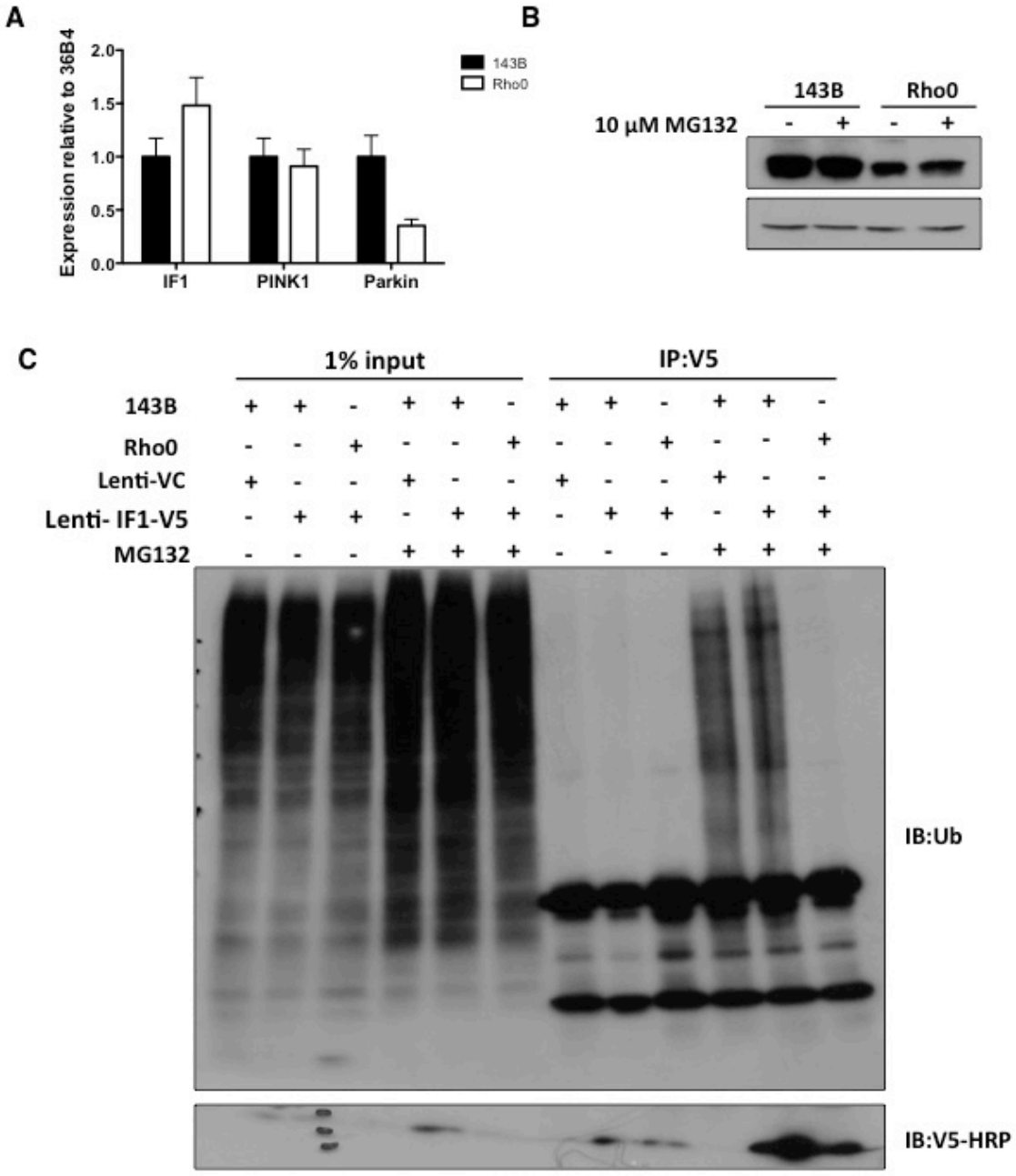

Figure 19- IF1 protein levels in Rho0 cells are not regulated at the transcriptional level or through proteasomal degradation. (A) qPCR analysis of IF1, PINK1, and Parkin levels in 143B control cells and Rho0 cells. Expression levels are relative to 36B4. (B) Levels of IF1 protein in 143B control and Rho0 cell lines following 6 h treatment with 10 μM MG132. (C) Ubiquitin western blot of immunoprecipitated V5 from 143B and Rho0 cell extracts infected with control (VC) or IF1-V5 lentivirus. 1% of the input was loaded as a control.

Chapter 4 – Discussion

4.1 IF1 is required for the recruitment of Parkin to damaged mitochondria

This work exemplifies the power of a genome-wide siRNA screen to identify new molecular players in mitophagy. siRNA knockdown of IF1 in HeLa cells effectively blocked the recruitment of GFP-Parkin to the mitochondria following depolarization with the chemical uncoupler CCCP. A caveat associated with RNAi screens is the off-target effects that occur (reviewed in [201]). As such, rigorous validations methods must be employed to ensure the results observed are caused by knockdown of the target gene. Secondary validation was performed using the unpooled siRNA to reveal that three out of four siRNAs against IF1 blocked Parkin recruitment. In addition we used an alternative RNAi technique and saw the same results using shRNA. The gold standard when it comes to siRNA validation is to perform genetic rescue using cDNA mutated such that RNAi cannot bind to it. Introduction of an siRNA resistant IF1 cDNA restored Parkin recruitment whereas an siRNA resistant IF1 mutant could not. The combination of these validation techniques eradicated any concern that the initial result observed in the genome-wide siRNA screen was due to off-target effects.

4.2 IF1 is required for loss of $\Delta\Psi_m$

Loss of $\Delta\Psi_m$ is recognized as the trigger for Parkin recruitment and subsequent mitophagy. When mitochondria lose potential they lose the ability to import mitochondrially-targeted proteins through the inner membrane transporter complexes [202]. Such is the case for PINK1 which gets stuck in the OMM following mitochondrial depolarization leaving the active kinase domain facing the cytoplasm where it can initiate Parkin recruitment to mitochondria [103]. Given the role of IF1 as an inhibitor

of the reverse reaction of the ATP synthase [189, 190], we hypothesized it would prevent the depolarization of mitochondria following a mitochondrial insult thus preventing the stabilization of PINK1 on the OMM. Indeed loss of $\Delta\Psi_m$ was prevented in HeLa cells in response to treatment with CCCP or Antimycin A following IF1 knockdown. In addition we identified an absence of full-length PINK1 accumulation in IF1 KD cells placing IF1 upstream of PINK1 in mitophagy (Figure 20) [188].

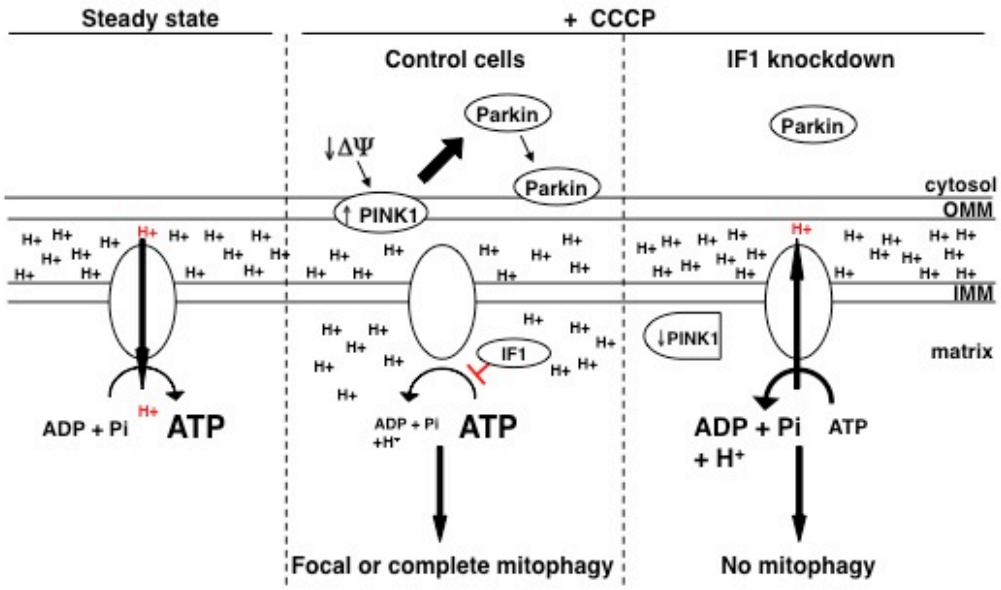

Figure 20- Mechanistic role of IF1 in the PINK1/Parkin mitophagy pathway. Under steady-state conditions, the ATP synthase runs uninhibited, coupling the electrochemical energy from protons pumped across the IMM by the ETC to oxidative phosphorylation of ADP generating ATP. Depolarization of mitochondria and the dissipation of protons results in the activation of IF1 to inhibit the reverse reaction of the ATP synthase, and the consumption of ATP. This protective mechanism allows for loss of $\Delta\Psi_m$. Loss of $\Delta\Psi_m$ results in the activation of PINK1 on the OMM and subsequent relocalization of Parkin to mitochondria to initiate mitophagy. Knockdown of IF1 protein levels allows the ATPase to run freely in reverse in the presence of a chemical uncoupler or mitochondrial stressor, preventing loss of potential across the IMM and the activation of PINK1, thus preventing the mitophagy pathway from eliminating defective mitochondria.

These data reveal a novel function of IF1 in the regulation of Parkin-mediated mitophagy that was not previously appreciated. They highlight the importance of the

dissipation of $\Delta\Psi_m$ in triggering mitophagy. There is some debate as to whether ROS is the initial trigger for mitophagy. Treatment with Antimycin A and CCCP result in the production of superoxide in addition to loss of membrane potential. Interestingly, pre-treatment with the antioxidant NAC could prevent this loss of membrane potential. It is likely that a positive feed-back loop occurs where ROS accumulation impairs function of ETC resulting in reduced $\Delta\Psi_m$ while impaired transport of protons across the ETC results in increased ROS.

Treatment of cells with direct ROS using either H_2O_2 or Menadione resulted in the accumulation of Parkin to foci of mitochondria within the cell. Since this treatment resulted in cytoplasmic ROS as opposed to mitochondrially derived ROS, it is possible that these foci of Parkin recruitment indicate subsets of the mitochondrial population that had lost $\Delta\Psi_m$ due to damage. Whether prolonged treatment with H_2O_2 or Menadione would result in increased Parkin recruitment was not verified. Knockdown of IF1 was unable to completely block Parkin recruitment to cells treated with H_2O_2 or Menadione. It is likely that the damage induced was too great for $\Delta\Psi_m$ to be restored by the ATPase activity of the F_1F_o-ATP synthase. Similar observations were observed using increasing concentrations of CCCP suggesting that in these cases, the rate of loss of $\Delta\Psi_m$ is greater than the rate at which the ATPase could restore it, or that ROS accumulation induced damage to the F_1F_o-ATP synthase machinery rendering its ATPase function inutile.

4.3 IF1 levels are regulated to maintain mitochondrial function

IF1 expression is notably higher in oxidative cell lines indicating an advantage in preventing cells from depleting ATP when electron transport is compromised [203]. We

wondered whether IF1 levels might be modulated in patients with mitochondrial myopathy in response to increased mitochondrial dysfunction. It has been demonstrated by Suen *et* al that Parkin overexpression can protect against mtDNA defects in cybrid cell lines suggesting that mitophagy can serve to protect against the propagation of mitochondrial myopathies [103]. We found that Rho0 cells, which lack mtDNA, had surprisingly low levels of IF1 suggesting that IF1 downregulation served as a protective mechanism against mitophagy [198-200]. Indeed, Rho0 cells are dependent on the reversal of the F_1F_o-ATP synthase in order to maintain membrane potential and mitochondrial functions such as protein import and iron metabolism.

These data suggest that IF1 may be downregulated in certain cases of mitochondrial disease, and that IF1 overexpression may serve to eliminate the dysfunctional population of mitochondria. Overexpression of IF1 in Rho0 cells resulted in loss of $\Delta\Psi_m$ and recruitment of Parkin to mitochondria, in the absence of any other pharmacological stimulus. This supports our conclusion that IF1 is required for the initiation of PINK1/Parkin mediated mitophagy and that its expression levels can be modulated to preserve or eliminate mitochondria.

How IF1 protein levels are regulated are not known. Our study did not detect a decrease in IF1 transcript levels by qPCR, nor did IF1 protein levels appear to be modulated by the proteasomal degradation pathway. We suspect that IF1 is regulated at the translational level, however experiments supporting this hypothesis have not been performed. Interestingly, loss of IF1 protein is presented in Luft's disease, an extremely rare form of mitochondrial myopathy in which patients suffer from extremely high ATPase rates [204, 205]. No mutations in the ATPIF1 gene have been

detected in the two known cases of the disease so the cause of IF1 protein downregulation is unknown. It would be interesting to see if a common pathway is involved in the suppression of IF1 levels in both Luft's disease and Rho0 cells.

4.4 IF1 in PD

It is important to gain an understanding of how mitochondrial integrity is maintained in neurons in order to transfer this knowledge to the treatment of PD. Many of the observations about the PINK1/Parkin mitophagy pathway have been made in cell lines using pharmacological agents to induce mitochondrial depolarization. These methods do not lend well to the study of mitophagy in a PD relevant models because neurons are not capable of coping with harsh metabolic insults due to their inability to switch to glycolytic metabolism. The current evidence for Parkin recruitment and mitophagy in neurons is dependent on the use of apoptotic inhibitors, very long treatment times, or manipulation of the media [125, 128, 129]. These techniques result in significant stress to the cell and likely activate other stress-related pathways making it difficult to interpret these observations. Nevertheless, it would be important to examine the impact of IF1 on mitochondrial quality control in neurons and in PD patients.

Whether IF1 levels are altered in PD patients is unknown and no GWAS studies have identified mutation of IF1 in PD or any other disease. Examining the modulation of IF1 in PD would be extremely interesting. It is possible that overexpression of IF1 could help to delay the progression of the disease by increasing clearance of damaged mitochondria. Conversely, the effect of tissue specific or IF1 knockout on neuronal function would provide additional information on the importance of IF1 in

mitochondrial quality control. In relation to this, understanding whether the downregulation of IF1 is pathogenic or protective would be instrumental in relationship to any disease association.

4.5 Concluding remarks and future directions

In this study we identify IF1 as a novel member of the PINK1/Parkin mitophagy pathway. These results implicate loss of $\Delta\Psi_m$ as a critical step in the recruitment of Parkin to damaged mitochondria. Additionally, we observed that IF1 protein levels can be modulated to protect mitochondria from elimination in Rho0 cells. This, coupled with the dramatic increase in IF1 levels in neurons, suggests that IF1 plays an important role in the maintenance of healthy mitochondria. Future work should evaluate the mechanism by which levels of IF1 are regulated and if they are affected in PD. It would be intriguing to determine whether upregulation of IF1 could serve to protect cells from mitochondrial stress through increased mitophagy.

Chapter 5 – References

1. Jankovic, J., *Parkinson's disease and movement disorders: moving forward.* Lancet Neurol, 2008. **7**(1): p. 9-11.
2. Gallagher, D.A., A.J. Lees, and A. Schrag, *What are the most important nonmotor symptoms in patients with Parkinson's disease and are we missing them?* Mov Disord, 2010. **25**(15): p. 2493-500.
3. Park, A. and M. Stacy, *Non-motor symptoms in Parkinson's disease.* J Neurol, 2009. **256 Suppl 3**: p. 293-8.
4. Davie, C.A., *A review of Parkinson's disease.* Br Med Bull, 2008. **86**: p. 109-27.
5. Nussbaum, R.L. and C.E. Ellis, *Alzheimer's disease and Parkinson's disease.* N Engl J Med, 2003. **348**(14): p. 1356-64.
6. Hindle, J.V., *Ageing, neurodegeneration and Parkinson's disease.* Age Ageing, 2010. **39**(2): p. 156-61.
7. Langston, J.W. and P.A. Ballard, Jr., *Parkinson's disease in a chemist working with 1-methyl-4-phenyl-1,2,5,6-tetrahydropyridine.* N Engl J Med, 1983. **309**(5): p. 310.
8. Langston, J.W., et al., *Chronic Parkinsonism in humans due to a product of meperidine-analog synthesis.* Science, 1983. **219**(4587): p. 979-80.
9. Uversky, V.N., *Neurotoxicant-induced animal models of Parkinson's disease: understanding the role of rotenone, maneb and paraquat in neurodegeneration.* Cell Tissue Res, 2004. **318**(1): p. 225-41.
10. Wirdefeldt, K., et al., *Epidemiology and etiology of Parkinson's disease: a review of the evidence.* Eur J Epidemiol, 2011. **26 Suppl 1**: p. S1-58.
11. Goldman, S.M., et al., *Solvent exposures and Parkinson disease risk in twins.* Ann Neurol, 2012. **71**(6): p. 776-84.
12. Antony, P.M., et al., *The hallmarks of Parkinson's disease.* FEBS J, 2013.
13. Klein, C. and A. Westenberger, *Genetics of Parkinson's disease.* Cold Spring Harb Perspect Med, 2012. **2**(1): p. a008888.
14. Polymeropoulos, M.H., et al., *Mutation in the alpha-synuclein gene identified in families with Parkinson's disease.* Science, 1997. **276**(5321): p. 2045-7.
15. Paisan-Ruiz, C., et al., *Cloning of the gene containing mutations that cause PARK8-linked Parkinson's disease.* Neuron, 2004. **44**(4): p. 595-600.
16. Valente, E.M., et al., *Hereditary early-onset Parkinson's disease caused by mutations in PINK1.* Science, 2004. **304**(5674): p. 1158-60.
17. Kitada, T., et al., *Mutations in the parkin gene cause autosomal recessive juvenile parkinsonism.* Nature, 1998. **392**(6676): p. 605-8.
18. Bonifati, V., et al., *Mutations in the DJ-1 gene associated with autosomal recessive early-onset parkinsonism.* Science, 2003. **299**(5604): p. 256-9.
19. Ramirez, A., et al., *Hereditary parkinsonism with dementia is caused by mutations in ATP13A2, encoding a lysosomal type 5 P-type ATPase.* Nat Genet, 2006. **38**(10): p. 1184-91.
20. Turrens, J.F., *Mitochondrial formation of reactive oxygen species.* J Physiol, 2003. **552**(Pt 2): p. 335-44.
21. Balaban, R.S., S. Nemoto, and T. Finkel, *Mitochondria, oxidants, and aging.* Cell, 2005. **120**(4): p. 483-95.

22. Bereiter-Hahn, J. and M. Voth, *Dynamics of mitochondria in living cells: shape changes, dislocations, fusion, and fission of mitochondria.* Microsc Res Tech, 1994. **27**(3): p. 198-219.
23. Westermann, B., *Mitochondrial fusion and fission in cell life and death.* Nat Rev Mol Cell Biol, 2010. **11**(12): p. 872-84.
24. Smirnova, E., et al., *A human dynamin-related protein controls the distribution of mitochondria.* J Cell Biol, 1998. **143**(2): p. 351-8.
25. Smirnova, E., et al., *Dynamin-related protein Drp1 is required for mitochondrial division in mammalian cells.* Mol Biol Cell, 2001. **12**(8): p. 2245-56.
26. James, D.I., et al., *hFis1, a novel component of the mammalian mitochondrial fission machinery.* J Biol Chem, 2003. **278**(38): p. 36373-9.
27. Yoon, Y., et al., *The mitochondrial protein hFis1 regulates mitochondrial fission in mammalian cells through an interaction with the dynamin-like protein DLP1.* Mol Cell Biol, 2003. **23**(15): p. 5409-20.
28. Gandre-Babbe, S. and A.M. van der Bliek, *The novel tail-anchored membrane protein Mff controls mitochondrial and peroxisomal fission in mammalian cells.* Mol Biol Cell, 2008. **19**(6): p. 2402-12.
29. Ingerman, E., et al., *Dnm1 forms spirals that are structurally tailored to fit mitochondria.* J Cell Biol, 2005. **170**(7): p. 1021-7.
30. Roux, A., et al., *GTP-dependent twisting of dynamin implicates constriction and tension in membrane fission.* Nature, 2006. **441**(7092): p. 528-31.
31. Santel, A. and M.T. Fuller, *Control of mitochondrial morphology by a human mitofusin.* J Cell Sci, 2001. **114**(Pt 5): p. 867-74.
32. Koshiba, T., et al., *Structural basis of mitochondrial tethering by mitofusin complexes.* Science, 2004. **305**(5685): p. 858-62.
33. Cipolat, S., et al., *OPA1 requires mitofusin 1 to promote mitochondrial fusion.* Proc Natl Acad Sci U S A, 2004. **101**(45): p. 15927-32.
34. McQuibban, G.A., S. Saurya, and M. Freeman, *Mitochondrial membrane remodelling regulated by a conserved rhomboid protease.* Nature, 2003. **423**(6939): p. 537-41.
35. Cipolat, S., et al., *Mitochondrial rhomboid PARL regulates cytochrome c release during apoptosis via OPA1-dependent cristae remodeling.* Cell, 2006. **126**(1): p. 163-75.
36. Ishihara, N., et al., *Regulation of mitochondrial morphology through proteolytic cleavage of OPA1.* EMBO J, 2006. **25**(13): p. 2966-77.
37. Head, B., et al., *Inducible proteolytic inactivation of OPA1 mediated by the OMA1 protease in mammalian cells.* J Cell Biol, 2009. **187**(7): p. 959-66.
38. Griparic, L., T. Kanazawa, and A.M. van der Bliek, *Regulation of the mitochondrial dynamin-like protein Opa1 by proteolytic cleavage.* J Cell Biol, 2007. **178**(5): p. 757-64.
39. Ehses, S., et al., *Regulation of OPA1 processing and mitochondrial fusion by m-AAA protease isoenzymes and OMA1.* J Cell Biol, 2009. **187**(7): p. 1023-36.
40. Frezza, C., et al., *OPA1 controls apoptotic cristae remodeling independently from mitochondrial fusion.* Cell, 2006. **126**(1): p. 177-89.

41. Song, Z., et al., *OPA1 processing controls mitochondrial fusion and is regulated by mRNA splicing, membrane potential, and Yme1L.* J Cell Biol, 2007. **178**(5): p. 749-55.
42. DeVay, R.M., et al., *Coassembly of Mgm1 isoforms requires cardiolipin and mediates mitochondrial inner membrane fusion.* J Cell Biol, 2009. **186**(6): p. 793-803.
43. Wong, E.D., et al., *The dynamin-related GTPase, Mgm1p, is an intermembrane space protein required for maintenance of fusion competent mitochondria.* J Cell Biol, 2000. **151**(2): p. 341-52.
44. Chen, H., et al., *Mitofusins Mfn1 and Mfn2 coordinately regulate mitochondrial fusion and are essential for embryonic development.* J Cell Biol, 2003. **160**(2): p. 189-200.
45. Chen, X.J. and R.A. Butow, *The organization and inheritance of the mitochondrial genome.* Nat Rev Genet, 2005. **6**(11): p. 815-25.
46. Nakada, K., et al., *Inter-mitochondrial complementation: Mitochondria-specific system preventing mice from expression of disease phenotypes by mutant mtDNA.* Nat Med, 2001. **7**(8): p. 934-40.
47. Chen, H., et al., *Mitochondrial fusion is required for mtDNA stability in skeletal muscle and tolerance of mtDNA mutations.* Cell, 2010. **141**(2): p. 280-9.
48. Twig, G., et al., *Fission and selective fusion govern mitochondrial segregation and elimination by autophagy.* Embo J, 2008. **27**(2): p. 433-46.
49. Li, Z., et al., *The importance of dendritic mitochondria in the morphogenesis and plasticity of spines and synapses.* Cell, 2004. **119**(6): p. 873-87.
50. Chinta, S.J. and J.K. Andersen, *Redox imbalance in Parkinson's disease.* Biochim Biophys Acta, 2008. **1780**(11): p. 1362-7.
51. Richter, C., J.W. Park, and B.N. Ames, *Normal oxidative damage to mitochondrial and nuclear DNA is extensive.* Proc Natl Acad Sci U S A, 1988. **85**(17): p. 6465-7.
52. Trimmer, P.A., et al., *Abnormal mitochondrial morphology in sporadic Parkinson's and Alzheimer's disease cybrid cell lines.* Exp Neurol, 2000. **162**(1): p. 37-50.
53. Barsoum, M.J., et al., *Nitric oxide-induced mitochondrial fission is regulated by dynamin-related GTPases in neurons.* EMBO J, 2006. **25**(16): p. 3900-11.
54. Benard, G., et al., *Mitochondrial bioenergetics and structural network organization.* J Cell Sci, 2007. **120**(Pt 5): p. 838-48.
55. Exner, N., et al., *Loss-of-function of human PINK1 results in mitochondrial pathology and can be rescued by parkin.* J Neurosci, 2007. **27**(45): p. 12413-8.
56. Greene, J.C., et al., *Mitochondrial pathology and apoptotic muscle degeneration in Drosophila parkin mutants.* Proc Natl Acad Sci U S A, 2003. **100**(7): p. 4078-83.
57. Irrcher, I., et al., *Loss of the Parkinson's disease-linked gene DJ-1 perturbs mitochondrial dynamics.* Hum Mol Genet, 2010. **19**(19): p. 3734-46.
58. Wang, X., et al., *LRRK2 regulates mitochondrial dynamics and function through direct interaction with DLP1.* Hum Mol Genet, 2012. **21**(9): p. 1931-44.
59. de Brito, O.M. and L. Scorrano, *Mitofusin 2 tethers endoplasmic reticulum to mitochondria.* Nature, 2008. **456**(7222): p. 605-10.
60. Friedman, J.R., et al., *ER tubules mark sites of mitochondrial division.* Science, 2011. **334**(6054): p. 358-62.

61. Rizzuto, R., M.R. Duchen, and T. Pozzan, *Flirting in little space: the ER/mitochondria Ca2+ liaison.* Sci STKE, 2004. **2004**(215): p. re1.
62. Rizzuto, R., et al., *Close contacts with the endoplasmic reticulum as determinants of mitochondrial Ca2+ responses.* Science, 1998. **280**(5370): p. 1763-6.
63. Szabadkai, G., et al., *Chaperone-mediated coupling of endoplasmic reticulum and mitochondrial Ca2+ channels.* J Cell Biol, 2006. **175**(6): p. 901-11.
64. Baughman, J.M., et al., *Integrative genomics identifies MCU as an essential component of the mitochondrial calcium uniporter.* Nature, 2011. **476**(7360): p. 341-5.
65. Glater, E.E., et al., *Axonal transport of mitochondria requires milton to recruit kinesin heavy chain and is light chain independent.* J Cell Biol, 2006. **173**(4): p. 545-57.
66. Kornmann, B., C. Osman, and P. Walter, *The conserved GTPase Gem1 regulates endoplasmic reticulum-mitochondria connections.* Proc Natl Acad Sci U S A, 2011. **108**(34): p. 14151-6.
67. Saotome, M., et al., *Bidirectional Ca2+-dependent control of mitochondrial dynamics by the Miro GTPase.* Proc Natl Acad Sci U S A, 2008. **105**(52): p. 20728-33.
68. Berridge, M.J., *The endoplasmic reticulum: a multifunctional signaling organelle.* Cell Calcium, 2002. **32**(5-6): p. 235-49.
69. Scorrano, L., et al., *BAX and BAK regulation of endoplasmic reticulum Ca2+: a control point for apoptosis.* Science, 2003. **300**(5616): p. 135-9.
70. Hamasaki, M., et al., *Autophagosomes form at ER-mitochondria contact sites.* Nature, 2013. **495**(7441): p. 389-93.
71. Hailey, D.W., et al., *Mitochondria supply membranes for autophagosome biogenesis during starvation.* Cell, 2010. **141**(4): p. 656-67.
72. Schon, E.A. and E. Area-Gomez, *Mitochondria-associated ER membranes in Alzheimer disease.* Mol Cell Neurosci, 2013. **55**: p. 26-36.
73. Cali, T., et al., *alpha-Synuclein controls mitochondrial calcium homeostasis by enhancing endoplasmic reticulum-mitochondria interactions.* J Biol Chem, 2012. **287**(22): p. 17914-29.
74. Cali, T., et al., *Enhanced parkin levels favor ER-mitochondria crosstalk and guarantee Ca(2+) transfer to sustain cell bioenergetics.* Biochim Biophys Acta, 2013. **1832**(4): p. 495-508.
75. Ottolini, D., et al., *The Parkinson disease-related protein DJ-1 counteracts mitochondrial impairment induced by the tumour suppressor protein p53 by enhancing endoplasmic reticulum-mitochondria tethering.* Hum Mol Genet, 2013. **22**(11): p. 2152-68.
76. Cummins, J.M., *Fertilization and elimination of the paternal mitochondrial genome.* Hum Reprod, 2000. **15 Suppl 2**: p. 92-101.
77. Al Rawi, S., et al., *Postfertilization autophagy of sperm organelles prevents paternal mitochondrial DNA transmission.* Science, 2011. **334**(6059): p. 1144-7.
78. Novak, I., et al., *Nix is a selective autophagy receptor for mitochondrial clearance.* EMBO Rep, 2010. **11**(1): p. 45-51.

79. Lemasters, J.J., *Selective mitochondrial autophagy, or mitophagy, as a targeted defense against oxidative stress, mitochondrial dysfunction, and aging.* Rejuvenation Res, 2005. **8**(1): p. 3-5.
80. Jin, S.M. and R.J. Youle, *PINK1- and Parkin-mediated mitophagy at a glance.* J Cell Sci, 2012. **125**(Pt 4): p. 795-9.
81. Yorimitsu, T. and D.J. Klionsky, *Autophagy: molecular machinery for self-eating.* Cell Death Differ, 2005. **12 Suppl 2**: p. 1542-52.
82. Yang, Z. and D.J. Klionsky, *Mammalian autophagy: core molecular machinery and signaling regulation.* Curr Opin Cell Biol, 2010. **22**(2): p. 124-31.
83. Wirawan, E., et al., *Autophagy: for better or for worse.* Cell Res, 2012. **22**(1): p. 43-61.
84. Schworer, C.M., K.A. Shiffer, and G.E. Mortimore, *Quantitative relationship between autophagy and proteolysis during graded amino acid deprivation in perfused rat liver.* J Biol Chem, 1981. **256**(14): p. 7652-8.
85. Jung, C.H., et al., *ULK-Atg13-FIP200 complexes mediate mTOR signaling to the autophagy machinery.* Mol Biol Cell, 2009. **20**(7): p. 1992-2003.
86. Hosokawa, N., et al., *Nutrient-dependent mTORC1 association with the ULK1-Atg13-FIP200 complex required for autophagy.* Mol Biol Cell, 2009. **20**(7): p. 1981-91.
87. Ganley, I.G., et al., *ULK1.ATG13.FIP200 complex mediates mTOR signaling and is essential for autophagy.* J Biol Chem, 2009. **284**(18): p. 12297-305.
88. Fujita, N., et al., *The Atg16L complex specifies the site of LC3 lipidation for membrane biogenesis in autophagy.* Mol Biol Cell, 2008. **19**(5): p. 2092-100.
89. Kabeya, Y., et al., *LC3, a mammalian homologue of yeast Apg8p, is localized in autophagosome membranes after processing.* EMBO J, 2000. **19**(21): p. 5720-8.
90. Yang, Z. and D.J. Klionsky, *Eaten alive: a history of macroautophagy.* Nat Cell Biol, 2010. **12**(9): p. 814-22.
91. Itakura, E., et al., *Beclin 1 forms two distinct phosphatidylinositol 3-kinase complexes with mammalian Atg14 and UVRAG.* Mol Biol Cell, 2008. **19**(12): p. 5360-72.
92. Liang, C., et al., *Autophagic and tumour suppressor activity of a novel Beclin1-binding protein UVRAG.* Nat Cell Biol, 2006. **8**(7): p. 688-99.
93. Sun, Q., et al., *Identification of Barkor as a mammalian autophagy-specific factor for Beclin 1 and class III phosphatidylinositol 3-kinase.* Proc Natl Acad Sci U S A, 2008. **105**(49): p. 19211-6.
94. Zhong, Y., et al., *Distinct regulation of autophagic activity by Atg14L and Rubicon associated with Beclin 1-phosphatidylinositol-3-kinase complex.* Nat Cell Biol, 2009. **11**(4): p. 468-76.
95. Liang, C., et al., *Beclin1-binding UVRAG targets the class C Vps complex to coordinate autophagosome maturation and endocytic trafficking.* Nat Cell Biol, 2008. **10**(7): p. 776-87.
96. Lemasters, J.J., et al., *The mitochondrial permeability transition in cell death: a common mechanism in necrosis, apoptosis and autophagy.* Biochim Biophys Acta, 1998. **1366**(1-2): p. 177-96.
97. Narendra, D., et al., *Parkin is recruited selectively to impaired mitochondria and promotes their autophagy.* J Cell Biol, 2008. **183**(5): p. 795-803.

98. Lee, J.Y., et al., *Disease-causing mutations in parkin impair mitochondrial ubiquitination, aggregation, and HDAC6-dependent mitophagy.* J Cell Biol, 2010. **189**(4): p. 671-9.
99. Matsuda, N., et al., *PINK1 stabilized by mitochondrial depolarization recruits Parkin to damaged mitochondria and activates latent Parkin for mitophagy.* J Cell Biol, 2010. **189**(2): p. 211-21.
100. Clark, I.E., et al., *Drosophila pink1 is required for mitochondrial function and interacts genetically with parkin.* Nature, 2006. **441**(7097): p. 1162-6.
101. Park, J., et al., *Mitochondrial dysfunction in Drosophila PINK1 mutants is complemented by parkin.* Nature, 2006. **441**(7097): p. 1157-61.
102. Yang, Y., et al., *Mitochondrial pathology and muscle and dopaminergic neuron degeneration caused by inactivation of Drosophila Pink1 is rescued by Parkin.* Proc Natl Acad Sci U S A, 2006. **103**(28): p. 10793-8.
103. Narendra, D.P., et al., *PINK1 is selectively stabilized on impaired mitochondria to activate Parkin.* PLoS Biol, 2010. **8**(1): p. e1000298.
104. Vives-Bauza, C., et al., *PINK1-dependent recruitment of Parkin to mitochondria in mitophagy.* Proc Natl Acad Sci U S A, 2010. **107**(1): p. 378-83.
105. Jin, S.M., et al., *Mitochondrial membrane potential regulates PINK1 import and proteolytic destabilization by PARL.* J Cell Biol, 2010. **191**(5): p. 933-42.
106. Meissner, C., et al., *The mitochondrial intramembrane protease PARL cleaves human Pink1 to regulate Pink1 trafficking.* J Neurochem, 2011. **117**(5): p. 856-67.
107. Muqit, M.M., et al., *Altered cleavage and localization of PINK1 to aggresomes in the presence of proteasomal stress.* J Neurochem, 2006. **98**(1): p. 156-69.
108. Geisler, S., et al., *The PINK1/Parkin-mediated mitophagy is compromised by PD-associated mutations.* Autophagy, 2010. **6**(7): p. 871-8.
109. Shiba-Fukushima, K., et al., *PINK1-mediated phosphorylation of the Parkin ubiquitin-like domain primes mitochondrial translocation of Parkin and regulates mitophagy.* Sci Rep, 2012. **2**: p. 1002.
110. Chen, Y. and G.W. Dorn, 2nd, *PINK1-phosphorylated mitofusin 2 is a Parkin receptor for culling damaged mitochondria.* Science, 2013. **340**(6131): p. 471-5.
111. Chan, N.C., et al., *Broad activation of the ubiquitin-proteasome system by Parkin is critical for mitophagy.* Hum Mol Genet, 2011. **20**(9): p. 1726-37.
112. Geisler, S., et al., *PINK1/Parkin-mediated mitophagy is dependent on VDAC1 and p62/SQSTM1.* Nat Cell Biol, 2010. **12**(2): p. 119-31.
113. Okatsu, K., et al., *Mitochondrial hexokinase HKI is a novel substrate of the Parkin ubiquitin ligase.* Biochem Biophys Res Commun, 2012. **428**(1): p. 197-202.
114. Sarraf, S.A., et al., *Landscape of the PARKIN-dependent ubiquitylome in response to mitochondrial depolarization.* Nature, 2013. **496**(7445): p. 372-6.
115. Narendra, D., et al., *p62/SQSTM1 is required for Parkin-induced mitochondrial clustering but not mitophagy; VDAC1 is dispensable for both.* Autophagy, 2010. **6**(8): p. 1090-106.
116. Gegg, M.E., et al., *Mitofusin 1 and mitofusin 2 are ubiquitinated in a PINK1/parkin-dependent manner upon induction of mitophagy.* Hum Mol Genet, 2010. **19**(24): p. 4861-70.
117. Poole, A.C., et al., *The mitochondrial fusion-promoting factor mitofusin is a substrate of the PINK1/parkin pathway.* PLoS One, 2010. **5**(4): p. e10054.

118. Rakovic, A., et al., *Mutations in PINK1 and Parkin impair ubiquitination of Mitofusins in human fibroblasts.* PLoS One, 2011. **6**(3): p. e16746.
119. Tanaka, A., et al., *Proteasome and p97 mediate mitophagy and degradation of mitofusins induced by Parkin.* J Cell Biol, 2010. **191**(7): p. 1367-80.
120. Ziviani, E., R.N. Tao, and A.J. Whitworth, *Drosophila Parkin requires PINK1 for mitochondrial translocation and ubiquitinates Mitofusin.* Proc Natl Acad Sci U S A. **107**(11): p. 5018-23.
121. Russo, G.J., et al., *Drosophila Miro is required for both anterograde and retrograde axonal mitochondrial transport.* J Neurosci, 2009. **29**(17): p. 5443-55.
122. Zinsmaier, K.E., M. Babic, and G.J. Russo, *Mitochondrial transport dynamics in axons and dendrites.* Results Probl Cell Differ, 2009. **48**: p. 107-39.
123. Weihofen, A., et al., *Pink1 forms a multiprotein complex with Miro and Milton, linking Pink1 function to mitochondrial trafficking.* Biochemistry, 2009. **48**(9): p. 2045-52.
124. Wang, X., et al., *PINK1 and Parkin target Miro for phosphorylation and degradation to arrest mitochondrial motility.* Cell, 2011. **147**(4): p. 893-906.
125. Cai, Q., et al., *Spatial parkin translocation and degradation of damaged mitochondria via mitophagy in live cortical neurons.* Curr Biol, 2012. **22**(6): p. 545-52.
126. Van Laar, V.S., et al., *Bioenergetics of neurons inhibit the translocation response of Parkin following rapid mitochondrial depolarization.* Hum Mol Genet, 2011. **20**(5): p. 927-40.
127. Almeida, A., et al., *Different responses of astrocytes and neurons to nitric oxide: the role of glycolytically generated ATP in astrocyte protection.* Proc Natl Acad Sci U S A, 2001. **98**(26): p. 15294-9.
128. Seibler, P., et al., *Mitochondrial Parkin recruitment is impaired in neurons derived from mutant PINK1 induced pluripotent stem cells.* J Neurosci, 2011. **31**(16): p. 5970-6.
129. Joselin, A.P., et al., *ROS-dependent regulation of Parkin and DJ-1 localization during oxidative stress in neurons.* Hum Mol Genet, 2012. **21**(22): p. 4888-903.
130. Rakovic, A., et al., *Phosphatase and tensin homolog (PTEN)-induced putative kinase 1 (PINK1)-dependent ubiquitination of endogenous Parkin attenuates mitophagy: study in human primary fibroblasts and induced pluripotent stem cell-derived neurons.* J Biol Chem, 2013. **288**(4): p. 2223-37.
131. Suen, D.F., et al., *Parkin overexpression selects against a deleterious mtDNA mutation in heteroplasmic cybrid cells.* Proc Natl Acad Sci U S A, 2010. **107**(26): p. 11835-40.
132. Vincow, E.S., et al., *The PINK1-Parkin pathway promotes both mitophagy and selective respiratory chain turnover in vivo.* Proc Natl Acad Sci U S A, 2013. **110**(16): p. 6400-5.
133. Hoshino, A., et al., *Cytosolic p53 inhibits Parkin-mediated mitophagy and promotes mitochondrial dysfunction in the mouse heart.* Nat Commun, 2013. **4**: p. 2308.
134. Ekstrand, M.I., et al., *Progressive parkinsonism in mice with respiratory-chain-deficient dopamine neurons.* Proc Natl Acad Sci U S A, 2007. **104**(4): p. 1325-30.

135. Sterky, F.H., et al., *Impaired mitochondrial transport and Parkin-independent degeneration of respiratory chain-deficient dopamine neurons in vivo.* Proc Natl Acad Sci U S A, 2011. **108**(31): p. 12937-42.
136. Matsui, H., et al., *PINK1 and Parkin complementarily protect dopaminergic neurons in vertebrates.* Hum Mol Genet, 2013. **22**(12): p. 2423-34.
137. Park, J., Y. Kim, and J. Chung, *Mitochondrial dysfunction and Parkinson's disease genes: insights from Drosophila.* Dis Model Mech, 2009. **2**(7-8): p. 336-40.
138. Gorman, A.M., *Neuronal cell death in neurodegenerative diseases: recurring themes around protein handling.* J Cell Mol Med, 2008. **12**(6A): p. 2263-80.
139. Cardoso, S.M., *The mitochondrial cascade hypothesis for Parkinson's disease.* Curr Pharm Des, 2011. **17**(31): p. 3390-7.
140. Byers, B., et al., *SNCA triplication Parkinson's patient's iPSC-derived DA neurons accumulate alpha-synuclein and are susceptible to oxidative stress.* PLoS One, 2011. **6**(11): p. e26159.
141. Choong, C.J. and Y.H. Say, *Neuroprotection of alpha-synuclein under acute and chronic rotenone and maneb treatment is abolished by its familial Parkinson's disease mutations A30P, A53T and E46K.* Neurotoxicology, 2011. **32**(6): p. 857-63.
142. Li, W.W., et al., *Localization of alpha-synuclein to mitochondria within midbrain of mice.* Neuroreport, 2007. **18**(15): p. 1543-6.
143. Nakamura, K., et al., *Optical reporters for the conformation of alpha-synuclein reveal a specific interaction with mitochondria.* J Neurosci, 2008. **28**(47): p. 12305-17.
144. Nakamura, K., et al., *Direct membrane association drives mitochondrial fission by the Parkinson disease-associated protein alpha-synuclein.* J Biol Chem, 2011. **286**(23): p. 20710-26.
145. Kamp, F., et al., *Inhibition of mitochondrial fusion by alpha-synuclein is rescued by PINK1, Parkin and DJ-1.* EMBO J, 2010. **29**(20): p. 3571-89.
146. Choubey, V., et al., *Mutant A53T alpha-synuclein induces neuronal death by increasing mitochondrial autophagy.* J Biol Chem, 2011. **286**(12): p. 10814-24.
147. Chinta, S.J., et al., *Mitochondrial alpha-synuclein accumulation impairs complex I function in dopaminergic neurons and results in increased mitophagy in vivo.* Neurosci Lett, 2010. **486**(3): p. 235-9.
148. Devi, L., et al., *Mitochondrial import and accumulation of alpha-synuclein impair complex I in human dopaminergic neuronal cultures and Parkinson disease brain.* J Biol Chem, 2008. **283**(14): p. 9089-100.
149. Mitsumoto, A. and Y. Nakagawa, *DJ-1 is an indicator for endogenous reactive oxygen species elicited by endotoxin.* Free Radic Res, 2001. **35**(6): p. 885-93.
150. Kinumi, T., et al., *Cysteine-106 of DJ-1 is the most sensitive cysteine residue to hydrogen peroxide-mediated oxidation in vivo in human umbilical vein endothelial cells.* Biochem Biophys Res Commun, 2004. **317**(3): p. 722-8.
151. Canet-Aviles, R.M., et al., *The Parkinson's disease protein DJ-1 is neuroprotective due to cysteine-sulfinic acid-driven mitochondrial localization.* Proc Natl Acad Sci U S A, 2004. **101**(24): p. 9103-8.

152. Blackinton, J., et al., *Formation of a stabilized cysteine sulfinic acid is critical for the mitochondrial function of the parkinsonism protein DJ-1.* J Biol Chem, 2009. **284**(10): p. 6476-85.
153. Zhou, W. and C.R. Freed, *DJ-1 up-regulates glutathione synthesis during oxidative stress and inhibits A53T alpha-synuclein toxicity.* J Biol Chem, 2005. **280**(52): p. 43150-8.
154. Zhong, N. and J. Xu, *Synergistic activation of the human MnSOD promoter by DJ-1 and PGC-1alpha: regulation by SUMOylation and oxidation.* Hum Mol Genet, 2008. **17**(21): p. 3357-67.
155. Clements, C.M., et al., *DJ-1, a cancer- and Parkinson's disease-associated protein, stabilizes the antioxidant transcriptional master regulator Nrf2.* Proc Natl Acad Sci U S A, 2006. **103**(41): p. 15091-6.
156. Im, J.Y., et al., *DJ-1 induces thioredoxin 1 expression through the Nrf2 pathway.* Hum Mol Genet, 2012. **21**(13): p. 3013-24.
157. Bai, J., et al., *Does thioredoxin-1 prevent mitochondria- and endoplasmic reticulum-mediated neurotoxicity of 1-methyl-4-phenyl-1,2,3,6-tetrahydropyridine?* Antioxid Redox Signal, 2007. **9**(5): p. 603-8.
158. Kim, R.H., et al., *DJ-1, a novel regulator of the tumor suppressor PTEN.* Cancer Cell, 2005. **7**(3): p. 263-73.
159. Guzman, J.N., et al., *Oxidant stress evoked by pacemaking in dopaminergic neurons is attenuated by DJ-1.* Nature, 2010. **468**(7324): p. 696-700.
160. Krebiehl, G., et al., *Reduced basal autophagy and impaired mitochondrial dynamics due to loss of Parkinson's disease-associated protein DJ-1.* PLoS One, 2010. **5**(2): p. e9367.
161. Thomas, K.J., et al., *DJ-1 acts in parallel to the PINK1/parkin pathway to control mitochondrial function and autophagy.* Hum Mol Genet, 2011. **20**(1): p. 40-50.
162. Tsika, E. and D.J. Moore, *Mechanisms of LRRK2-mediated neurodegeneration.* Curr Neurol Neurosci Rep, 2012. **12**(3): p. 251-60.
163. Biskup, S., et al., *Localization of LRRK2 to membranous and vesicular structures in mammalian brain.* Ann Neurol, 2006. **60**(5): p. 557-69.
164. Mortiboys, H., et al., *Mitochondrial impairment in patients with Parkinson disease with the G2019S mutation in LRRK2.* Neurology, 2010. **75**(22): p. 2017-20.
165. Hardy, J., *Genetic analysis of pathways to Parkinson disease.* Neuron, 2010. **68**(2): p. 201-6.
166. Jiang, H., et al., *Parkin protects human dopaminergic neuroblastoma cells against dopamine-induced apoptosis.* Hum Mol Genet, 2004. **13**(16): p. 1745-54.
167. Lo Bianco, C., et al., *Lentiviral vector delivery of parkin prevents dopaminergic degeneration in an alpha-synuclein rat model of Parkinson's disease.* Proc Natl Acad Sci U S A, 2004. **101**(50): p. 17510-5.
168. Rosen, K.M., et al., *Parkin protects against mitochondrial toxins and beta-amyloid accumulation in skeletal muscle cells.* J Biol Chem, 2006. **281**(18): p. 12809-16.
169. Staropoli, J.F., et al., *Parkin is a component of an SCF-like ubiquitin ligase complex and protects postmitotic neurons from kainate excitotoxicity.* Neuron, 2003. **37**(5): p. 735-49.

170. Bouman, L., et al., *Parkin is transcriptionally regulated by ATF4: evidence for an interconnection between mitochondrial stress and ER stress.* Cell Death Differ, 2011. **18**(5): p. 769-82.
171. Lutz, A.K., et al., *Loss of parkin or PINK1 function increases Drp1-dependent mitochondrial fragmentation.* J Biol Chem, 2009. **284**(34): p. 22938-51.
172. Scarpulla, R.C., *Metabolic control of mitochondrial biogenesis through the PGC-1 family regulatory network.* Biochim Biophys Acta, 2011. **1813**(7): p. 1269-78.
173. Shin, J.H., et al., *PARIS (ZNF746) repression of PGC-1alpha contributes to neurodegeneration in Parkinson's disease.* Cell, 2011. **144**(5): p. 689-702.
174. Henn, I.H., et al., *Parkin mediates neuroprotection through activation of IkappaB kinase/nuclear factor-kappaB signaling.* J Neurosci, 2007. **27**(8): p. 1868-78.
175. Tokunaga, F., et al., *Involvement of linear polyubiquitylation of NEMO in NF-kappaB activation.* Nat Cell Biol, 2009. **11**(2): p. 123-32.
176. Muller-Rischart, A.K., et al., *The E3 ligase parkin maintains mitochondrial integrity by increasing linear ubiquitination of NEMO.* Mol Cell, 2013. **49**(5): p. 908-21.
177. Dagda, R.K., et al., *Loss of PINK1 function promotes mitophagy through effects on oxidative stress and mitochondrial fission.* J Biol Chem, 2009. **284**(20): p. 13843-55.
178. Sandebring, A., et al., *Mitochondrial alterations in PINK1 deficient cells are influenced by calcineurin-dependent dephosphorylation of dynamin-related protein 1.* PLoS One, 2009. **4**(5): p. e5701.
179. Gautier, C.A., T. Kitada, and J. Shen, *Loss of PINK1 causes mitochondrial functional defects and increased sensitivity to oxidative stress.* Proc Natl Acad Sci U S A, 2008. **105**(32): p. 11364-9.
180. Heeman, B., et al., *Depletion of PINK1 affects mitochondrial metabolism, calcium homeostasis and energy maintenance.* J Cell Sci, 2011. **124**(Pt 7): p. 1115-25.
181. Gandhi, S., et al., *PINK1-associated Parkinson's disease is caused by neuronal vulnerability to calcium-induced cell death.* Mol Cell, 2009. **33**(5): p. 627-38.
182. Youle, R.J. and D.P. Narendra, *Mechanisms of mitophagy.* Nat Rev Mol Cell Biol, 2011. **12**(1): p. 9-14.
183. Pridgeon, J.W., et al., *PINK1 protects against oxidative stress by phosphorylating mitochondrial chaperone TRAP1.* PLoS Biol, 2007. **5**(7): p. e172.
184. Costa, A.C., S.H. Loh, and L.M. Martins, *Drosophila Trap1 protects against mitochondrial dysfunction in a PINK1/parkin model of Parkinson's disease.* Cell Death Dis, 2013. **4**: p. e467.
185. Plun-Favreau, H., et al., *The mitochondrial protease HtrA2 is regulated by Parkinson's disease-associated kinase PINK1.* Nat Cell Biol, 2007. **9**(11): p. 1243-52.
186. Tain, L.S., et al., *Drosophila HtrA2 is dispensable for apoptosis but acts downstream of PINK1 independently from Parkin.* Cell Death Differ, 2009. **16**(8): p. 1118-25.
187. Grenier, K., G.L. McLelland, and E.A. Fon, *Parkin- and PINK1-Dependent Mitophagy in Neurons: Will the Real Pathway Please Stand Up?* Front Neurol, 2013. **4**: p. 100.
188. Lefebvre, V.D., Qiujiang; Ng, Andy; Baird, Stephen; Nascimento, Mirna; Campanella, Michelangelo; McBride, Heidi; Screaton, Robert *Genome-wide RNAi*

screen identifies ATPase Inhbitory Factor 1 (ATPIF1) as essential for PARK2 recruitment and mitophagy. Autophagy, 2013. **9**(11).
189. Harris, D.A., V. von Tscharner, and G.K. Radda, *The ATPase inhibitor protein in oxidative phosphorylation. The rate-limiting factor to phosphorylation in submitochondrial particles.* Biochim Biophys Acta, 1979. **548**(1): p. 72-84.
190. Schwerzmann, K. and P.L. Pedersen, *Synthesis and use of an azido-labeled form of the ATPase inhibitor peptide of rat liver mitochondria.* Methods Enzymol, 1986. **126**: p. 660-6.
191. Zanotti, F., et al., *Proton translocation by the H+-ATPase of mitochondria. Effect of modification by monofunctional reagents of thiol residues in F0 polypeptides.* Eur J Biochem, 1987. **164**(3): p. 517-23.
192. Campanella, M., et al., *Regulation of mitochondrial structure and function by the F1Fo-ATPase inhibitor protein, IF1.* Cell Metab, 2008. **8**(1): p. 13-25.
193. Bason, J.V., et al., *Binding of the inhibitor protein IF(1) to bovine F(1)-ATPase.* J Mol Biol, 2011. **406**(3): p. 443-53.
194. Penefsky, H.S., *Mechanism of inhibition of mitochondrial adenosine triphosphatase by dicyclohexylcarbodiimide and oligomycin: relationship to ATP synthesis.* Proc Natl Acad Sci U S A, 1985. **82**(6): p. 1589-93.
195. Perry, S.W., et al., *Mitochondrial membrane potential probes and the proton gradient: a practical usage guide.* Biotechniques, 2011. **50**(2): p. 98-115.
196. Perry, S.W., et al., *HIV-1 transactivator of transcription protein induces mitochondrial hyperpolarization and synaptic stress leading to apoptosis.* J Immunol, 2005. **174**(7): p. 4333-44.
197. Campanella, M., et al., *IF1, the endogenous regulator of the F(1)F(o)-ATPsynthase, defines mitochondrial volume fraction in HeLa cells by regulating autophagy.* Biochim Biophys Acta, 2009. **1787**(5): p. 393-401.
198. Appleby, R.D., et al., *Quantitation and origin of the mitochondrial membrane potential in human cells lacking mitochondrial DNA.* Eur J Biochem, 1999. **262**(1): p. 108-16.
199. Buchet, K. and C. Godinot, *Functional F1-ATPase essential in maintaining growth and membrane potential of human mitochondrial DNA-depleted rho degrees cells.* J Biol Chem, 1998. **273**(36): p. 22983-9.
200. Wittig, I., et al., *Assembly and oligomerization of human ATP synthase lacking mitochondrial subunits a and A6L.* Biochim Biophys Acta, 2010. **1797**(6-7): p. 1004-11.
201. Jackson, A.L. and P.S. Linsley, *Recognizing and avoiding siRNA off-target effects for target identification and therapeutic application.* Nat Rev Drug Discov, 2010. **9**(1): p. 57-67.
202. Wiedemann, N., A.E. Frazier, and N. Pfanner, *The protein import machinery of mitochondria.* J Biol Chem, 2004. **279**(15): p. 14473-6.
203. Campanella, M., et al., *IF(1): setting the pace of the F(1)F(o)-ATP synthase.* Trends Biochem Sci, 2009. **34**(7): p. 343-50.
204. Yamada, E.W. and N.J. Huzel, *Distribution of the ATPase inhibitor proteins of mitochondria in mammalian tissues including fibroblasts from a patient with Luft's disease.* Biochim Biophys Acta, 1992. **1139**(1-2): p. 143-7.

205. DiMauro, S., et al., *Luft's disease. Further biochemical and ultrastructural studies of skeletal muscle in the second case.* J Neurol Sci, 1976. **27**(2): p. 217-32.

Chapter 6 – Appendices

Appendix I – Ranking of genes from the kinome screen based on z-score. GFP-Parkin recruitment was analyzed in HeLa cells following 1 h of CCCP treatment. Data are average of three replicates screens.

Gene Symbol	Well	score	Gene Symbol	Well	score	Gene Symbol	Well	score
NA	pos	7.46	PRKACG	sample	2.59	NME1	sample	1.46
NA	pos	7.43	CAMK1D	sample	2.59	PRKACB	sample	1.46
MAP2K2	sample	7.42	PRKCDBP	sample	2.58	TNNI3K	sample	1.45
NA	other	7.41	NA	neg	2.53	DGKG	sample	1.44
RIOK2	sample	7.35	MAP3K12	sample	2.48	PAK2	sample	1.41
NA	pos	7.29	MAP3K8	sample	2.46	DCAMKL1	sample	1.4
NA	pos	7.26	MASTL	sample	2.4	AURKC	sample	1.39
NA	pos	7.25	FGFR3	sample	2.4	CDC42BPA	sample	1.38
NA	pos	7.24	EEF2K	sample	2.38	FLJ13052	sample	1.36
NA	pos	7.2	PRKR	sample	2.37	CNKSR1	sample	1.36
NA	pos	7.18	UCK1	sample	2.37	RAGE	sample	1.36
NA	pos	7.11	PRKRIR	sample	2.35	DYRK1B	sample	1.32
NA	pos	7.05	TGFBR2	sample	2.35	NA	sample	1.28
NA	pos	7.05	ACVR2B	sample	2.35	MAPK13	sample	1.28
NA	pos	6.97	STK25	sample	2.27	MAP3K7IP1	sample	1.28
NA	pos	6.94	NA	neg	2.27	TNIK	sample	1.27
NA	pos	6.82	DGKE	sample	2.26	URKL1	sample	1.25
NA	pos	6.8	CDK8	sample	2.24	PRKCBP1	sample	1.24
NA	pos	6.65	DYRK3	sample	2.23	ADK	sample	1.24
NA	pos	6.65	FLT1	sample	2.2	PIK3C2B	sample	1.23
NA	pos	6.63	TRAF3IP3	sample	2.11	ULK1	sample	1.22
NA	pos	6.5	AK3	sample	2.04	RET	sample	1.22
NA	pos	6.49	PFKFB2	sample	2.02	DGKB	sample	1.21
NA	pos	6.44	IKBKB	sample	2	STK22B	sample	1.2
PINK1	sample	6.28	FLJ10761	sample	2	BRAF	sample	1.2
PIM2	sample	6.22	CDK2	sample	1.98	RFK	sample	1.19
NA	pos	6.06	MAP2K3	sample	1.97	SPHK1	sample	1.19
NA	pos	6.03	FLJ14800	sample	1.96	IRAK1BP1	sample	1.19
NA	pos	5.54	MAP3K5	sample	1.96	NA	other	1.19
STK3	sample	5.26	PLK3	sample	1.95	ROR1	sample	1.18
MAPKAP1	sample	4.9	DOK1	sample	1.95	TXK	sample	1.18
BCR	sample	4.84	IKBKE	sample	1.88	ICK	sample	1.18
NEK4	sample	4.64	EPHA5	sample	1.87	CKMT2	sample	1.16
PIK3R4	sample	4.51	CDC2	sample	1.85	MAP3K6	sample	1.16
PRKCL2	sample	4.43	ACVR2	sample	1.84	CDKN2A	sample	1.15
PLK1	sample	4.41	PRKAG2	sample	1.83	FN3K	sample	1.15
EIF2AK4	sample	4.22	SIK2	sample	1.81	PCTK3	sample	1.15
SKIP	sample	3.79	ROCK1	sample	1.79	RIPK3	sample	1.12
MAPK8IP1	sample	3.69	CAMK1	sample	1.79	CDC2L1	sample	1.09
MAPK8IP2	sample	3.48	NA	other	1.79	MST1R	sample	1.08
LTK	sample	3.4	JAK2	sample	1.78	AK7	sample	1.08
DGKD	sample	3.34	NME6	sample	1.77	CALM1	sample	1.07
TNK1	sample	3.27	CAMK1G	sample	1.75	STK19	sample	1.06
PRKAR1A	sample	3.2	GAK	sample	1.74	DAPK1	sample	1.06
STK38	sample	3.08	PAK3	sample	1.71	TEK	sample	1.06
MAP2K1IP1	sample	3.07	LRRK2	sample	1.67	PLK4	sample	1.05
ITK	sample	3.06	AKT3	sample	1.67	EPHA8	sample	1.04
PAK4	sample	3.05	MAST3	sample	1.63	AKAP6	sample	1.03
MGC45428	sample	3.03	SKP2	sample	1.62	EPS8L1	sample	1.03
RPS6KA6	sample	3.02	P101-PI3K	sample	1.62	NA	sample	1.02
NA	other	2.99	NAGK	sample	1.62	STK32C	sample	1.02
GALK1	sample	2.95	PIK3R2	sample	1.58	TYROBP	sample	1
TEC	sample	2.94	KHK	sample	1.57	PDK2	sample	1
HIPK2	sample	2.91	PRKCE	sample	1.56	FER	sample	0.98
FUK	sample	2.88	MAPK6	sample	1.56	MGC40579	sample	0.97
PTK6	sample	2.83	NA	neg	1.55	discontinued	sample	0.97
NA	other	2.8	DGUOK	sample	1.53	EPHA7	sample	0.96
CSNK2A1	sample	2.77	STYK1	sample	1.53	ERK8	sample	0.96
PTK2B	sample	2.74	PIP5K1C	sample	1.49	RP6-213H19.1	sample	0.95
CIT	sample	2.67	CDK5	sample	1.48	AK5	sample	0.94
CDK10	sample	2.63	PIP5K2B	sample	1.47	PAK7	sample	0.94
ROCK2	sample	2.61	ANKK1	sample	1.47	FES	sample	0.93

Gene Symbol	Well	score
PRKACA	sample	0.91
PIM1	sample	0.9
NA	sample	0.9
ULK4	sample	0.89
NEK1	sample	0.89
RPS6KA3	sample	0.89
SNF1LK	sample	0.88
IRAK4	sample	0.86
PRKCN	sample	0.85
PIK3CD	sample	0.85
HRI	sample	0.84
NA	sample	0.84
MAP3K1	sample	0.84
PDK4	sample	0.84
IKBKG	sample	0.83
PHKA1	sample	0.83
KIAA1446	sample	0.83
GK2	sample	0.83
TTK	sample	0.8
ITPKB	sample	0.79
PIK3C3	sample	0.78
STK39	sample	0.78
ATM	sample	0.78
PDIK1L	sample	0.77
CDK9	sample	0.77
MAPK9	sample	0.77
BMPR1A	sample	0.76
JAK1	sample	0.76
PRKAR2A	sample	0.74
PKIG	sample	0.73
AAK1	sample	0.73
CDKL2	sample	0.71
ZAP70	sample	0.71
MAP3K11	sample	0.71
PSKH1	sample	0.69
GIT2	sample	0.69
NYD-SP25	sample	0.69
TYRO3	sample	0.68
RYK	sample	0.67
GK	sample	0.67
EGFR	sample	0.67
CINP	sample	0.67
TTBK1	sample	0.67
NA	sample	0.66
MAST2	sample	0.66
RIOK1	sample	0.65
CDK5R2	sample	0.62
discontinued	sample	0.62
MAP3K13	sample	0.61
LOC392265	sample	0.61
HIPK4	sample	0.61
PRKG1	sample	0.61
ERN2	sample	0.61
MAPK14	sample	0.6
PFKL	sample	0.6
PRKWNK3	sample	0.59
NIPA	sample	0.58
IRAK3	sample	0.56
EPHA4	sample	0.56
PCK1	sample	0.55
DUSTYPK	sample	0.55
DYRK4	sample	0.55

Gene Symbol	Well	score
NA	neg	0.54
ITPK1	sample	0.54
HIPK3	sample	0.53
AK1	sample	0.53
MAPKBP1	sample	0.51
PRKCI	sample	0.51
PLAU	sample	0.51
STK33	sample	0.5
FYN	sample	0.5
PANK2	sample	0.5
PRKCB1	sample	0.49
NA	sample	0.49
TESK2	sample	0.48
PRKCA	sample	0.48
MAP4K4	sample	0.47
CDKN2B	sample	0.47
GRK7	sample	0.46
FGFR2	sample	0.45
PFKP	sample	0.44
GSK3B	sample	0.43
AURKA	sample	0.42
VRK3	sample	0.41
CHEK1	sample	0.41
AKAP3	sample	0.4
PDK3	sample	0.4
SPEC2	sample	0.39
LYN	sample	0.39
AKAP7	sample	0.39
CSNK1G3	sample	0.38
IHPK1	sample	0.37
PSKH2	sample	0.36
ACVR1	sample	0.36
SPEG	sample	0.36
FN3KRP	sample	0.35
ETNK1	sample	0.35
SYK	sample	0.34
MAPK4	sample	0.34
PIK3AP1	sample	0.34
ERBB3	sample	0.33
PIK3R3	sample	0.33
TESK1	sample	0.32
PTK7	sample	0.31
ADCK2	sample	0.31
discontinued	sample	0.28
EPHB2	sample	0.28
NA	sample	0.28
DDR2	sample	0.28
TYK2	sample	0.27
CAMKIINALPH	sample	0.26
AURKB	sample	0.26
CLK2	sample	0.25
AKAP10	sample	0.25
KIAA1804	sample	0.25
KIAA1361	sample	0.25
ARHGAP26	sample	0.25
PKIB	sample	0.24
NME3	sample	0.24
NA	sample	0.23
CRK7	sample	0.23
NRK	sample	0.23
AXL	sample	0.22
ROR2	sample	0.22

Gene Symbol	Well	score
STK4	sample	0.22
XYLB	sample	0.21
NA	sample	0.21
MADD	sample	0.2
TBK1	sample	0.19
LAK	sample	0.18
AKAP4	sample	0.18
BUB1B	sample	0.16
MKNK2	sample	0.15
CLK1	sample	0.15
PDXK	sample	0.15
MAP2K4	sample	0.14
DDR1	sample	0.14
CDKN2D	sample	0.14
ASK	sample	0.14
NA	sample	0.13
MAK	sample	0.13
CALM2	sample	0.13
NEK7	sample	0.12
BCKDK	sample	0.11
STK35	sample	0.11
SKP1A	sample	0.1
NA	sample	0.1
TAO1	sample	0.1
CDKL4	sample	0.08
LRRK1	sample	0.08
STK23	sample	0.08
ADCK5	sample	0.08
GUK1	sample	0.08
EPHA2	sample	0.08
MYLK2	sample	0.07
MAP4K3	sample	0.07
MET	sample	0.07
PGK2	sample	0.07
NA	sample	0.07
PTK2	sample	0.06
ADRBK2	sample	0.06
CDKL3	sample	0.05
PRKAG3	sample	0.04
MVK	sample	0.04
LOC407835	sample	0.03
NYD-SP25	sample	0.03
PIK4CA	sample	0.03
CDKN1C	sample	0.03
IRAK1	sample	0.03
MAP3K3	sample	0.03
KALRN	sample	0.03
DGKA	sample	0.03
MYLK	sample	0.02
NA	sample	0.02
RPS6KA4	sample	0.02
MAPK7	sample	0.02
PXK	sample	0.02
ALS2CR2	sample	0.02
NA	sample	0.01
PKN3	sample	0.01
ZAK	sample	0.01
STK32A	sample	0.01
LCK	sample	0.01
TK2	sample	0.01
CKM	sample	0.01
CKMT1B	sample	0

Gene Symbol	Well	score
MELK	sample	-0.54
PANK1	sample	-0.55
ILK	sample	-0.55
MARK3	sample	-0.55
TAO1	sample	-0.56
CKS2	sample	-0.56
JAK3	sample	-0.56
HGS	sample	-0.57
LIMK1	sample	-0.57
DGKQ	sample	-0.59
STK17A	sample	-0.6
STK29	sample	-0.6
RIPK1	sample	-0.6
DTYMK	sample	-0.61
IKBKAP	sample	-0.61
NA	neg	-0.62
MAP3K14	sample	-0.62
NEK3	sample	-0.63
MARCKS	sample	-0.63
EPHA1	sample	-0.64
NA	sample	-0.64
TNK2	sample	-0.64
NME7	sample	-0.64
TIE	sample	-0.65
TGFBR1	sample	-0.65
PDLIM5	sample	-0.65
ANKRD3	sample	-0.66
PCTK1	sample	-0.67
TLK2	sample	-0.67
SMG1	sample	-0.67
PRKCZ	sample	-0.67
discontinued	sample	-0.67
PRKWNK2	sample	-0.69
SRPK1	sample	-0.69
CDK5R1	sample	-0.69
CDKN1A	sample	-0.7
MLCK	sample	-0.7
PRKAG1	sample	-0.7
MAPKAPK3	sample	-0.71
BUB1	sample	-0.71
MARK2	sample	-0.71
CDK11	sample	-0.71
CAMKK2	sample	-0.72
HK3	sample	-0.73
STK11IP	sample	-0.74
MUSK	sample	-0.74
PRKCQ	sample	-0.74
NEK5	sample	-0.75
LMTK3	sample	-0.75
PHKB	sample	-0.76
IRAK2	sample	-0.76
NEK2	sample	-0.77
PIK3C2G	sample	-0.77
CNKSR3	sample	-0.77
ADRBK1	sample	-0.78
FLT4	sample	-0.78
NA	sample	-0.78
HCK	sample	-0.79
NA	other	-0.79
MAP4K1	sample	-0.8
MAP3K9	sample	-0.8
CSK	sample	-0.81

Gene Symbol	Well	score
SGKL	sample	-0.82
HK2	sample	-0.83
NA	sample	-0.83
NA	neg	-0.83
NA	sample	-0.84
CERK	sample	-0.86
ALK	sample	-0.86
NTRK2	sample	-0.86
GRK5	sample	-0.89
PIK3CG	sample	-0.9
LOC283155	sample	-0.91
TRIO	sample	-0.92
NA	sample	-0.93
SRPK2	sample	-0.93
GRK6	sample	-0.95
NA	sample	-0.95
FLT3	sample	-0.96
PACSIN2	sample	-0.97
DAPK2	sample	-0.97
LYK5	sample	-0.98
FLT3LG	sample	-0.98
CDC2L5	sample	-0.99
ACVRL1	sample	-0.99
BTK	sample	-0.99
PIK4CB	sample	-0.99
KIAA1811	sample	-1.01
MAPK8IP3	sample	-1.02
LOC55971	sample	-1.02
PKIA	sample	-1.02
STK17B	sample	-1.02
PDXK	sample	-1.03
EPHB4	sample	-1.03
PRKG2	sample	-1.03
PRKCG	sample	-1.04
RPS6KA1	sample	-1.04
DYRK1A	sample	-1.05
STK22D	sample	-1.05
EPHA3	sample	-1.05
RIPK2	sample	-1.07
MAP3K7	sample	-1.07
AKAP8L	sample	-1.09
SLK	sample	-1.12
CDKN1B	sample	-1.14
GCK	sample	-1.15
SGK2	sample	-1.16
PFKFB3	sample	-1.16
CAMK2B	sample	-1.17
DAPK3	sample	-1.18
HUNK	sample	-1.19
TPK1	sample	-1.2
BMP2K	sample	-1.2
PRKAB1	sample	-1.2
NA	sample	-1.21
CAMK4	sample	-1.22
PACSIN3	sample	-1.22
ITPKC	sample	-1.23
MAP3K2	sample	-1.23
STK31	sample	-1.25
AKAP1	sample	-1.25
AK3L1	sample	-1.27
STK16	sample	-1.27
IBTK	sample	-1.28

Gene Symbol	Well	score
PIP5K2C	sample	-1.3
PAK1	sample	-1.31
NA	sample	-1.32
LATS2	sample	-1.33
CSNK1A1P	sample	-1.33
PIP5K1A	sample	-1.33
PRPF4B	sample	-1.34
NA	neg	-1.34
UMP-CMPK	sample	-1.35
RPS6KA5	sample	-1.37
TSKS	sample	-1.37
NTRK3	sample	-1.41
MAPK11	sample	-1.41
GRK1	sample	-1.42
MARK1	sample	-1.44
HSMDPKIN	sample	-1.44
MAPK8	sample	-1.45
PKLR	sample	-1.45
PDGFRA	sample	-1.45
PFKFB4	sample	-1.46
CAMK2G	sample	-1.46
PFKFB1	sample	-1.47
PRKCM	sample	-1.48
MARK4	sample	-1.49
CDK7	sample	-1.49
SHARPIN	sample	-1.53
BMX	sample	-1.54
IHPK3	sample	-1.55
ADCK4	sample	-1.56
SORCS3	sample	-1.57
EPHB3	sample	-1.58
NA	sample	-1.58
NA	neg	-1.59
MAP2K1	sample	-1.59
ULK2	sample	-1.63
TK1	sample	-1.64
SRMS	sample	-1.65
MKNK1	sample	-1.68
AKAP8	sample	-1.69
MINK	sample	-1.69
OSR1	sample	-1.73
FGFR4	sample	-1.76
PDPK1	sample	-1.77
MERTK	sample	-1.77
PASK	sample	-1.77
GNE	sample	-1.81
PMVK	sample	-1.91
NEK6	sample	-1.95
ARK5	sample	-1.96
ROS1	sample	-1.97
MAPK10	sample	-1.99
TOPK	sample	-2
PRKAA1	sample	-2.02
BLK	sample	-2.02
WNK4	sample	-2.03
UGP2	sample	-2.04
LMTK2	sample	-2.04
FGFR1	sample	-2.09
UHMK1	sample	-2.1
PI4KII	sample	-2.11
PCTK2	sample	-2.11
CDC42BPB	sample	-2.2

Gene Symbol	Well	score
PRKDC	sample	0
CSNK2A2	sample	0
ATR	sample	0
PAK6	sample	0
MAGI-3	sample	0
RIOK3	sample	0
PRSS7	sample	0
PHKG2	sample	0
AATK	sample	0
FRK	sample	0
CARKL	sample	0
EIF2AK3	sample	0
PANK3	sample	0
PIK3R1	sample	0
PRKAB2	sample	0
EPHB6	sample	0
NRGN	sample	0
PDK1	sample	0
BMPR2	sample	0
STK22C	sample	0
SNARK	sample	0
RPS6KB2	sample	0
MAPK12	sample	0
AKT2	sample	0
PFTK1	sample	0
NME4	sample	0
ERBB2	sample	0
PRKAR2B	sample	0
PIP5K2A	sample	0
PRKWNK1	sample	0
MAPKAPK2	sample	0
DKFZP434C131	sample	0
GRK4	sample	0
AKAP5	sample	0
PHKG1	sample	0
PRKY	sample	0
CDKL1	sample	0
HIPK1	sample	0
CLK4	sample	0
CSNK1G2	sample	0
PRKCH	sample	0
RPS6KA2	sample	0
CLK3	sample	0
DGKI	sample	-0.01
VRK2	sample	-0.01
KSR2	sample	-0.01
KIT	sample	-0.01
PIP5K3	sample	-0.01
IHPK2	sample	-0.01
PACSIN1	sample	-0.01
NA	sample	-0.01
TTBK2	sample	-0.02
STK32B	sample	-0.02
AKIP	sample	-0.02
MAPK1	sample	-0.02
LATS1	sample	-0.02
NA	sample	-0.02
DCK	sample	-0.03
CHEK2	sample	-0.03
MAP3K4	sample	-0.03
ITPKA	sample	-0.03
CDK6	sample	-0.03
TP53RK	sample	-0.03
SBK1	sample	-0.03
EPHB1	sample	-0.04
ABL1	sample	-0.06
MOS	sample	-0.06
AKAP13	sample	-0.06
NA	other	-0.06
FASTK	sample	-0.06
VRK1	sample	-0.06
PRKCL1	sample	-0.07
NME5	sample	-0.07
RPS6KL1	sample	-0.07
ALS2CR7	sample	-0.07
STK36	sample	-0.08
BMPR1B	sample	-0.08
CSNK2B	sample	-0.08
PKM2	sample	-0.09
CSNK1D	sample	-0.09
MAP4K5	sample	-0.09
NA	sample	-0.1
SGK	sample	-0.1
PNCK	sample	-0.11
AKAP9	sample	-0.11
NLK	sample	-0.12
KIDINS220	sample	-0.13
CDKN2C	sample	-0.13
CALM3	sample	-0.13
PRKX	sample	-0.13
CIB3	sample	-0.13
CHKB	sample	-0.13
SH3KBP1	sample	-0.13
MAPK3	sample	-0.13
MAPKAPK5	sample	-0.15
KSR	sample	-0.15
PRKAA2	sample	-0.15
NME2	sample	-0.15
CDK3	sample	-0.15
PIK3CB	sample	-0.16
PRKRA	sample	-0.16
MAP2K7	sample	-0.17
PRKAR1B	sample	-0.17
SPHK2	sample	-0.2
CKS1B	sample	-0.2
LIMK2	sample	-0.21
GSK3A	sample	-0.21
SSTK	sample	-0.22
PDGFRB	sample	-0.22
CSNK1G1	sample	-0.22
PIK3CA	sample	-0.23
AKT1	sample	-0.23
CSNK1A1	sample	-0.23
PIP5K1B	sample	-0.23
CASK	sample	-0.24
PGK1	sample	-0.24
STK38L	sample	-0.25
PHKA2	sample	-0.25
AKAP11	sample	-0.25
RPS6KB1	sample	-0.26
NA	sample	-0.27
PTK9L	sample	-0.27
ACVR1B	sample	-0.28
NUCKS	sample	-0.28
discontinued	sample	-0.28
YES1	sample	-0.28
AKAP28	sample	-0.29
NA	sample	-0.29
CKB	sample	-0.29
NEK8	sample	-0.3
PTK9	sample	-0.3
AK2	sample	-0.3
GALK2	sample	-0.31
MAP2K6	sample	-0.31
STK10	sample	-0.32
CCRK	sample	-0.32
RAF1	sample	-0.32
CAMK2D	sample	-0.32
PRKCABP	sample	-0.32
CAMK2A	sample	-0.32
ERN1	sample	-0.33
PFKM	sample	-0.33
STK24	sample	-0.34
PIK3C2A	sample	-0.35
MAST4	sample	-0.36
MATK	sample	-0.36
DMPK	sample	-0.36
NA	sample	-0.37
PKMYT1	sample	-0.37
JIK	sample	-0.38
CDK4	sample	-0.38
GIT1	sample	-0.38
MAP2K5	sample	-0.39
MAP3K10	sample	-0.39
ARAF1	sample	-0.4
CAMKK1	sample	-0.4
PLK2	sample	-0.4
PRKCD	sample	-0.41
PRPS1L1	sample	-0.42
UMPK	sample	-0.42
CHKA	sample	-0.42
NA	other	-0.42
MAP3K7IP2	sample	-0.42
NTRK1	sample	-0.42
DGKZ	sample	-0.43
HK1	sample	-0.43
RBKS	sample	-0.43
STK11	sample	-0.43
FGR	sample	-0.44
HAK	sample	-0.44
NEK11	sample	-0.44
CDKL5	sample	-0.44
ERBB4	sample	-0.45
NA	sample	-0.45
WDSUB1	sample	-0.46
ADCK1	sample	-0.47
NRBP	sample	-0.47
CSNK1E	sample	-0.47
ABL2	sample	-0.47
SRC	sample	-0.48
PRKD2	sample	-0.49
CHUK	sample	-0.5
KDR	sample	-0.52
PI4K2B	sample	-0.53
NJMU-R1	sample	-0.53
NA	neg	-0.53

Gene Symbol	Well	score
MAST4	sample	-2.21
DGKH	sample	-2.22
CIB2	sample	-2.26
MAP4K2	sample	-2.3
SNRK	sample	-2.32
GKAP1	sample	-2.32
FLJ10986	sample	-2.39
DYRK2	sample	-2.39
RPS6KC1	sample	-2.42
TLK1	sample	-2.52
NEK9	sample	-2.53
AKAP12	sample	-2.56
CSNK1A1L	sample	-2.58
MGC4796	sample	-2.7
PANK4	sample	-2.78
HSPB8	sample	-3.2
WEE1	sample	-4.14

Appendix II- Analysis of deconvoluted siRNA sets of gene candidates from the genome-wide Parkin recruitment screen. Data are mean ±SD of four replicate experiments measuring % cytoplasmic localization on deconvoluted siRNA sets. The scrambled negative control siRNA is shown as a blue square and the PINK1 positive control siRNA is shown as a red triangle. The siRNAs against candidate hits are shown as black circles.

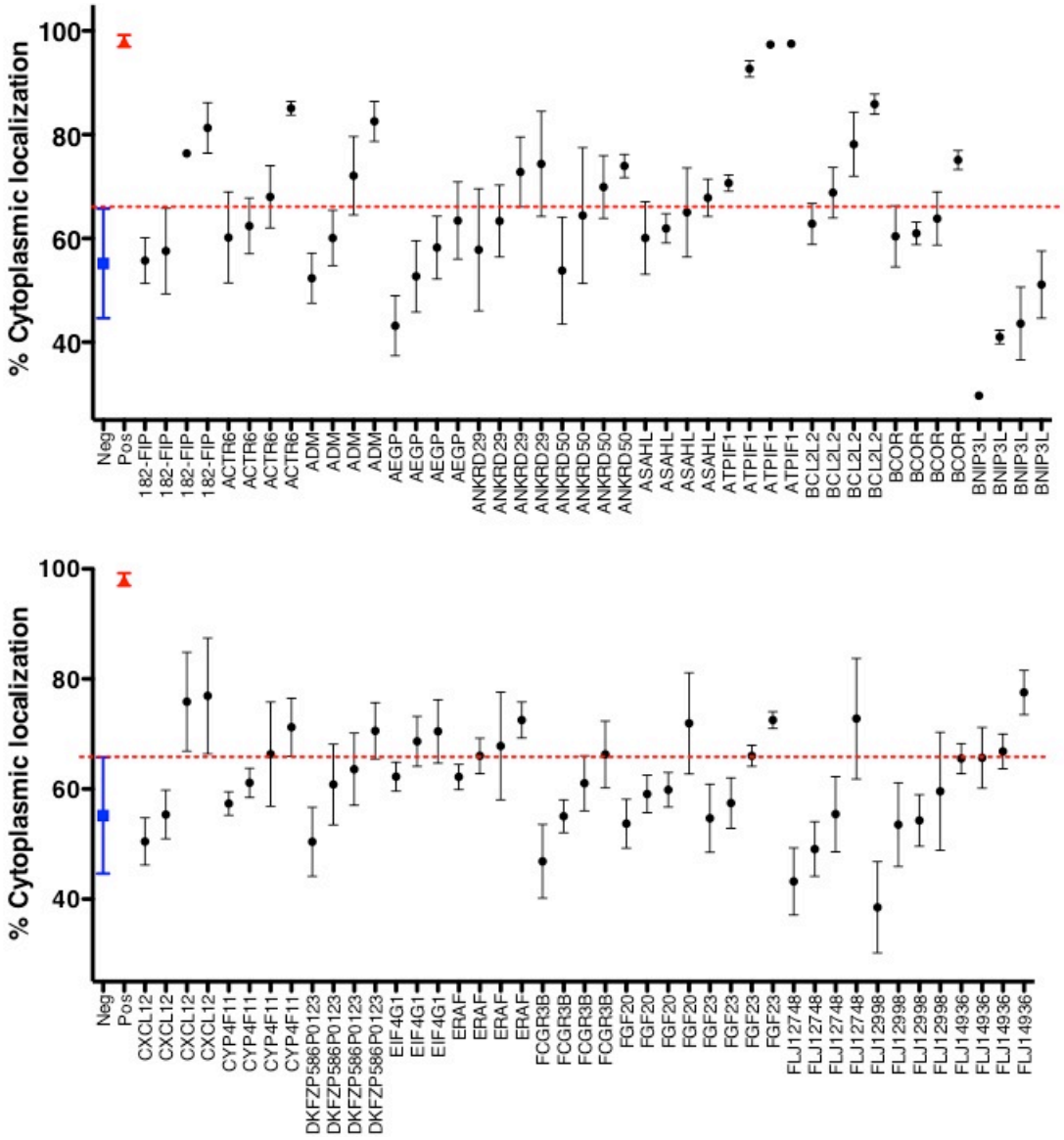

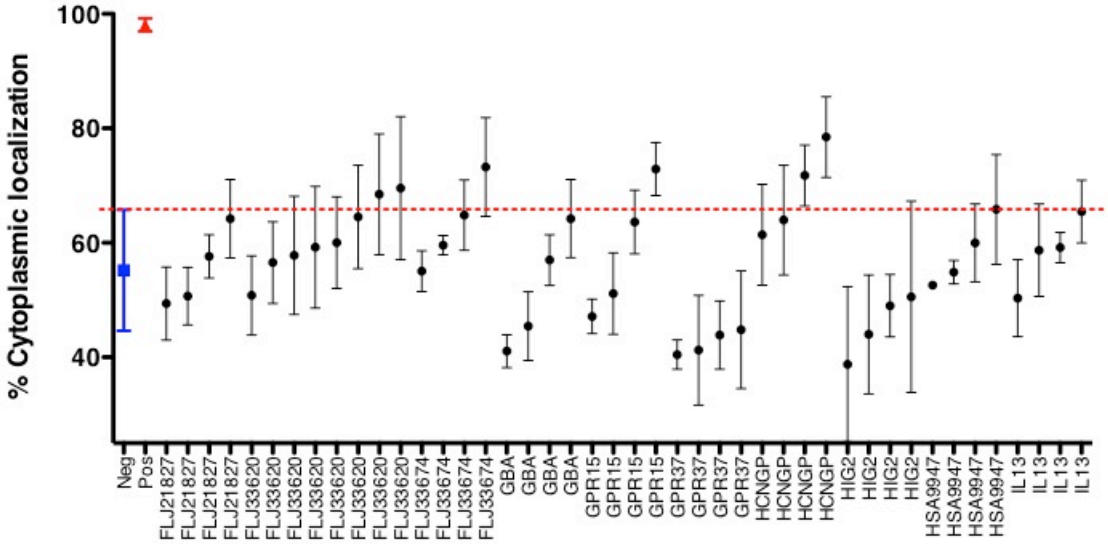
% Cytoplasmic localization
100
80
60
40
Neg
Pos
FLJ21827
FLJ33620
FLJ33674
GBA
GPR15
GPR37
HCNGP
HIG2
HSA9947
IL13

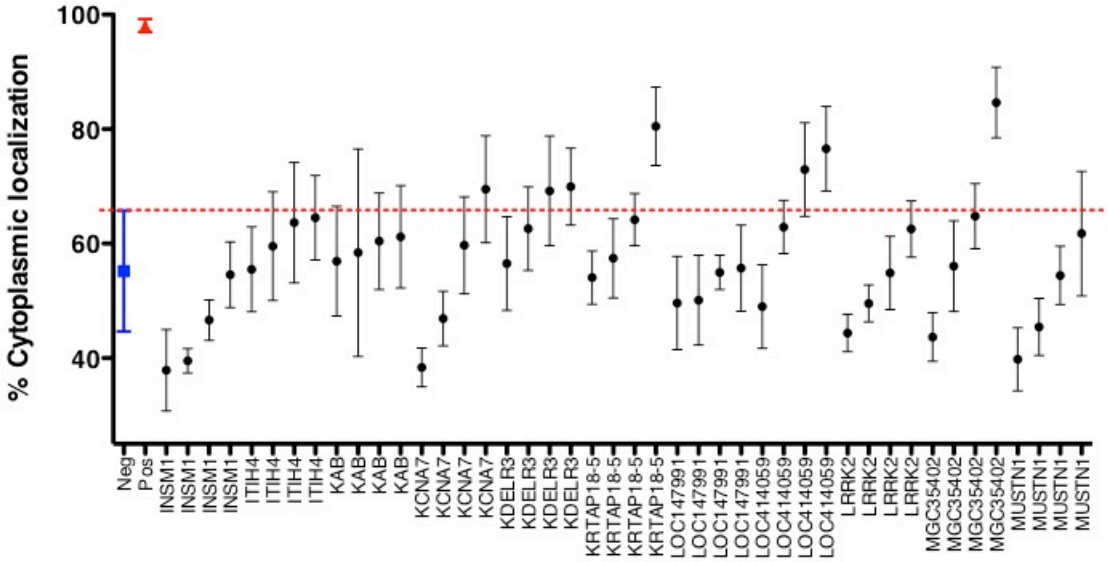
% Cytoplasmic localization
100
80
60
40
Neg
Pos
INSM1
ITIH4
KAB
KCNA7
KDELR3
KRTAP18-5
LOC147991
LOC414059
LRRK2
MGC35402
MUSTN1

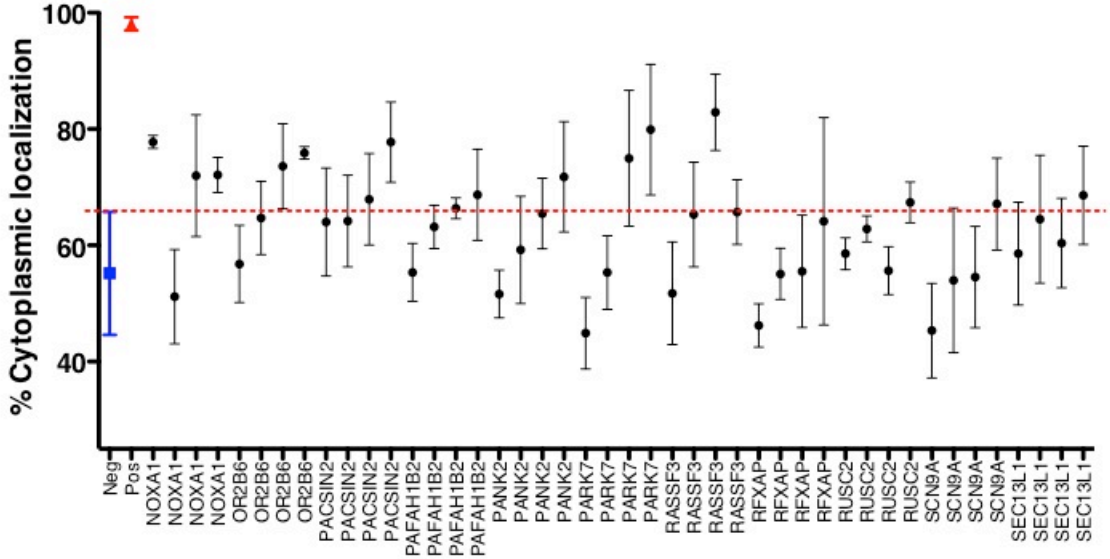
% Cytoplasmic localization
100
80
60
40
Neg
Pos
NOXA1
NOXA1
NOXA1
NOXA1
OR2B6
OR2B6
OR2B6
OR2B6
PACSIN2
PACSIN2
PACSIN2
PACSIN2
PAFAH1B2
PAFAH1B2
PAFAH1B2
PAFAH1B2
PANK2
PANK2
PANK2
PANK2
PARK7
PARK7
PARK7
PARK7
RASSF3
RASSF3
RASSF3
RASSF3
RFXAP
RFXAP
RFXAP
RFXAP
RUSC2
RUSC2
RUSC2
RUSC2
SCN9A
SCN9A
SCN9A
SCN9A
SEC13L1
SEC13L1
SEC13L1
SEC13L1

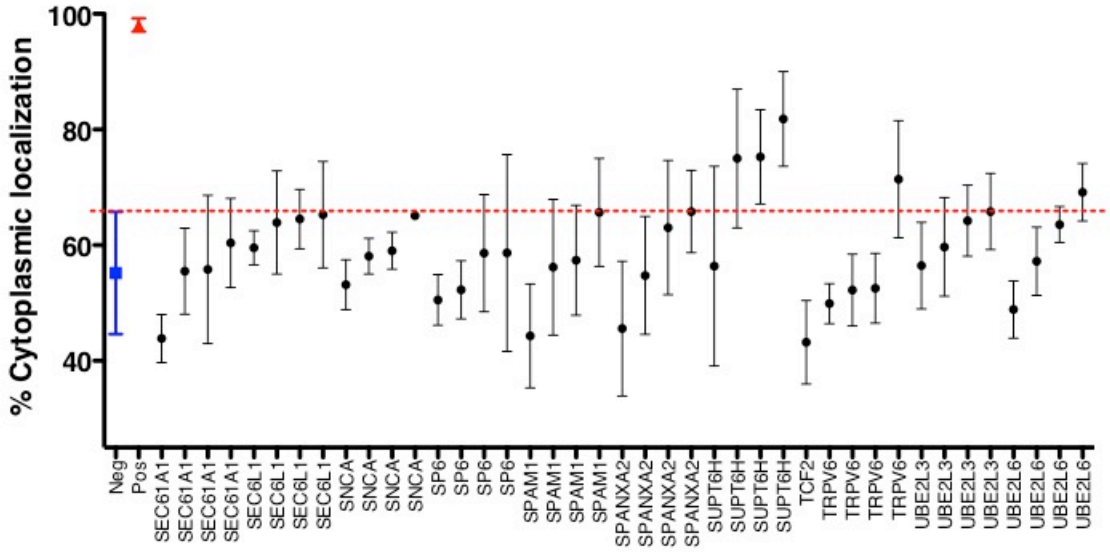
% Cytoplasmic localization
100
80
60
40
Neg
Pos
SEC61A1
SEC61A1
SEC61A1
SEC61A1
SEC6L1
SEC6L1
SEC6L1
SEC6L1
SNCA
SNCA
SNCA
SNCA
SP6
SP6
SP6
SP6
SPAM1
SPAM1
SPAM1
SPAM1
SPANXA2
SPANXA2
SPANXA2
SUPT6H
SUPT6H
SUPT6H
SUPT6H
TCF2
TRPV6
TRPV6
TRPV6
TRPV6
UBE2L3
UBE2L3
UBE2L3
UBE2L3
UBE2L6
UBE2L6
UBE2L6
UBE2L6

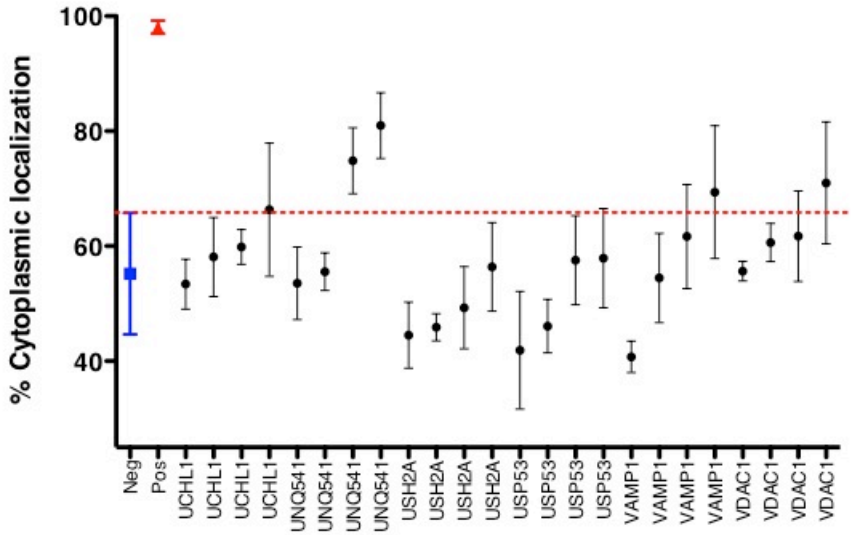
% Cytoplasmic localization
100
80
60
40
Neg
Pos
UCHL1
UCHL1
UCHL1
UCHL1
UNQ541
UNQ541
UNQ541
UNQ541
USH2A
USH2A
USH2A
USH2A
USP53
USP53
USP53
USP53
VAMP1
VAMP1
VAMP1
VAMP1
VDAC1
VDAC1
VDAC1
VDAC1

Appendix III- Analysis of a panel of mitochondrial disease cell lines for changes in the regulation of mitophagy genes. IF1 protein levels were assessed by WB and densitometry relative to the levels of the β subunit of the ATP synthase. Changes in Δψ were assessed by TMRE staining intensity. mRNA levels were assessed by qPCR relative to the house keeping gene 36B4. Changes relative to control (MCH73 for fibroblast cell lines, and 143B for cybrid and Rho0 cell lines) are highlighted in red for an increase and in blue for a decrease.

					mRNA levels		
Cell line	mutation	cell type	IF1 levels (protein)	ΔΨ	IF1	PINK1	Parkin
143B	parent line	osteosarcoma	1	1	1	1	1
Da1B	Melas 100% wt	cybrid	3.1	1.5			
Da10B	Melas	cybrid	1.5	0.7			
Da6	Melas	cybrid	2.8	0.7			
Da8	Melas	cybrid	1.8	0.7			
Da13	Melas	cybrid	2	0.7			
143B Rho0	mtDNA		0.4	0.5	1.5	0.9	0.4
MCH74	control		1	1	1	1	1
Complex III	Complex III	fibroblast	0.8	1.2	1.4	0.9	79
EFG1	mitochondrial elongation factor	fibroblast	1.8	1	1.5	0.8	7.6
NDUFS4	complex I	fibroblast	1.4	1.3	1.2	1.6	2.5
Taco1	Complex IV	fibroblast	2.4	1.5	0.7	0.2	0.3
Surf1	ComplexIV	fibroblast	0.5	1.5	2.3	3	1.8
B17.2L	NDUFAF (complex I assembly)	fibroblast	1.5	0.6	1.5	0.8	1.3
GM10625	leber optic atrophy (MTND1/MTND4)	fibroblast	1	0.6			
GM13078	myoclonic epilepsy	fibroblast	1.2				
GM13411	leigh syndrom (MTATP6)	fibroblast	1.5				